A NEW SOLUTION FOR IMPROVING TRANSMISSION LINE DISTANCE PROTECTION SECURITY DURING SYSTEM-WIDE CASCADING FAILURES

A Dissertation

by

Ahmad Muhammad Abdullah

Submitted to the Office of Graduate and Professional Studies of
Texas A&M University
in partial fulfillment of the requirements for the degree of

DOCTOR OF PHILOSOPHY

Chair of Committee,	Karen L. Butler-Purry
Committee Members,	Joseph D. Ward
	Mehrdad Ehsani
	Panganamala R. Kumar
	Mahmoud El-Halwagi
Head of Department,	Miroslav M. Begovic

May 2018

Major Subject: Electrical Engineering

ABSTRACT

Protection misoperation is responsible for a large portion of all cascading failures. These cascading failures can lead to blackouts that have tremendous social impacts. This dissertation proposes a new method that uses local distance relay instantaneous three-phase currents to enhance the security of distance protection of transmission lines during wide-area cascading events. The method incorporates advanced signal processing techniques and pattern recognition approaches to prevent zone 3 distance protection misoperation.

Prevention of misoperation is done through three major stages. The first stage is fault detection. In this first stage, the proposed method merely recognizes that a fault exists somewhere in the transmission system. The second stage determines whether this fault is within the distance relay's protective reach. The last stage detects whether this fault has been cleared. If the second stage determines that the fault is outside the zone 3 reach of the relay, a blocking signal will be sent to the relay to prevent operation even if the impedance falls within the operating characteristics of the relay. Alternatively, if the second stage determines that the fault is indeed within zone 3 protection reach of the relay, a permissive trip signal will be sent to the relay only if the third stage determines that the fault has not been cleared yet.

The first and second stages use three different k-nearest neighbor classifiers that are trained using level 3 detail coefficients of discrete wavelet transform of the aerial mode currents. The third stage uses the current fundamental to detect fault clearing.

Several wide area cascading scenarios were simulated, and various performance metrics were analyzed to study the effectiveness of the proposed methodology.

DEDICATION

To Shorouk, my wife, and Jana, my daughter, for the joy they bring to my life.

To my father, mother, brothers and sister, and their small families, for their unconditional love.

To my late father-in-law and mother-in-law, for accepting me into their families.

To my friends, especially those with whom I witnessed the 2011 revolution, for all the time we spent together. We will be heroes.

To all my teachers, instructors, and professors who taught me how to think.

To my uncle, Ahmed, and his wife, Mona, for all their help and support since I was an undergrad.

To my late grandmother, Ekram, who would have been very proud.

To the random Egyptian man who told me: “No halva without oven fire”.

To the random American girl who wore a hoodie that read:

“Life without risk is like victory without glory”.

Lastly, to my late math teacher, Saad, who taught me how to do mathematics.

ACKNOWLEDGEMENTS

First and foremost, I would like to thank my adviser Dr. Karen Butler-Purry for her strong support throughout the Ph.D. program. I have learned, indeed, a lot from her experience and knowledge.

This research could not have been completed without the mentorship of Dr. Mahmoud El-Halwagi. I am determined to be as great mentor for my students.

I would like to thank Dr. Joseph Ward for his deep mathematical insight into wavelets, the Fourier transform, and vector spaces which became the basis for this work.

I would like to express my gratitude for both Dr. Mehrdad Ehsani and Dr. Panganamala R. Kumar for investing the time to serve on my committee.

I would like to thank Dr. Gurunath Gurrala of the Indian Institute of Science for his guidance and support during the first year of my Ph.D. program.

Dr. Krishna Narayanan and Dr. Jose Silva-Martinez supported me during an extremely turbulent period of my Ph.D. program. Without their genuine help, I would not have completed the Ph.D. program.

Lastly, Ms. Tammy Carda, has done a tremendous job in facilitating registration and meeting tight deadlines. My wish is that I will serve any position I hold as faithfully as she did.

CONTRIBUTORS AND FUNDING SOURCES

This work was supervised by a dissertation committee consisting of Professor Karen Butler-Purry, Professors Mehrdad Ehsani and Panganamala R. Kumar of the Electrical and Computer Engineering Department, Professor. Joseph D. Ward of the Mathematics Department, and Professor Mahmoud El-Halwagi of the Chemical Engineering Department.

All work conducted for dissertation was completed by the student independently.

The Electrical and Computer Engineering Department at Texas A&M University provided travel grants to present the conference papers that resulted from the research in this dissertation.

NOMENCLATURE

DWT	Discrete Wavelet Transform
KNN	k-nearest neighbors
I_{index}	Current, the index can refer to different quantities
V_{index}	Voltage, the index can refer to different quantities
HFCOs	High Frequency Current Oscillations
CVT	Capacitive Voltage Transformer
CT	Current Transformer
EMTP	Electromagnetic Transients Program
ATP	Alternative Transients Program
A, kA	Ampere, Kiloampere
V, kV	Volt, Kilovolt
Db4	Daubechies type 4
MVA	mega Volt-Ampere

TABLE OF CONTENTS

Page

LIST OF FIGURES

Page

LIST OF TABLES

Page

1. INTRODUCTION AND LITERATURE SURVEY[1, *]

With the deregulated market structure in the United States and Europe, grid operators are under more pressure to reap more profits of existing infrastructure due to increased competition. The grid is thus increasingly operated near the threshold of stability and failure. Failure of the grid, better known as blackouts, carries catastrophic economic and societal consequences. Large blackouts tend to be due to either extreme natural events such as hurricanes, or a series of events called cascading failures [1]. In this dissertation, we only focus on cascading events. Those events can be any of the following: line tripping, overloading of other lines, malfunctions of protection systems, power oscillations and voltage instability [2]. The event that is considered in this dissertation is distance protection misoperation which is a contributing factor in seventy percent of all cascading events [3]. If not discovered and mitigated in an early stage, cascading events generally lead to a complete blackout. With today's society much dependence on electricity as a form of energy, preventing such damage is of high importance.

Cascading failures are defined as "a sequence of dependent failures of individual components that successively weaken the power system" [4]. Since the 2003 US-Canada

---

[1] This dissertation follows the style of IEEE Transactions on Power Systems

blackout, cascading events have drawn much attention in the industrial and academic community. Even though the world has witnessed many blackouts prior to the 2003 blackout [1], the dramatic causes and consequences of the 2003 blackout have left industrial and academic community with the burden of exploring this phenomenon in more detail. To understand the severity of the 2003 blackout [5], it sufficient to say it had caused the loss of 62 GW which caused the lights to turn off for more than 51 million people in the eastern interconnection. Considering the many components and the bits and pieces involved, a domino effect of events evolved slowly (hours) or fast (seconds) according to the region causing a degradation of the integrity of the system leading ultimately to a complete blackout. The main reason of the 2003 blackout was distance relay misoperation. Daunting efforts had to be exerted to gain more knowledge and understanding of the underlying phenomenon.

Relays by design act quickly to remove the fault from the system by disconnecting faulted lines. However, sometimes relays fail to perform such function which is considered a protection system misoperation. Of all protection system misoperations that lead to cascading events, this dissertation focuses exclusively on distance protection misoperation. A protection system misoperation is defined as "a failure to operate as intended for protection purposes" [6]. Various categories are given for misoperation in [6]. However, in this dissertation the word misoperation will be used exclusively to mean only one of them, namely, an operation in which a protection system trips a healthy line due to heavy loading when no fault exists. Notable cascading events [2], [7] begin with lines that were tripped due to actual faults. The tripping of

those faulty line causes the current flowing in those lines to be redistributed to adjacent and nearby lines. Those lines may be overloaded and thus tripped incorrectly -protection misoperation- which may trigger a sequence of cascading events that might ultimately lead to a blackout. It should be noted that regardless of the initial triggering events- whether a fault or not- that cause cascading events, historically those cascading events were triggered under stressful system conditions [5], [8].

As mentioned in [2], one of the effective ways to prevent cascading events is to specify potential undesirable relay operations ahead of time. In this chapter, we show that even though distance protection misoperation can be anticipated ahead of time, prevention of this misoperation is not possible with distance protection principle only because the distance protection principle is not able to be selective in some regions of its operation.

This chapter is organized as follows: Section 1.1 provides a sample distance relay that is set according to NERC standards. Once this relay is set according to NERC directives, it will be explained in the same section that the relay may still misoperate under various operating conditions. Anticipation and detection of distance relay misoperation in the planning stage is described section 1.2. Section 1.3 provides an overview of the communication assisted schemes that have been proposed to eliminate the distance protection misoperation. Lastly, section 1.4 offers a survey on the methods that were suggested in literature to enhance the distance protection security using local data only.

1.1 The distance protection misoperation problem

On August 14th of 2003 [5], the US eastern interconnection suffered one of the largest blackouts in the recent US history. Three 345 kV transmission lines sagged into untrimmed trees during the hot summer days. The tripping of those lines caused another 345 kV transmission line to carry substantial system load. The heavy loading of this last line coupled with relatively low system voltage, caused the distance relay to confuse a heavy loading situation for uncleared zone 3 fault as the impedance entered the third zone of protection which in turn resulted in tripping of the heavily loaded line. The tripping of the healthy yet heavily loaded line worsened system conditions leading to a chain of events that ultimately led to system collapse. Also, on March 31st of 2015 [9], the Turkish grid suffered the worst blackout ever recorded since 1999 when an earthquake caused a complete shutdown of the grid. On the contrary to the 1999 earthquake, the 2015 blackout was caused by an impedance protection misoperation that tripped a heavily loaded line on the 400 kV transmission level even though there was no fault on the tripped line or anywhere in the transmission network. As can be seen from the examples in [5], [9] in which distance protection misoperation have been the main cause of the blackouts or in [10] in which distance protection misoperation have been studied in the IEEE 118 bus system, a distance protection misoperation is characterized by a distance protection system seeing a heavy load on a line as a fault. This confusion arises from the fact that the impedance measured by the impedance protection system coincides with that of a fault. The reason for the heavy load can be due to load shifting after a fault as in the 2003 US-Canada blackout [5], due to lines out of service for

maintenance causing one line to carry substantial system power transfer as in the 2015 Turkish blackout [9], or due to any unforeseen reasons.

To illustrate that this confusion is not tied up with certain system conditions but rather inherent insecurity in the distance protection principle [11], the single line diagram shown in Figure 1 is used to formulate the problem in general terms. It will be shown below that this insecurity always exists, and the degraded system conditions only excite it; that is, for some regions in the impedance protection zone the protection system is not able to be selective between a fault and non-fault condition. Without the degraded system conditions, it is highly unlikely that a distance protection misoperates. Even though, degraded system conditions can be anticipated in the planning stage, the system operator will have nothing in hand to prevent a distance protection misoperation if local function of the distance protection is used alone. It is important to keep in mind that distance protection systems are set locally with the help of the impedance of adjacent lines without any information about the system load until the coordination study phase. In the coordination study phase, the transmission line owner checks all settings against applicable standards. This is explained in detail in [12]. In the following paragraphs, we will set up the relay settings first then discuss what happens in system wide cascading events.

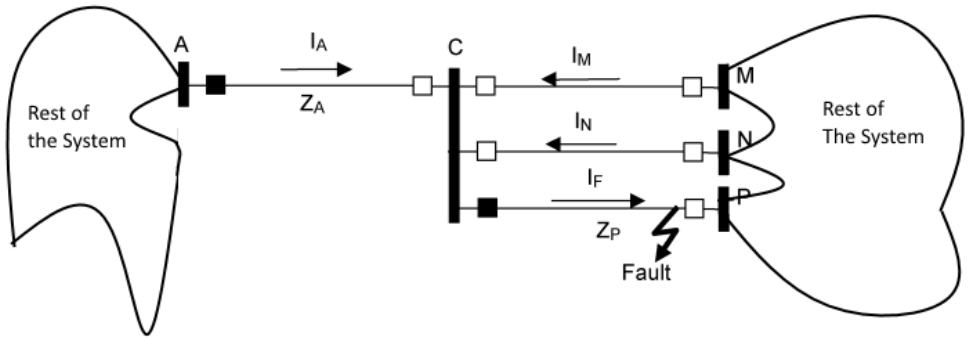

Figure 1. System configuration for formulating the problem

In Figure 1, the distance protection relay that will be studied is the relay at point A of line A-C. Line A-C is connected to three (3) lines: C-M, C-N, and C-P. The number of lines connected to line A-C will not affect zone 1 or zone 2 settings, but will affect zone 3 settings as will be shown in Equation (2). It is clear that the system in Figure 1 is a general topology and does not affect the problem formulation. As will be seen below, tripping in Zone 3 becomes more insecure with more lines connected to line A-C as zone 3 reach becomes larger. To simplify the analysis, all lines are assumed to have the same impedance as well as the short circuit level. However, as will be explained below, this simplification does not affect the generality of the problem formulation. The impedance and the rating of the lines are 60 Ω and 3000 Amp, respectively and are taken from [13]. The setting of zone 1 is assumed to be 0.85 of the line impedance. Zone 2 setting is assumed to be 1.2 of the line impedance. However, some consideration is needed to set the third zone. The third zone has to be set such that it can protect the longest adjacent line (assumed to be line C-P in this case) and to protect 20% beyond that line to provide backup to the remote circuit breakers. In case of a bolted three-phase fault on line C-P

and assuming that the short circuit contributions of all buses is given in Figure 1 by I_{index} where index is the bus name (being M , N, A or P), the voltage at distance protection system at A can be written as given in Equation (1)

$$V_A = I_A \times Z_A + Z_p \times (I_M + I_A + I_N) \qquad \text{Equation (1)}$$

The impedance that is seen by the relay A can then be written as in Equation (2)

$$Z_R = \frac{V_A}{I_A} = Z_A + Z_p \times \left(1 + \frac{I_M + I_N}{I_A}\right) \qquad \text{Equation (2)}$$

Equation (2) will only be applicable to faults on line C-P, if we need to include 20% for the line that is beyond bus P, then the impedance Z_p in Equation (2) has be replaced by $1.2 \times Z_p$. Using the data in [13] and assuming all lines are identical as well as their short circuit contribution, then the setting of zone 3 will be $Z_A + 3.6 \times Z_p = 4.6 \times Z_A$. The three zones are plotted in Figure 2.

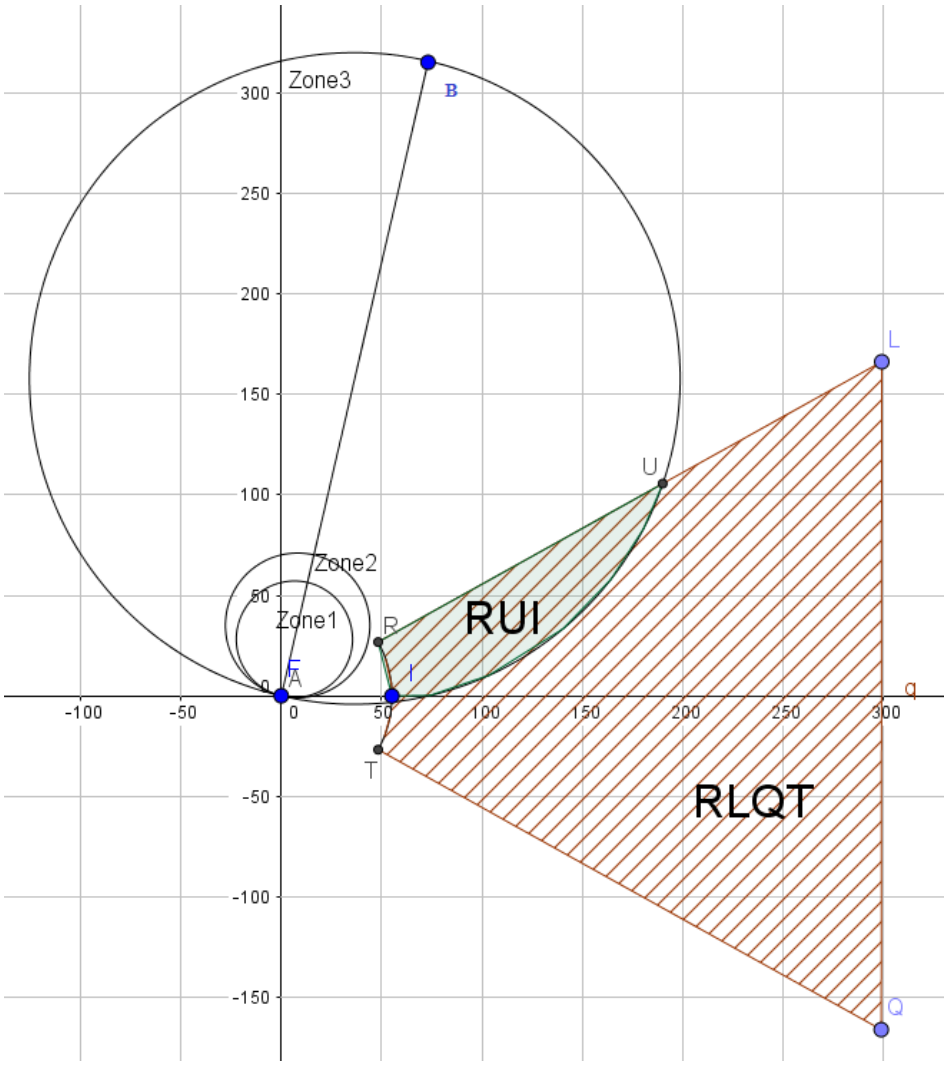

Figure 2. MHO Distance protection characteristic for relay A in Figure 1

After setting up the relay locally, applicable standards and directives need to be applied to the settings for compliance purposes. This step involves running worst case power flow in the summer peak case. The most notable directive is the load encroachment. The load encroachment zone is an area of the protection zone in which the load impedance "encroaches" –intrudes- upon the fault impedance. Load encroachment will obviously cause misoperation and should be removed from the zone

of protection [13]. To plot the load encroachment zone according to NERC [6], [13], [14], the load zone should include the point which corresponds to 150% line loading and 0.85 per unit voltage. Thus, the load encroachment locus of the distance relay at A will consist of two parts. The first part will be an arc of circle of radius given in Equation (3) which is given as arc **RIT** in Figure 2. This arc **RIT** corresponds to the least impedance that the relay should not issue a trip command for. The other characteristic load lines will be two lines making an angle of $\pm 30^o$ with the x-axis ($\pm 30^o$ represents the power factor of the line under worst case loading condition)

$$Z_{load} = \frac{V_A}{I_A} = \frac{\frac{345\ kV}{\sqrt{3}} \times 0.85}{1.5 \times 3000} = 57\ \Omega \qquad \text{Equation (3)}$$

The orange hashed area **RLQT** is the load encroachment area. NERC directives [6], [13], [14] states that this load encroachment zone has to be removed from the relay operating zone. It can be seen at once that if the impedance seen by the relay lies within the solid green area **URI** then a relay may confuse this operating point for a fault since the point lies already in zone 3. This confusion arises if the fault resistance is high enough to cause the fault point to lie within the solid green area **URI**. In Figure 2, this fault resistance ranges from 30 Ω to 90 Ω. The fault resistance can be obtained by measuring the distance between the diameter **AB** of zone 3 circle to point **R** and **U** of the green zone. If it is known in advance that the fault resistance calculated cannot be attained along the route of the transmission line, then the risk of misoperation is nonexistence and the green area can be removed from zone 3 without affecting the security or reliability of the distance protection system. However, fault resistance along

the route of the transmission line is not known in advance. Also, one should note that solid state and electromechanical relays cannot be programmed, only microprocessor relays can. This really means that older relays will have to comply with NERC standards by disabling zone 3 altogether. It is shown in [15] that disabling zone 3 in some cases will force protection engineers to provide back-up protection solutions to remote circuit breakers. This might involve a considerable cost. Additionally, not all countries around the world have standards as strict as NERC, so the solid green area **URI** exist in the zone of protection without regard from the protection engineer. Lastly, even if the relay complies with NERC directives, an impedance can still fall anywhere in zone 3, not only the solid green area **URI,** under stressed system conditions as Phadke and Horowitz pointed out in their paper [15]. This shows clearly the impedance protection is inherently insecure under stressed system conditions.

Attention is now given to the assumptions stated in the beginning. It was assumed that all lines have the same impedance and all of them are contributing equal currents to the fault. It can be seen at once from Figure 2 that this assumption is not restricting the generality of the problem formulation. Because in any case the green area **URI** will exist due to the load profile under stressed conditions. Additionally, the fault contribution of the transmission lines will only affect the diameter **BA** of zone 3 which will only affect point **U**. Point **U** correspond to the max fault resistance. Stated differently, there will always be an overlap between the dynamic rating of the line and zone 3 and the short circuit levels from nearby lines will only affect the size of the overlap (area **URI)** not the overlap itself. Lastly, to derive Equation (1) and Equation (2),

a three-phase fault has been assumed. This is due to the fact that line overload is a three-phase phenomenon. However, it should not be hard to be able to envision a single line to ground fault causing the same effect if one important line is operated with only one phase due to a line to line fault under heavy loading conditions.

It should be apparent from the description above that the major issue that is faced by traditional impedance protection system is that the steady state impedance corresponding to a heavy load is coincident to the impedance under a fault on a remote line to which the distance protection system provides backup protection. It could be argued that impedance protection should be supervised by other steady state protection principles to enhance its selectivity, i.e., the ability to differentiate between a load and a fault current. However, other protection principles -such as over current protection- that can make the distinction between a load and a fault depend on the anticipated power flow for operation while the problem in hand is different. The confusion that is seen by the distance protection is because the power flow under system wide cascading failures changes considerably from the planned power flow. In other words, the load encroachment zone has to be set for system wide cascading scenarios that are not known in advance, which is close to impossible undertaking. One of the authors [15] states this fact as:

"The overwhelming thrust of the NERC rules and other instructions regarding the application of zone 3 elements has been to prevent its operation during emergency conditions. Although this is a desirable goal, it should be recognized that even with all the intelligence available to modern computer relays, the problem of distinguishing a

fault from a heavy load in a relatively short time and using only the current and voltage signals available to the relay cannot be solved in every single imaginable (and some unimaginable) power system scenarios".

1.2 Detection and mitigation of zone 3 misoperation in planning

Most Independent System Operators (ISOs) [16], [17] today use N-1 criterion to judge whether the system is secure after the removal of one line in planning stage. However, given that zone 3 distance protection misoperation is not triggered until two or three lines go out of service [5], the distribution of power flow is hard to be taken into account in the planning stage as it would mean performing N-2 and N-3 contingency analysis which is expensive computationally. Thus, it is increasingly hard to assess protection system capability under the most stressful system conditions. Due to that, the authors in [18], [19] provided an efficient method to study the sensitivity of zone 3 under various operating conditions without the need for performing large number of power flow studies. In [18], [19], the authors define a linearized impedance margin of a distance relay using system voltages, injected power and shunt susceptance. The impedance margin is defined as the distance between the measured impedance locus in the R-X plane to the boundary of the operating characteristic of the relay and is shown in Figure 3. By doing so, the relays that may misoperate can be anticipated ahead of time in an efficient manner in the planning stage using simple formulas. However, it is shown in the paper that if the changes in the voltages or power injections are electrically far away

from the relay under study, a situation that always exists in wide area cascading scenarios, the error in the analysis becomes unacceptable especially for long lines.

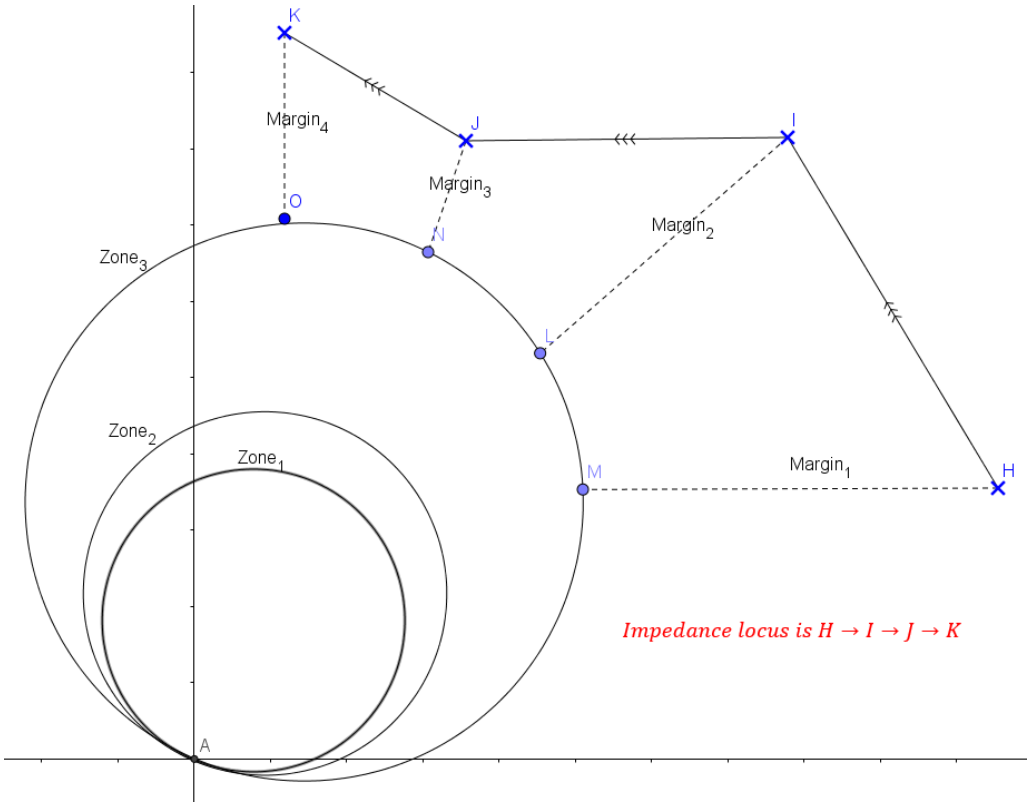

Figure 3. Impedance margin and impedance locus plot for a distance relay during a wide area cascading scenario

In [20], the authors propose blocking zone 3 of certain distance relays ahead of time based on offline simulations. The authors propose that the system operator perform contingency analysis using credible historical contingencies in planning stage to observe the impedance trajectory at each distance relay in the system. The contingency scenarios to be performed have to include more than one contingency to create an impedance trajectory. The relays that misoperate during each contingency scenario due to the impedance trajectory entering zone 3 when no fault conditions exist should be short

listed. Of those relays that are short listed, certain relays are selected such that their zone 3 protection will be disabled. The relays that will be disabled are common to all contingency scenarios and are selected based on a specific criterion explained in the paper. However, the contingency scenarios can be hard to design in the planning stage for modern power systems that have thousands of buses. Additionally, disabling zone 3 effectively disables backup protection for remote circuit breakers which is a situation that should be avoided unless another form of backup is available.

The authors in [21] proposed certain indices that can accurately gauge the severity of system conditions and the likelihood of cascades in real time. An index that is used to monitor distance relays is also proposed. If the indies associated with the distance relays exceed their threshold, then distance protection misoperation is about to occur and the system operator has the option to stop distance relays from operation. However, in practice only N-1 contingencies are studied and thus the severity index is chosen based on these cases. Nevertheless, if the system enters N-2 or N-3 contingency conditions, tuning of the "severity" threshold will be a difficult task computationally.

Lastly, distance protection co-ordination has been explored in [22], [23]. An SVM for each relay is trained using the impedance trajectory that is seen by the relay during fault conditions. The impedance trajectory is obtained by using a transient stability program. SVM is then trained for various scenarios to distinguish zone 1, zone 2 and zone 3 faults. Training scenarios include cases for different fault types at different distances away from the relay that has the SVM and at different fault resistances. Testing scenarios for SVM include faults that have not used in training. By ensuring that the

relays are well co-coordinated under various contingency conditions, unnecessary trip could be avoided. However, the impedance trajectory will depend on the system topology at the time of fault occurrence and this has not been taken into consideration in [22], [23] which could lead to large offline training set.

Due to the fact that distance protection co-ordination requires large amount of offline simulations by performing many contingency conditions, the authors in [24] introduced the idea of "distance of impact" to automate the distance protection co-ordination. However, the authors use the super computer to perform their computations at the first stage. Once the distance of impact of each relay has been calculated, co-ordination of the distance relays becomes straight forward. A shortcoming of the distance co-ordination approach is that even though it can ensure that distance relays never overreach for faults beyond their reach, little research has been performed to study whether the co-ordination can ensure that relays will not misoperate under heavy loading conditions.

As can be seen above, anticipation detection of distance protection misoperation in the planning stage is a hard task. To be able to fully prevent distance protection misoperation, an N-x, where x is greater than 1, contingency analysis need to be done. Even though this could be done for small benchmark systems, contingency analysis, under uncertain load and generation, is computationally intensive for large system consisting of thousands of buses. Many ISOs may not have access to supercomputers to run such intensive computations.

1.3 Communication assisted schemes

The 2003 blackouts pointed out the importance of storing events along with the time they occurred. Investigators spent much of their time trying to match up the waveforms to reconstruct the sequence of events that led to the blackout. It was then apparent that to facilitate the transfer and comparison of waveforms, all samples need to have a time stamp for this purpose. Phasor Measurement Unit (PMU) or synchrophasor technology was then recommended to address this shortcoming [5]. By the time of 2003 blackout, state estimation was a very mature field, but PMUs opened new areas for the application of state estimation by reducing the time needed to do state estimation due to wide spread deployment in the transmission network. A PMU measures the positive sequence voltage and current (both the magnitude and angle), which opens new areas for adaptive relaying and wide area control and protection. In typical distance protection schemes, the relay is only applied to a single transmission line. However, in a wide area protection scheme, a complete area (several transmission lines) can be protected using selected PMU devices without the need to apply PMUs to each single bus in the system. By transferring information in between PMUs in the power system, accurate decision regarding the nature of the impedance falling in zone 3 can be made and misoperation can be avoided.

With the introduction of PMUs, several fault detection and locations methods have been proposed. The salient feature of PMU detection schemes [25] is that using the communication links to transfer data between the two ends of the lines, several conclusions can be drawn regarding whether the line is undergoing abnormal conditions.

A salient feature of the PMU algorithm is the ability to monitor the status of the line and compute the parameters of the line online in a very accurate way.

Due to the fact that zone 3 of distance relays may not be able differentiate between heavy line load and an actual fault on the system, the authors in [26] proposed that a tool be installed at the control center, also known as Independent System Operator (ISO), to continuously supervise the operation of zone 3 elements. The tool will consist of two modules, a central control unit (CCU) and several regional control units (RCUs). The CCU will be installed in the ISO while the RCUs will be installed at select individual substations. The CCU measures the line outage distribution factors and generation shift factors for the entire power grid and sends all factors to the individual RCUs. RCUs use local measurements at the substation and communicate with one another. The individual RCUs will differentiate between faults and transfer of power flow and supervise distance relays based on the information received from the CCU and other RCUs. Even though this solution might be able to prevent all zone-3 misoperations, it needs considerable cost to construct the communication infrastructure that is needed to transmit the data between the individual substation and the ISO.

The authors in [27] uses synchronized samples from both ends of the line to check whether the transmission line has been tripped successfully or not. The instantaneous power from both line ends are calculated. It is shown in the paper that after fault inception, the instantaneous power at both ends becomes positive. This hold true even under systems with week infeed. The method is applicable to all systems other than radial systems. However, due to the need to transfer data between both ends,

significant cost may be incurred to establish such algorithm across each transmission line in the grid. The approach that has been proposed in [27] has been validated using field data in [28].

In [29], distributed PMUs are used to reach a definitive decision about the existence of the fault in the system using a synchrophasor state estimator (SynSE). The SynSE is used to detect network topology changes as well as determine the fault locations as shown in Figure 4. However, the grid has to be completely observable by PMUs. Thus, siting PMUs has to be done carefully to not create unobservable islands under stressed system conditions and certain contingency conditions.

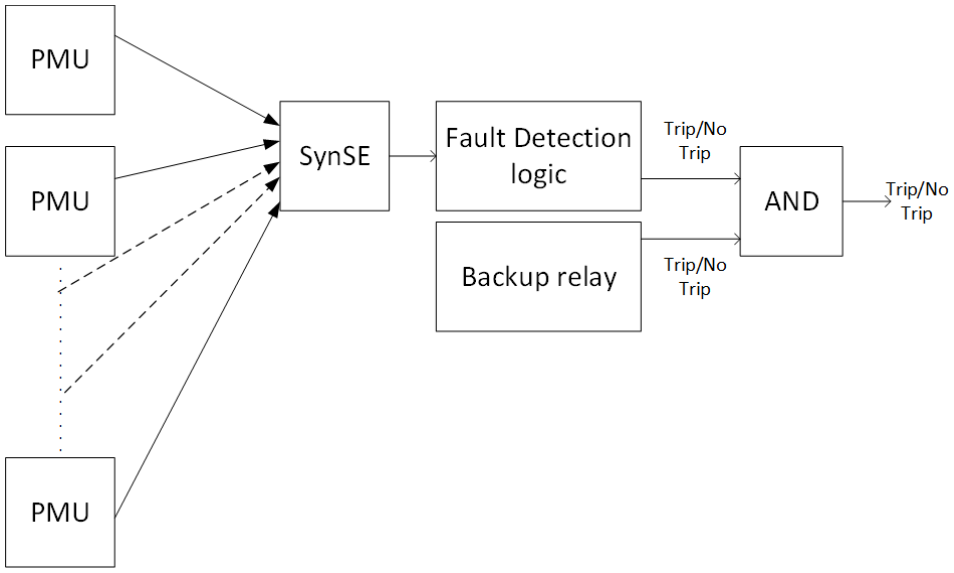

Figure 4. Protection logic of the paper in [29]

In [30] synchrophasors are proposed to supervise zone 3 operation. Specific indices are proposed to assert the fault using the currents which result in a very robust

zone 3 distance protection system. The algorithm forms a super node from the certain groups of PMUs. By summing the current going into the super node, a decision can be reached whether a disturbance exists or not. If a disturbance is detected, another logic is invoked to determine whether it is a fault for the group of PMUs with the higher deviation. The logic that is invoked after disturbance detection is impedance based. A weighted fault detection index is defined for this purpose. The weights used to define the index depend on the reach of the respective zone 3 distance protection relay. If after disturbance detection, the weighted fault index is exceeded, a fault in zone 3 is declared and the relay is restrained from operation. However, to fully take advantage of the method, strategically located PMUs have to exist in the system which makes the approach highly dependent on the topology and any transmission system upgrades. Additionally, certain contingency conditions can cause some faults not to be detected due to the location of the PMUs.

In [31], agents are used to aid zone 3 relay elements without enforcing a decision. In this scheme, each impedance relay will have the capability to communicate with other agents in the network that protect the same transmission line. If the majority of the agents informs the local distance relay that the impedance in its zone 3 reach is actually due to a fault, then the local distance relay should be energized, and a trip command has to be issued. An optimization approach is set up such that the communication delay between the various agents are less than 1 second, which is the time of operation of zone 3. A similar approach has been proposed in [32] where agents are installed everywhere without the optimization approach.

In [33], a limited number of PMUs are used to determine the faulted line as well as the location of the fault. An optimization approach is used to locate a set of PMUs such that the observability is independent of the generator models. A backup protection zone is then constructed using the lines and buses between each PMU such that a line in not included in two regions. The sum of zero and positive sequence currents are used as discriminant for fault detection and location. If the sum is not zero, then the area will be flagged as having a fault. Next comes the task of identifying the faulted line. For the area that is flagged as having a fault, a distance quantity will be calculated for each line within the area, i.e., each line will be assumed faulted and a distance quantity will be calculated. If the distance quantity falls between 0 to 1 then the faulted line will be determined. If more than one line is found to be faulted, an estimation of relative residual error is made and the line with the minimum residual error will be selected as the faulted line. It is clear from this description that two faults within any protected zone or cross-country faults will be detected as one fault only. And even though one of the two faults may have not been cleared, the algorithm may not be able to detect such situation.

In [34], a backup wide area protection scheme is proposed. Short window DFT is used to extract the phasor information from the three-phase voltages and currents. In this scheme, the absolute difference of the bus angles and currents are used to detect the fault. The minimum voltage magnitude establishes the closest bus to the fault and the maximum current angle difference between the buses establishes the faulted lines. However, for the method to work, the minimum voltage threshold has to be established.

It is shown in the paper that a voltage threshold less than 0.95 means that there is a fault on a system. This immediately points out that in case of voltage instability conditions, the method can operate erroneously.

In [35], another wide area protection scheme is proposed. The solution consists of two components: a fault element identification (FEI) and a fault area detection (FAD). The FEI is used to identify the faulted element in the zone being protected. After that, the fault isolation is realized by coordination among area circuit breakers. As part of the FEI, the measured voltage and current of one terminal of the protected area are used to estimate the voltages at the other end. If an internal fault occurs within the zone being monitored, then the estimated value will be different from the measured value at that bus causing a fault to be detected. On the other hand, the faulted area is detected through FAD. The substations that are within the faulted area need to send the information to the central control room. Afterwards, the central control room will search the suspected faulty lines and identify actual faulty lines quickly. The use of FAD concept reduces the communication overhead required by the scheme.

The authors in [36] use PMUs, that are in place as part of a wide area protection scheme, to detect the power flow transfer due to the removal of faulted line from service. In [36], the load flow transfer to a line can be calculated using the network topology via the distribution factors. If the measured power flow transfer significantly mismatches the calculated power flow transfer, then a fault will be declared. Based on that detection, zone 3 is adaptively adjusted to prevent misoperation which eliminates distance protection zone 3 misoperation.

Even though PMU based schemes and wide-area based schemes can offer attractive solutions to eliminate the problem of distance protection misoperation, these solutions require significant communication infrastructure cost. Additionally, the power grid is a critical infrastructure and the cybersecurity risk may be eminent if the grid is brought online for communications purposes.

1.4 Modifications to local distance protection

In addition to using PMUs for fault detection and assisting zone 3 tripping, various authors proposed making changes to the way impedance relays operate. In these methods, the authors proposed additional criteria to assist distance protection in order to assert that fault exists within the relay reach using local data.

Local measurements are used in [37] to assist zone-3 tripping. The authors proposed to distinguish three-phase faults from system overloads. The DC decaying component and the line load angle are used to determine whether a fault has occurred within the reach of local distance relay. The DC decaying fault component is reconstructed from the measured currents in all three phases. Since the fault is three-phase, a DC decaying component must exist in one of the phases. A transient monitoring function will then be defined to be the maximum of all three phases DC decaying components in one cycle. Also, for the three-phase fault to be asserted, the line load angle has to be greater than 50 degrees. Both the monitoring function as well as the line load angle has to be true for a three-phase fault to be declared. The drawback of this method is that the fault must have significant decaying DC component which makes it challenging for certain fault incipient angles and transmission line lengths as a

significant decaying DC component can only occur when the fault occurs at certain incipient angles and under certain X/R ratios. Additionally, the paper assumes the angle between the current and the voltage at the relay to be more than 50 degrees as a fault indicator. However, it has been pointed out in [15] that under stressed system conditions the angle may indeed exceed that threshold with no fault on the system. Also, if the swing frequency in the system is anticipated to be larger than 5 Hz, threshold selection for transient monitoring becomes a hard task which could mislead the scheme to confuse power system swing for three-phase faults. Lastly, the effect of fault resistance has not been studied in the paper. Fault resistance can potentially cause trouble setting the threshold for the transient monitoring function as it affects the DC decaying component.

In [38] the rate of change of voltage is used as a trip restraint to supervise distance protection misoperation. The idea is that fault occurrence or fault clearing causes the voltage seen by the relay to change drastically. The authors propose if the local relay senses that the system voltage is stressed according to the conditions listed in [39], the rate of voltage change ($\frac{\Delta V}{\Delta t}$) will be used to assert whether a fault has occurred and cleared within zone 3 protection using two thresholds for both fault occurrence and fault clearing. Additionally, the authors proposed to use a thermal loading monitoring function to decide whether the maximum conductor temperature has been reached. The temperature monitoring function will start operation after the fault has been detected. If the temperature monitoring function declares that the line temperature has reached maximum limit, the line will be tripped whether the fault has been cleared or not. However, for the trip command to be secure, large amount of offline simulations need to

be carried out to know the worst-case rate of change of voltage. The major disadvantage of the method is that under voltage instability, the $(\frac{\Delta V}{\Delta t})$ criterion is not exclusive property for faults as pointed in [40] since under voltage instability, a sudden generator tripping could cause the same $(\frac{\Delta V}{\Delta t})$.

Since it is hard to distinguish between evolving pre-blackout event and short circuit conditions using magnitude of voltage, another trip restraint quantity, namely $(\frac{\Delta I}{\Delta V})$ has been used along with $(\frac{\Delta V}{\Delta t})$ criterion to trip zone 3 securely in [40]. The $(\frac{\Delta I}{\Delta V})$ threshold value has also been obtained using offline simulations. The disadvantage of the method in [40] is that neither contingency analysis nor system loading levels have been taken into consideration.

The use of fault generated high frequency components has also been investigated in literature [41]. Such usage can give a more precise answer whether a fault has occurred thus making tripping in zone 3 more secure. In [42], the energy of the first three current levels and the third approximation is used to train a probabilistic classifier. The energy is calculated using certain levels of the discrete wavelet transform of the three-phase currents. Using this energy features, a decision is made whether a transient signal if due to a fault or non-fault condition on a line. A simpler online transient classifier has been proposed in [43], where the transient events occurring on the transmission lines nearby any distance relay are identified. Modal transformation is used to transform the phase currents into modal currents. The discrete wavelet transform coefficients of the aerial modes [44] are combined in a certain manner to train a

feedforward neural network to classify those transients. However, the major drawbacks of both [43] and [44] is that they cannot be used to tell whether the fault is within the relay protection reach even though they can tell whether a fault has occurred in the network. These papers can only be useful if another method is found to use the transient classification as an entrance point to determining whether the fault is within the protection reach of the relay, but this has not been done in literature to the best of our knowledge.

Various adaptive zone 3 settings were also investigated in literature where zone 3 reach is adjusted based on local information. In [45], [46], ANN has been used to predict the correct load blinder under various system conditions. The load blinder is then combined with the zone 3 settings to block any undesirable tripping. The load blinder is only activated under balanced conditions to make sure that the heavy loading is not confused for unbalanced fault conditions. The load blinder is determined based on offline simulations. The simulations take into account the loading level of the power system, fault incipient angle, source impedance ratio, fault resistance and fault location. The features used to train ANN is the active and reactive power, voltage as well as the rate of change of both the voltages and currents seen at the relay terminal as shown in Figure 5. A simple line connected to another line with a load in between is used to test the method which is a disadvantage of the method. Also, the effect of the system topology was not studied. It is also foreseen that the inclusion for contingency analysis in ANN training will require large offline simulations and will make load blinder selection difficult task. Additionally, only three phase-fault currents has been used to

train the ANN and in case a single line to ground fault occurs and cause the features to be different than the ones used in training, the method is expected to fail because ANN is known to have bad generalization capabilities [47].

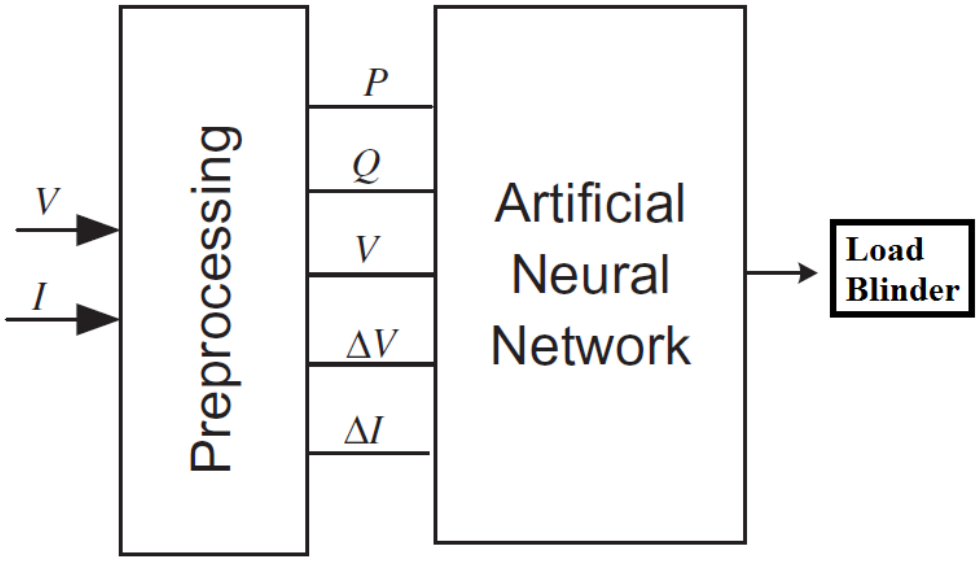

Figure 5. Creation of adaptive load blinder in [45]

In [48], [49] the authors propose changing zone 3 reach during emergency conditions to prevent distance protection misoperation if certain system conditions are met. If those system conditions are met, zone 3 protection reach will be shrunk to zone 2 which in turn gives maximum security. During stressed system conditions, the impedance seen by the local relay approaches the original zone 3 border, whether this border is MHO characteristics or polygonal one. The authors propose to define a fourth protection zone, called third zone proximity area (TZPA), as well as a fifth protection zone, called third zone modification area (TZMA), to change zone 3 protection reach based on certain criteria. The TZMA is a region within TZPA but closer to zone 3

protection zone. The authors provided rules on how to set both TZMA and TZPA. Once the impedance enters this TZPA and crosses zone 3 fast enough, the fault will be declared. However, if the impedance enters TZPA and stays within TZPA, the TZMA logic will be put into action. Zone 3 protection will be shrunk to zone 2 if the impedance crosses TZMA within a minute. This one minute is used to adjust for restorative corrective forces of the gird such as generator excitation controls and transformer load tap changer. In summary, zone 3 protection will only be changed if the impedance crosses TZMA with a certain rate within a specified time delay once it starts changing in TZPA. These ideas are illustrated in Figure 6. Although, the approach is very promising, a fast-evolving system instability could mislead the scheme. Additionally, it can be seen that the approach proposed sacrifices dependability for security as evident by shrinking zone 3; if a fault occurs within the original zone 3 protection zone beyond the original zone 2 reach after zone 3 protection zone is shrunk, the approach proposed by the authors will rely heavily on the closest relay and circuit breaker to clear the fault. However, if this relay or circuit breaker fails to clear the fault, the fault will go uncleared worsening the already stressed system conditions. Lastly, the proposed algorithm will fail definitely in case the impedance stays within TZPA, suddenly jumps to original zone 3 due to a zone 3 fault before the time delay expires then stays in zone 3 after fault clearing due to line heavy loading conditions.

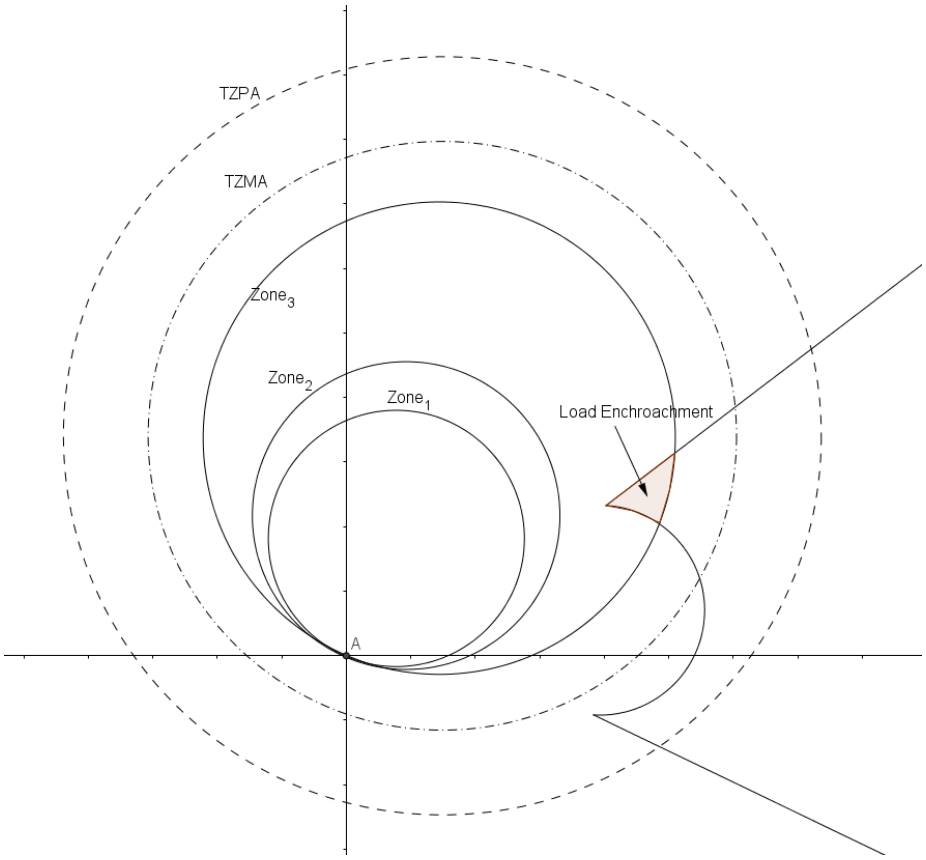

Figure 6. TZMA and TZPA of the method in [49]

Lastly, the authors in [50] proposed to identify power flow overload based on a newly proposed concept. This concept is based on the phasor relationships in the complex phasor plane. The paper only differentiates between three-phase faults and overloads as overloads are three-phase balanced phenomenon. Since the paper only aims to distinguish three-phase faults from overload, any three-phase fault on a transmission line can be analyzed without the need of information from the other end of line. This is due to the fact that the fault arc voltage is not affected by the infeed fault current making the fault point grounded through the arc resistance. This property is used to derive the criterion to differentiate between three-phase faults and overloads based on an

impedance criterion that can be adaptively adjusted using the measured phase angle between the voltage and current at the relay location as well as a constant safety factor. However, the method is not applicable when a three-phase fault occurs within the distance relay reach during an overload condition. Additionally, it is assumed that all three-phase to ground faults involve arc without the consideration of the other situations when three-phase downed conductors cause such faults which in turn could cause some of the assumptions used in deriving the impedance criterion to be invalid.

In summary, the use of rate of change of voltages and currents can prevent the problem of distance protection misoperation in most occasions but does not fully prevent it. Other methods use previous operational experience with distance relays to propose solutions to the problem of distance protection misoperation. However, system conditions and scenarios that were not previously encountered could mislead those proposed solutions. The use of high frequency fault generated transients seems to be a promising area, but it is scarcely researched in literature.

1.5 Summary

The problem of distance protection misoperation has been presented. Various approaches to solve the problem have been surveyed and organized into three main categories. The methods in each category have been explained. Additionally, the advantages and disadvantages of each method have been pointed out.

The first category is anticipation of distance protection misoperation in the planning stage. In this category, distance protection misoperation could be anticipated day ahead based on the forecasted load and generation as well as contingency

conditions. However, due to the large size of modern day power systems, such anticipation is computationally intensive.

The second category is communication assisted protection schemes. The main idea in this category is that using information from both ends of the line or information from various substations in the network, a blocking command can be issued to the affected distance relay. Nevertheless, these communication-assisted protection schemes have not found wide industry acceptance due to cybersecurity risks as well as the economic cost that is required to build such systems.

The third category is modification of the local distance protection function using local information. The main idea in this family of solutions is that using operational system experience as well as the local data, one can tell with certainty that a distance relay is about to misoperate. By detecting such conditions, a blocking command can be issued to guard the relay against misoperation. Nevertheless, the methods in this last category may fail under system conditions that were not taken into consideration while developing these methods. This dissertation belongs to this class of solutions.

The most appropriate method to mitigate zone 3 misoperation is dependent on what is the most important factor for the utility company. For example, one utility company may prefer a communication-assisted scheme using remote measurements to eliminate the possibility for distance protection misoperation while accepting the cybersecurity vulnerabilities that are introduced. Another utility may not be willing to accept the cybersecurity risks or the cost of constructing such scheme and requires a solution using local measurements or minimum remote measurements. We think that

methods which use local relay data are worthy of research attention as cybersecurity threats are becoming a major concern.

2. DATA ANALYSIS AND METHODOLOGY CONSIDERATIONS*

This chapter analyzes the features of disturbance data during wide-area of cascading events. A general theoretical background about the discrete wavelet transform is first explained. After that, the features that are available in the high frequency oscillatory components are presented. Based on the study of the features, general considerations regarding any acceptable solution methodology will be given.

2.1 Discrete wavelet transform

In this research, the dyadic wavelet transform is used [51]. The transform takes the signal and applies low and high pass filters to it. The transform converts the original signal into independent signals, each of which spans a certain frequency band. The frequency bands are determined by the number of levels the original signal sought to analyze; each level corresponds to a unique frequency band. The word "independent" (as it applies to signals) means that one level cannot be derived from another, i.e., level 2 cannot be derived from level 1. The frequency band of each level depends on the sampling frequency and Nyquist theory. The highest frequency in the decomposed signal will be equal to half of the sampling frequency.

---

* Parts of this chapter were reprinted with permission from "Towards a new paradigm for ultrafast transmission line relaying" by Ahmad Abdullah, 2016 IEEE Power and Energy Conference at Illinois (PECI), Pages 1–8, ©2016 IEEE

The DWT transform equation is provided in Equation (4) [51] where $\varphi(t)$is the mother wavelet used, and f(t) is the signal to be analyzed. Parameter "a" causes scaling (which determines the level) and "b" causes shifting in time.

$$Wf(a,b) = \frac{1}{\sqrt{a}} \int_{-\infty}^{\infty} f(t) \times \overline{\varphi(\frac{t-b}{a})}\ dt \qquad \text{Equation (4)}$$

As can be seen from the integral, the transform signal is successively approximated at each level given by the "a" scaling coefficient. In other words, after fixing the coefficient "a", the transform signal is a time series signal that is a function of the "b" coefficient. The "b" coefficient is a translation in time. It is evident from Equation (4) that the transform time series signal at a certain level cannot be derived from the time series at a different level (different value of the "a" coefficient).

The dyadic transform can be thought of as an application of high and low pass filters to the signal resulting in two signals. The signal corresponding to the output of the high-pass filter is called level 1, and the other signal is called approximation 1. Both signals are independent and cannot be derived from each other. One can stop at this step or choose to apply high and low pass filters to the first approximation to get level 2 and approximation 2. Level 2 will span a frequency band corresponding to the upper half of the frequency band of approximation 1, while approximation 2 will occupy the lower frequency band. Continuing in this manner, by applying successive low- and high-pass filters, one obtains a set of levels (also called details) and one last approximation. In theory, the last approximation should correspond to a pure sine wave, provided that the

high frequency components imposed on the power frequency contain frequencies that are not included in the frequency band of the last approximation.

Figure 7 illustrates a numerical example where the use of a 200 kHz sampling frequency results in discrete wavelet transform (DWT) decomposition. In practice, it is not needed to apply the transform all over the infinite time line. Since wavelets have a strong localization property, it is only necessary to apply the transform to the time period under study.

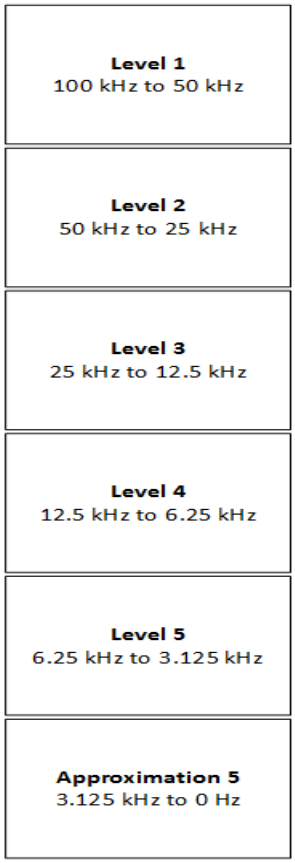

Figure 7. DWT analysis of a certain signal

2.2 Features available in the high frequency oscillatory components

Since it was determined, based on the literature survey, that high frequency oscillatory components are the best approach to increase the security of the distance relay, the question that remains open is: What features in the high frequency components can be used for fault detection?

When a fault or any transient event occurs, it launches a traveling wave, as well as high frequency oscillatory components [52]. Traveling waves can be easily quantified as they arrive at the line terminals, but the high frequency oscillatory components cannot. The reason these oscillatory components were difficult to quantify in previous research is explained below.

At this point, new terminology needs to be introduced. When speaking of a certain transmission line, a fault on that line is called a fault case. A fault case has its parameters. Those parameters are: incipient angle, fault resistance, fault type, and fault location. Thus, a certain fault case on a specific transmission line causes voltages and currents to oscillate in a manner that is in accordance with the parameters of that fault case. The formal solution of the currents and voltages of a single phase line is given by the following two equations (called telegrapher equations) [53]

$$\frac{\partial V}{\partial x} = I \times R + L \times \frac{\partial I}{\partial t} \qquad \text{Equation (5)}$$

$$\frac{\partial I}{\partial x} = G \times V + C \times \frac{\partial V}{\partial t} \qquad \text{Equation (6)}$$

where:

- I and V are the current and the voltage anywhere on the line (Ampere and Volt, respectively).
- R and G is the resistance and conductance per unit length of the line (Ohm and Mho), respectively.
- L and C are inductance and capacitance of the line per unit length (Henry and Farad), respectively.
- x is the distance from a zero-reference frame generally taken to be at either end of the line.

A general closed form solution of Equation (5) and Equation (6) is difficult and generally impossible, as it depends on the boundary and initial conditions of the case involved. Perhaps the most straightforward solution method is to obtain the solution in terms of an infinite time series expansion. However, infinite time series expansion is not applicable here because we intend to analyze the frequency content of the signal as the content changes over time. Application of Laplace and Fourier transforms to those equations produces integrals that have not yet been solved formally. Moreover, when a three-phase line is studied, the above equations become six equations (two equations for each phase: a voltage and current equation). Thus, decoupling them is a difficult undertaking, if not impossible, in most cases. If we have mutual coupling between two lines sharing the same tower, then we must generate three more equations for a total of nine equations. Bearing in mind that those nine equations are for one line only, those equations then need to be solved simultaneously along with all other equations in the

system. For today's power systems which consist of thousands of lines, solving all equations analytically in a closed form is beyond human capacity.

The main aim of analyzing the high frequency components is to detect the fault once it is initiated. It is very apparent that high-frequency fault-generated transients are different for each fault case on a specific line. This is because each fault case on a specific line has its own set of equations as given in Equation (5) and Equation (6) with unique boundary (lines connected to it) and initial conditions. Moreover, the same fault case on different lines will cause different fault-generated transients because each case has its own boundary and initial conditions, which are different for all neighboring lines. For this reason, no attempt is made to solve the equations in a closed form but instead, they are solved numerically by running electromagnetic transients (EMT) simulations, extracting the high frequency content and then analyzing this content.

To be able to see the high frequency features, one can analyze the three-phase currents and voltages using DWT. This way the time and frequency features in both the voltages and currents can be seen at once. In all of the following investigations, we found that DWT with Daubechies type 4 "db4" provides the best features. In theory, any wavelet type can be used as no emphasis is put on the smoothness and differentiability of the current or voltage signals since we are using the discrete wavelet transform to analyze numerical simulations. A discussion of the differentiability and smoothness of mother wavelets such as db4 would occupy too much space and time away from the main focus of this research. However, the interested reader is encouraged to read the book, *A Wavelet Tour of Signal Processing* by Mallat [54].

To identify features in both voltages and currents, realistic voltage transformer and current transformer models have to be used since distance relays see the currents and voltages at the secondary side of CTs and CVTs whereas the EMT simulations provide three-phase currents and voltages at the primary side of the measuring transformers. Most voltage transformers used across the transmission network are capacitive voltage transformers (CVTs) due to cost and size limitations. CVT models used are described in [55]. Also, most CTs are either air core CTs or bushing type CTs due to cost considerations. CT models used are described in [55].

To identify voltage and current features, one can create a fault case on a transmission line and analyze it using DWT to see what type of oscillatory components exist. Figure 8 illustrates the DWT decomposition of a signal

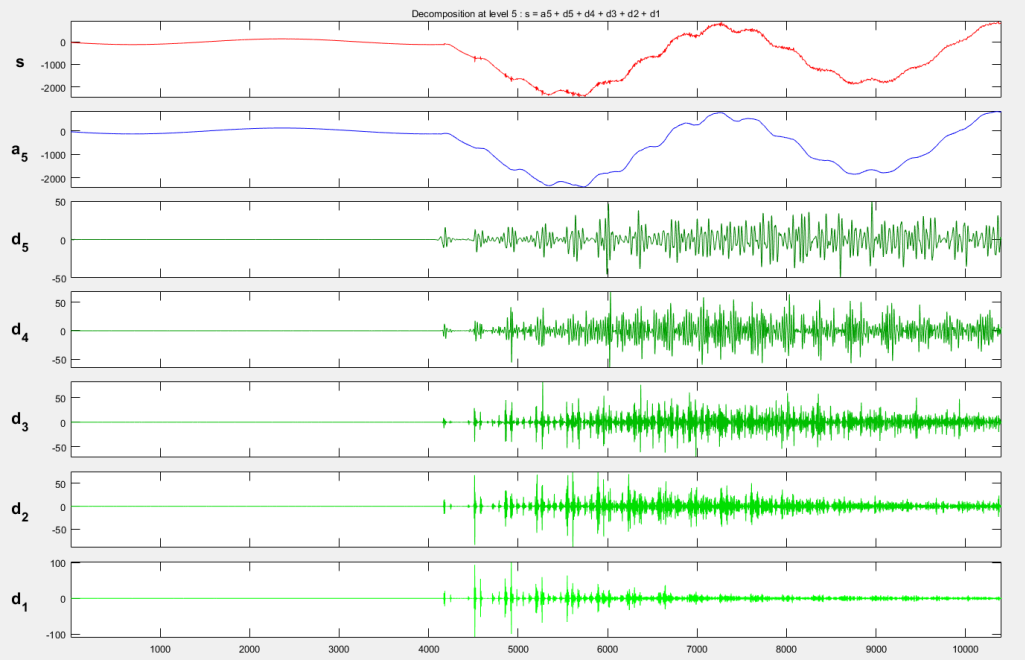

Figure 8. DWT decomposition of phase A current of a certain fault case

As can be seen from Figure 8, the details coefficients show the high frequency content of a phase current at each level. It is apparent that the pre-fault case does not contain any oscillations since it is at a steady state. However, once the fault occurs, the traveling waves as well as the high frequency components occur and can be seen in the decomposition. It is also clear from Figure 8 that traveling waves can easily be seen at level 1. But as levels go up, it becomes harder to determine when the traveling waves arrived at the line terminal.

On the other hand, small oscillatory components can be seen at voltages as the CVT attenuates all high frequency components. A CVT is a tuned RC filter that is supposed to pass the fundamental frequency signal only. A closer look at the voltages produced at CVT terminals based on CVT models adopted from [56] illustrate that this is indeed the case as shown in Figure 9. Figure 9 that was reproduced from [56] shows that the voltage contains no noticeable traveling waves and the fundamental frequency signal is clearly dominant.

Moreover, it is widely known [57] that if a fault occurs at the instant of zero-voltage crossing, no traveling waves occur and the fault will go undetected if traveling waves are used for fault detection. This can be clearly seen at Figure 10 where the fault has been created such that it occurs at the zero-voltage crossing at the point on the transmission line where the fault occurred. As shown in Figure 10, even though no traveling waves occur, high frequency oscillatory transients do exist even though they may be small. In fact, no traveling waves will appear if the fault occurs within the zero-

voltage crossing, i.e., there is a deadband around the zero-voltage crossing in which no traveling waves can be launched.

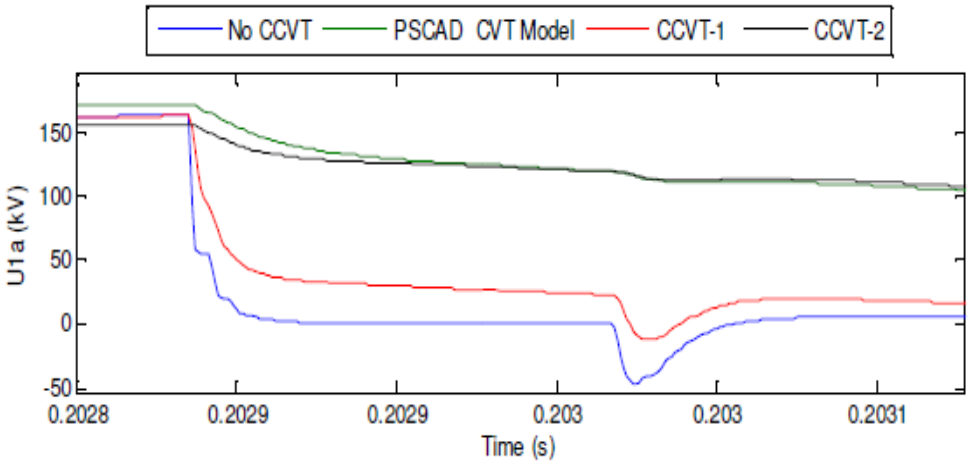

Figure 9. Voltage measurement with and without CVT model. CCVT-1 and CCVT-2

In summary, no voltage high-frequency components or traveling waves can be used because 1) a capacitive voltage transformer (CVT) attenuates them due to its characteristics, and 2) traveling waves are not generated in case the fault occurs around zero voltage at the point of fault on the transmission line. These two points cause three-phase voltages to be practically unusable for this application. On the other hand, high-frequency oscillations always exist at three-phase currents largely regardless of the fault incipient angle and the CT model used. For this purpose, features are extracted from the phase currents throughout this research.

It should be noted that transmission line faults are not the only reason for high frequency oscillations generated in the transmission network. The study of high-frequency oscillations due to faults must be done alongside other high-frequency oscillations with the reasons for all such occurrences taken into consideration. This is

done to ensure that the features seen in the three-phase currents are unique to faults and thus, the fault detection module is secure and does not cause a false alarm. Since transmission networks are isolated from the distribution network by relatively long sub-transmission and sub-distribution networks, the reasons for transmission line high-frequency components are limited and are given as follows:

- faults,
- line switching operations,
- lightning strikes,
- load dropping and load energization, which include:
    - load ramping,
    - line opening, and
    - line dropping operation.

In the next sections, all of these disturbance events are analyzed using the DWT to identify the features that can be unique to faults.

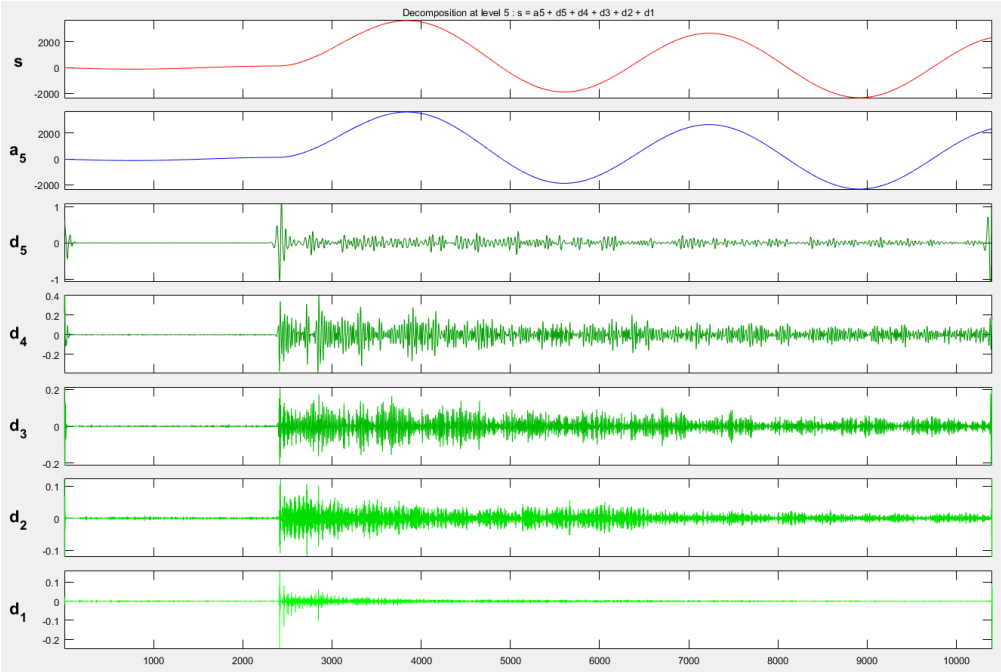

Figure 10. Fault at zero voltage crossing

2.2.1 Features available in three-phase currents

As has been explained in the previous chapter, only three-phase currents contain high frequency oscillatory components that are usable from a practical point of view. In this subsection, we provide an overview of the features used to represent high-frequency oscillatory components.

Samples of the three-phase currents were proposed in [58]–[60] to be used as the features. The samples were used with no pre-processing which required high computational resources. After the emergence of wavelet transform, it was discovered that not all samples are needed other than a compressed version of them. Researchers in [61]–[64] proposed using wavelet details as features. By combining those features in addition to some logic to distinguish internal and external faults, the authors in [61]–[64]

were able to construct a fault detection module. In addition to using the wavelet coefficients, authors in [42] proposed to use the energy of certain wavelet details coefficients as features.

When it comes to three-phase currents, various transformations can be defined to obtain different features in various domains. The following transformations can be defined:

- Symmetrical components [65],
- Clarke transformation [66],
- Karrenbauer transformation [67], and
- modal transformation

A well-established feature extraction method is given in [68] to extract the optimal or near optimal features from the details coefficients. We found that using a sampling rate of 200 kHz, the optimality condition in [68] removes considerable amount detail coefficients from level 1 and level 2 decompositions but not from level 3 if certain conditions are met. These conditions are: 1) we apply the modal transformation [44] to a half cycle of post disturbance data to remove the ground mode current and obtain the two aerial mode currents; 2) the DWT was then applied to extract level 3 detail coefficients corresponding to half a cycle of post-disturbance data of the two aerial mode currents. Thus, a design decision was taken not to apply the optimality condition to trade complexity for simplicity and practicality. If the CT bandwidth is 10 kHz, as is the case with some bushing type CTs, then level 1, corresponding to a frequency band ranging from 10 kHz to 5 kHz, will be used instead of level 3. In other words, we found that the

detail coefficients must correspond to frequencies of at least 5 kHz for accurate classification. Below is a summary of the modal transformation.

2.2.2 Modal transformation

The modal transformation is used in EMTP [69] as the only way to analyze power system transients [70]. Contrary to the above transformations, modal transformation depends on distances between the phases. This means that for each tower configuration, a transformation matrix is obtained. Briefly, the modal analysis corresponds to an eigenvalue analysis of the currents in the three phases, which means that the three-phase currents or voltages are separated into three independent sets of currents or voltages. The modal transformation removes any mutual coupling and untransposed line effects. The general form of the modal transformation is given in Equation (7) [44], [71]. In general, the entries of the matrix are complex, but the imaginary part is so small that the matrix can be approximated by real entries. The signs of entries of the matrix are constant and do not depend on the tower configuration. The current I_0 has the same physical meaning of the ground mode current in symmetrical components. However, since the entries do not have the same value as in the symmetrical component transformation matrix, I_0 is the weighted sum of the phase currents. The T entry is either zero or has a negative sign. $I_1$and $I_2$are called aerial mode currents.

$$\begin{pmatrix} I_0 \\ I_1 \\ I_2 \end{pmatrix} = \begin{pmatrix} + & + & + \\ + & T & - \\ + & + & - \end{pmatrix} \times \begin{pmatrix} I_a \\ I_b \\ I_c \end{pmatrix} \qquad \text{Equation (7)}$$

The modal transformation changes the system equations to the form given in Equation (8). As shown in the above equation, the mutual coupling is removed, and each phase is analyzed separately, which can be further expressed as

$$\begin{pmatrix} I_0 \\ I_1 \\ I_2 \end{pmatrix} = \begin{pmatrix} a_{11} & 0 & 0 \\ 0 & a_{22} & 0 \\ 0 & 0 & a_{33} \end{pmatrix} \times \begin{pmatrix} V_0 \\ V_1 \\ V_2 \end{pmatrix} \qquad \text{Equation (8)}$$

2.3 Study of the features available in the three-phase currents

The first step in the proposed algorithm is fault detection. This means that the local relay must be able to tell whether the high frequency components are due to a fault or not. It should be noted that in the following discussion, it is assumed that the three-phase currents are free from noise. The effect of noise will be studied in chapter 4. Thus, the pre-fault (or pre-event) data is assumed to be noise-free with no high frequency components. Figure 8 clearly shows that any event can be detected once the detail coefficients change to non-zero values. This change of coefficients would immediately signal that a disturbance occurred. What remains is to identify whether this disturbance is a fault or not. Since the problem at hand applies to the transmission network, one needs to understand what disturbances are observed at the transmission level. The disturbances that are seen at the transmission level are:

- Load switching (including ramping-up or down the load),
- lightning strikes,
- faults,
- line energization, and
- line dropping.

Notably, these disturbance events should only be detected within the distance relay reach, which is 220%. If one of those disturbance events, even faults, occur outside that reach, then the event can be ignored as the relay is not to respond to any of them, even if they cause heavy loading. In section 2.4, we show how to determine that a disturbance event is within the reach of a distance relay. After that, each of the disturbance events is studied to identify the features that are unique to faults.

2.4 Modified relay reach

A typical relay reach is shown in Figure 40. It is typical for the relay at bus A to provide back-up protection for two circuit breakers downstream in case of circuit breaker failure [72]. Thus, the relay at bus A of line A-B is supposed to provide backup protection for:

- the two circuit breakers at buses B of the lines BC and BD and
- the circuit breakers at the beginning of the lines emanating from both buses C and D.

For the distance protection to provide a secure back-up protection to the circuit breakers of the lines emanating from buses B and C, a conservative 20% protection of those lines is included in the third protection zone [72]. To determine whether a disturbance event is within the relay reach or not, various disturbance events were created just inside and just outside the relay reach. These events were then compared to reach a conclusion on how to determine whether the disturbance event is inside or outside the relay reach. As an example, refer to Figure 11, which provides the relay reach of the relay at bus 16 of line 16–42 of a certain benchmark network. Two three-phase to ground faults have been created. The first one is just within the relay reach of

the relay bus 16 at point Ω (219% of line length) and the other one is just outside that relay reach at point ∑ (221% of the line length). Phase A currents of both cases are provided in Figure 12 and a zoomed in version is shown in Figure 13, where both cases are nearly identical to each other since both faults are separated by a small line section (1 mile in this case). It is apparent from this figure that there is no way to identify which fault is outside the relay reach. This is because the high frequency content of the signal changes continuously as the event moves continuously along the line as is evident from the equations in section 2.2. This will be shown in more detail in section 2.6.

For this reason, the relay reach has to be changed such that a clear distinction can be made between the disturbances that are within the relay reach and the ones that are outside the relay reach. Increasing the relay reach is not an option as this will exacerbate the problem of zone 3 misoperation as it originates from a large relay reach. Thus, the only option is to decrease the relay reach. Decreasing the relay reach has to be done in such a way that the relay can still provide back-up to most of the area originally covered. In this research, we found that the best option is to decrease the relay reach to 200% of the line length. In this manner, we still protect most of area that was covered originally by the 220% reach of the relay but we, in effect, disable the second layer of backup to the circuit breakers two buses downstream of the relay. This can be understood by referring to Figure 11. If the relay reach at bus 16 is limited to 200% of line length, then the red 20% of line 46–81 will no longer be protected and the circuit breaker at bus 46 of line 46-81 will lose the second layer of backup provided by the relay at bus 16.

However, relay 46 of line 46–81 is still backed up by the relay at bus 42 of line 42–46. The modified relay reach is shown in Figure 14.

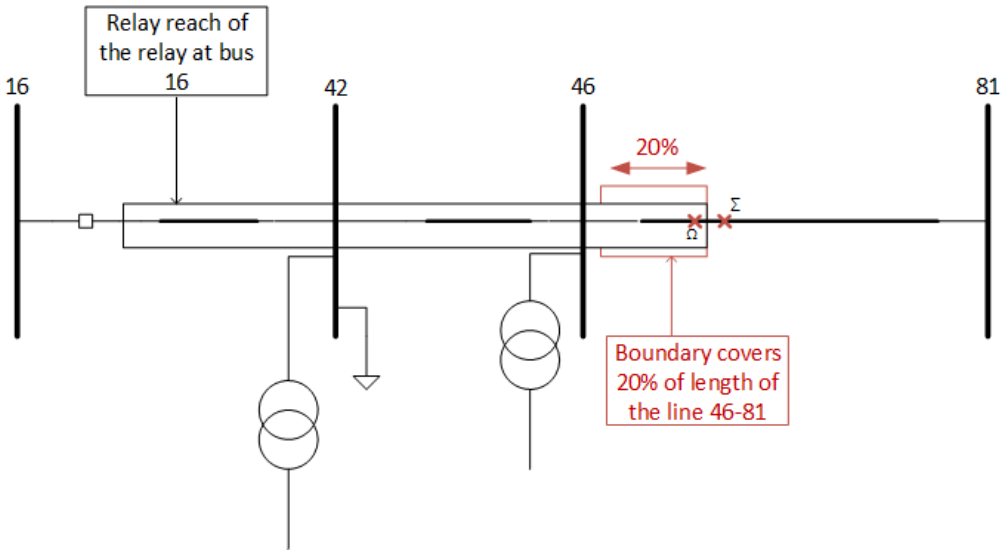

Figure 11. Original relay reach at bus 16 of line 16–42

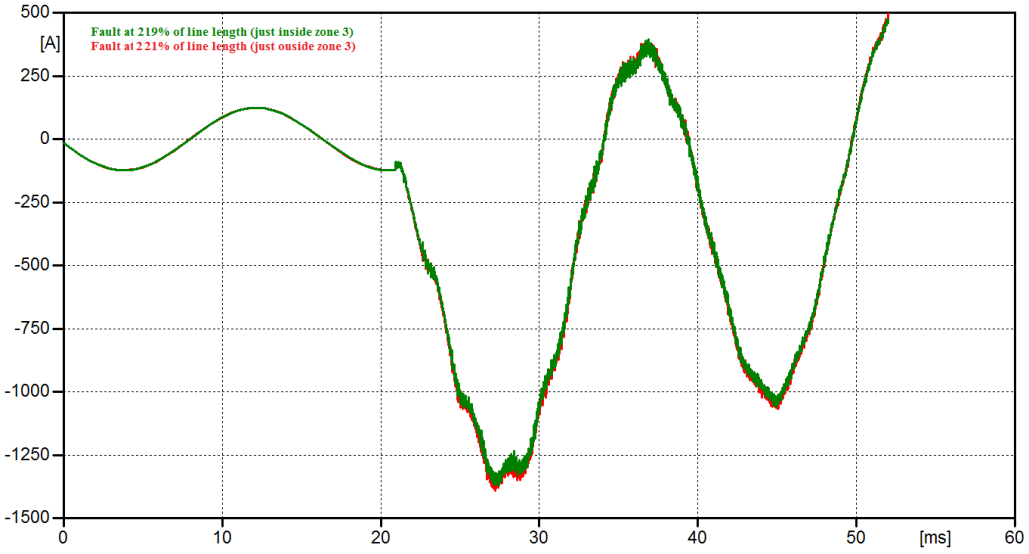

Figure 12. Current of phase A for the same fault case just inside zone 3 and just outside zone 3 for the original relay reach

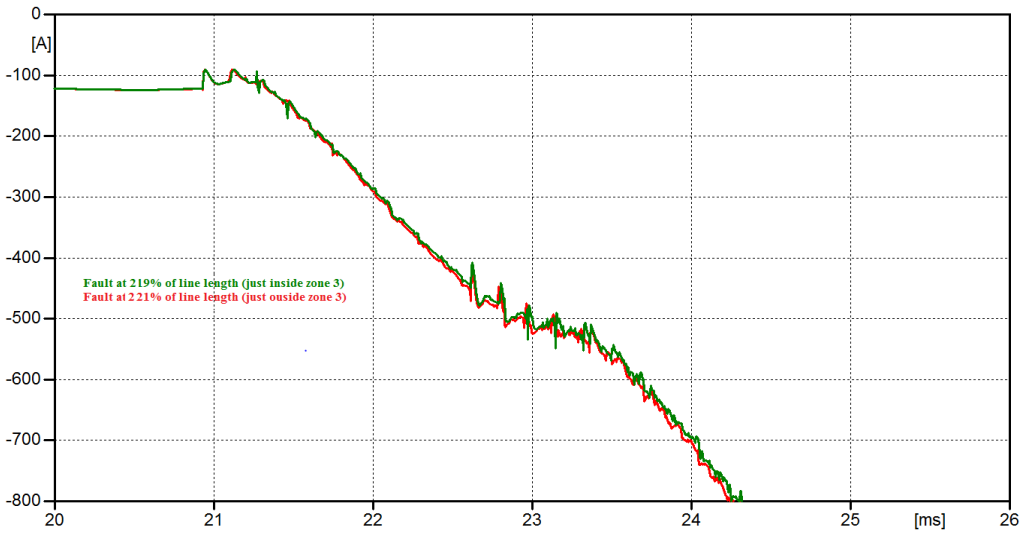

Figure 13. Zoomed in version of phase A current in Figure 12

The main reason for changing the relay reach to 200% of line length is to ensure that the features inside the relay reach (modified zone 3) and outside zone 3 will be different. When the relay reach is restricted in such a way, a physical discontinuity exists in the network which forces the high frequency components generated by the disturbances happening inside zone 3 to be different that the ones occurring outside zone 3. This can be understood by referring to section 2.2. In this section, it was explained that each disturbance event will have a unique boundary and initial conditions. In case two events are very close to each other on the same transmission line (such as in the case of the old 220% zone 3 relay reach), the solutions to the equations will be almost identical. But when the events are such that each one of them occurs on a different line, the disturbance equations will have different sets of initial and boundary conditions causing the solutions to be different. This can be clearly seen by referring to Figure 15 and the zoomed version in Figure 16 in which two faults have been created. The first one

is just within the newly created 200% relay reach and the other one is created just outside that new reach. The inside fault has been created on line 42–46 one meter away from bus 46. The fault outside has been created on line 46–81 one meter away from bus 46. As evident from the discussion in 2.2.1, the existence of the bus as a physical boundary makes both faults look different.

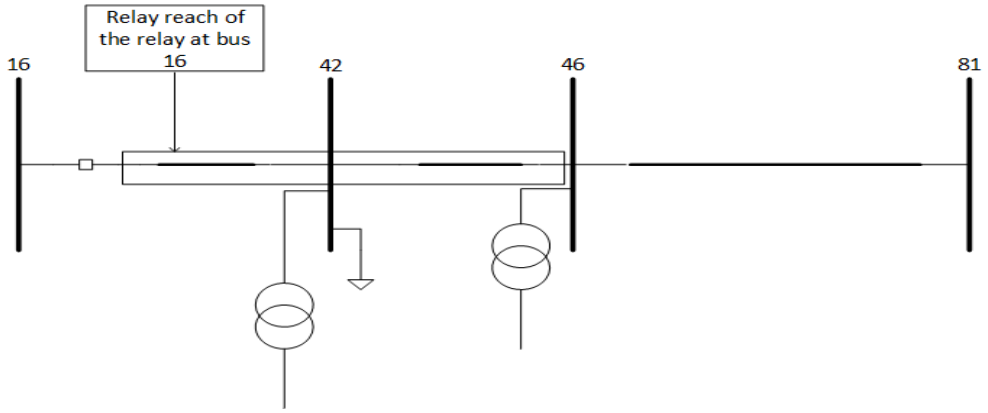

Figure 14. Modified relay reach of the relay at bus 16

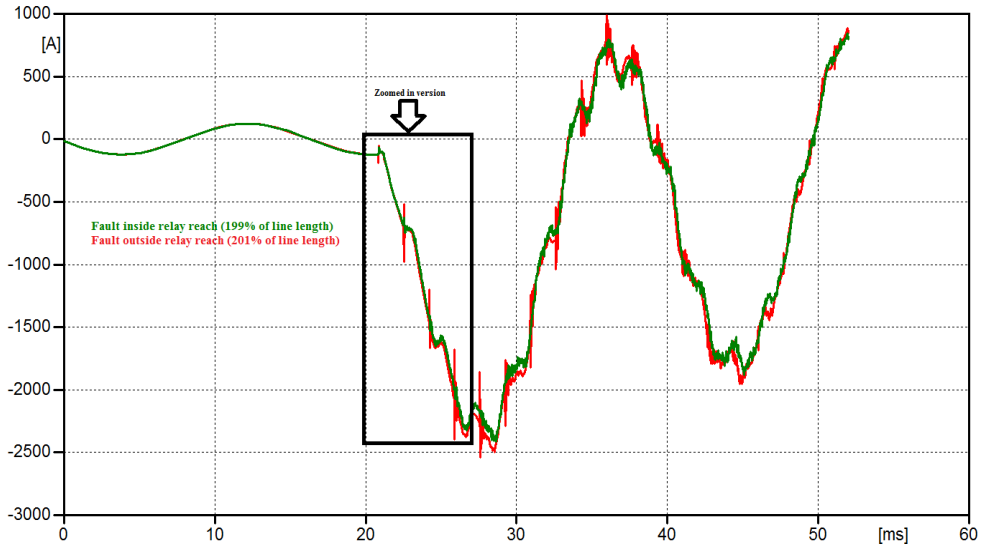

Figure 15. Current of phase A for the same fault case just inside zone 3 and just outside zone 3 for modified relay reach of relay 16 in Figure 14

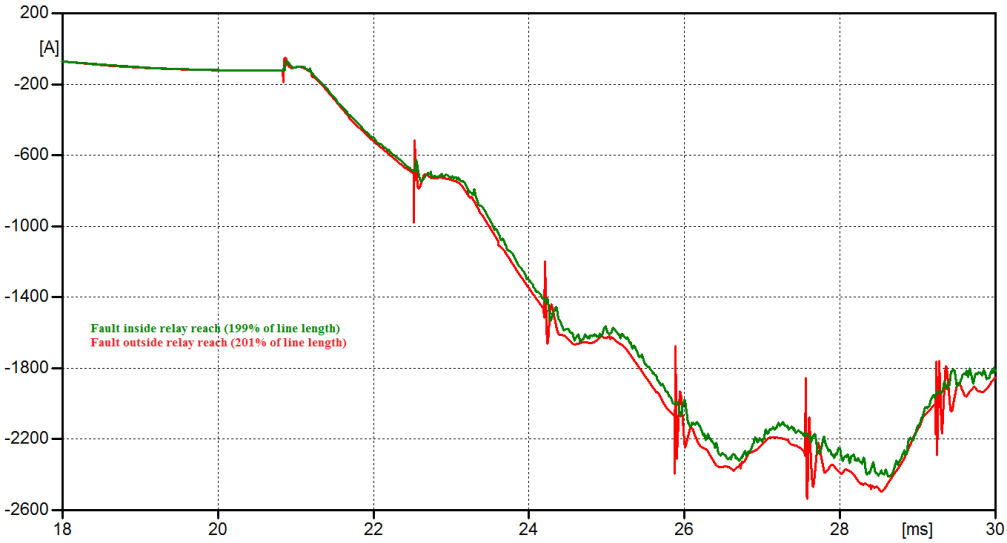

Figure 16. Zoomed in version of phase A current at Figure 15

It is self-evident that the logic given in this section applies to all tower configurations and all transmission lines in the network. In other words, the existence of a physical bus as a barrier defining the relay reach should be sufficient as a measure to

distinguish the events that are within the relay reach and the ones that are outside the relay reach.

2.5 Analysis of features available in the disturbance events

In this section, different disturbance events will be studied, and the features unique to each one of them will be analyzed. It will be assumed that the relay reach is only 200% of the line length. Thus, a fault detection module will be proposed in chapter 3.1.

2.5.1 Features in lightning

To know for sure that a fault has occurred using high frequency oscillations, other types of disturbance events must be ruled out. One of the most frequent disturbances in power systems is lightning. Lightning can evolve to a fault or not. For this reason, it is important to identify lightning and detect whether it has evolved to a fault. In this section, we will only explain how a lightning strike can be detected, saving the detection of lightning fault discussion for section 3.1.3.

Figure 17 shows a 10 kA lightning strike on line 16–42 of Figure 11 as seen from relay 16, and the phase current attains very high values. This can be seen at the DWT decomposition in Figure 19. It should be noted that a 10 kA lightning strike is very low compared to a recent lightning survey in which the least powerful lightning strike reported had values of no less than 20 kA [73]. Figure 18 shows the phase current of a 5 kA lightning strike on line 46–81 of Figure 11 as seen by relay 16 of line 16–42. As shown in Figure 18, the phase current still attains extremely high values, and this will be reflected in the DWT coefficients. Thus, the current in Figure 18 as seen from relay 16 of line 16–42 attains very high values even though the total distance between relay 16 to

the point of the lightning strike on line 46–81 is around 280 km. This indicates that the initial traveling wave arrives at the relay location at almost full strength. In all disturbance studies that were performed, it was found that if any level 3 detail coefficient reaches 500, then a lightning strike can be declared. In most cases this criterion works unless the lightning strike has a magnitude of 5000 amps or less. Thus, a threshold of 500 for level 1 detail coefficients is satisfactory for declaring lightning.

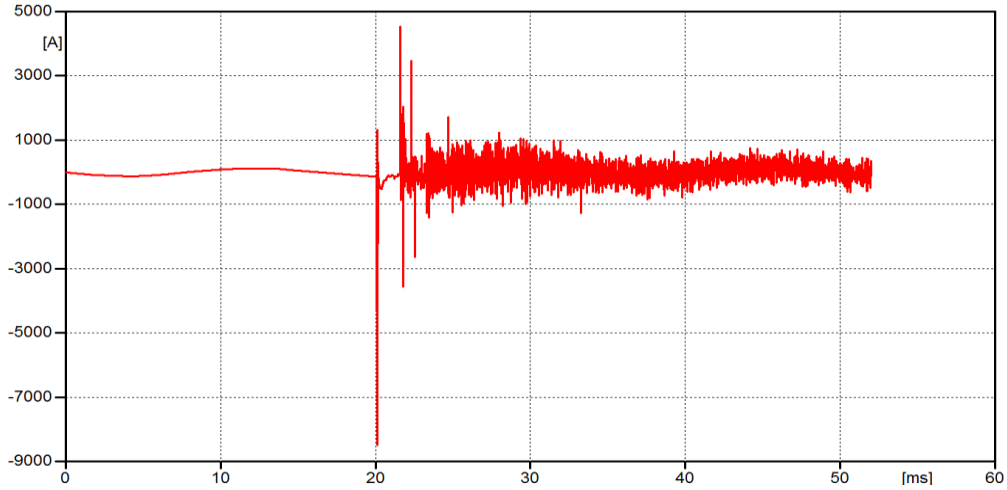

Figure 17. Phase A current of lightning strike at a 10 kA amplitude

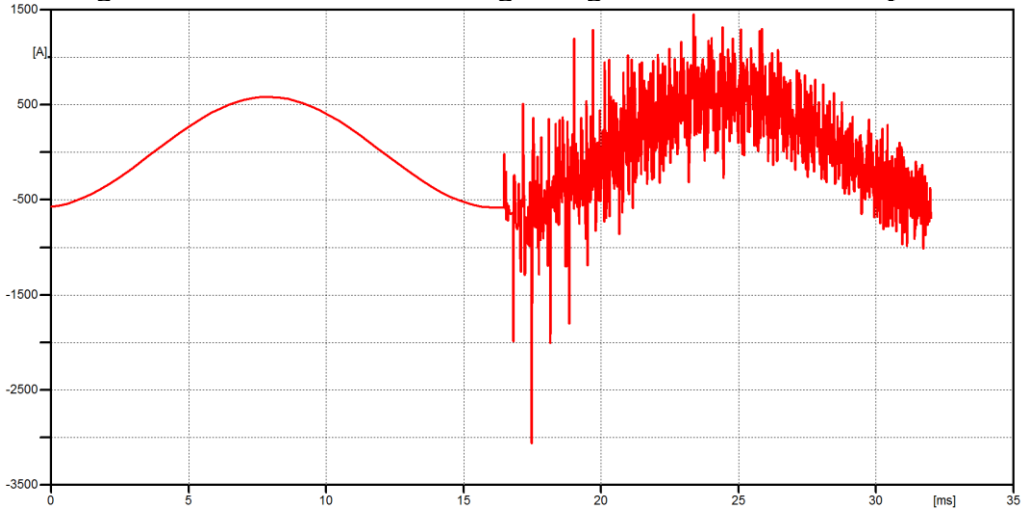

Figure 18. Phase A current of lightning strike at a 5 kA amplitude on linse 42-46 seen by relay 16 of line 16-42

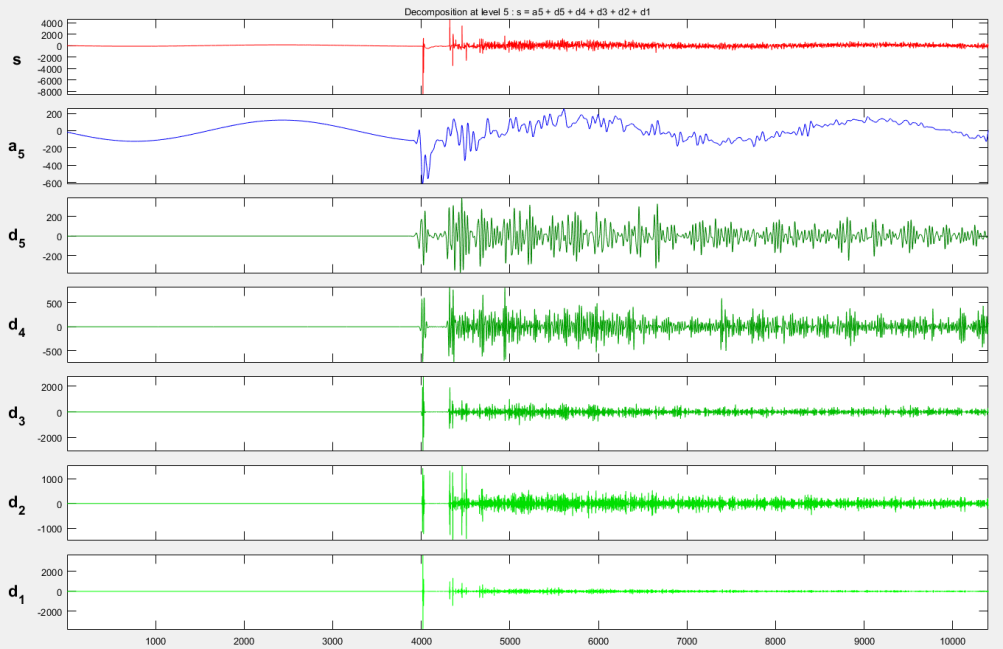

Figure 19. DWT of phase A current at Figure 17

2.5.2 Features in load switching

Another disturbance event that can be confused with faults is load switching. This includes: ramping up loads, ramping down loads, sudden load energization and sudden load rejection.

For this purpose, we studied how the disturbance data would look like if the load closest to the relay is suddenly switched ON or OFF. The worst load switching event was found to be switching on the load at the bus closest to the relay, irrespective of the system under study or the line under study. For example, the worst-case high frequency oscillatory components detected at bus 16 of line 16–42 of Figure 11 always corresponded to the load switching at bus 42. Figure 20 shows the DWT decomposition of phase A current observed at relay 16 of line 16-42 due to switching the load at bus 42.

The DWT decomposition of the phase A current observed at relay 16 of the line 16-42 due to switching the load at bus 46 is given in Figure 21. As can be seen from Figure 21, the detail coefficients are very small in comparison to the detail coefficients of Figure 20. In other words, switching ON load at buses beyond bus 42 causes very little, if any, transient oscillations and when a noise rejection module exists, these very low amplitude transient components are highly likely to get rejected by the noise rejection filter as will be explained in chapter 4.

Moreover, the DWT coefficients of load switching are very small compared to faults and lightning strikes. The detail coefficients also lie in a small band during the first cycle. This feature was used to detect load switching or rejection.

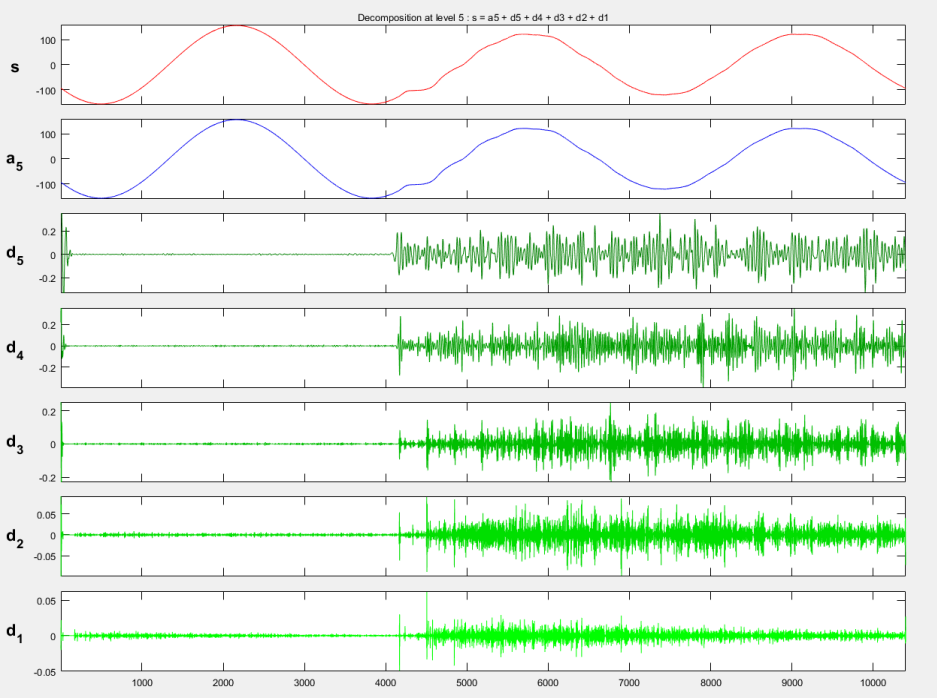

Figure 20. Phase A current of relay 16 of line 16–42 due to switching ON load at bus 42 of Figure 12

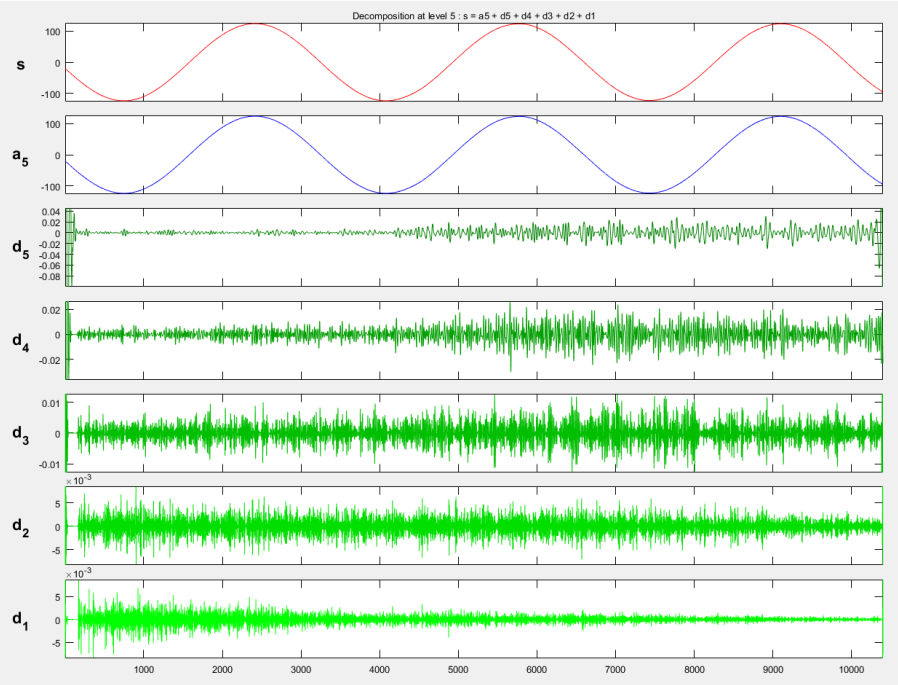

Figure 21. Phase A current of relay 16 of line 16–46 due to switching ON load at bus 46 of Figure 12

It is evident that since switching ON load causes the most severe transients, ramping the loads up or down will have features that are less than the ones given in Figure 20 and Figure 21. This has been also verified by simulations. Regarding Figure 11, any load switching other than the load at bus 42 or 16 will not cause any high frequency components to appear at the currents at either end of line 42–16.

2.5.3 Features in faults and line switching

Aside from lightning strikes and load switching that can easily be recognized using the magnitude of DWT coefficients, the magnitude criterion was not sufficient to distinguish faults and line switching operations. For faults, this is self-evident as the fault resistance affects the high frequency content of the data as will be seen in [43]. Nevertheless, it was found that the magnitude of the oscillations due to the load switching lies below the ones for lightning and the ones for faults irrespective of the

fault resistance. Figure 22 shows the high frequency content of a fault case on line for a fault resistance of 100 Ω. It can be seen from the figure that the magnitude of the oscillations is larger than the ones in Figure 20 and Figure 21 even for a 100-Ω fault. Various faults and load switching operations have been created, and the relationship between fault-generated high frequency components and load switching high-frequency components was determined.

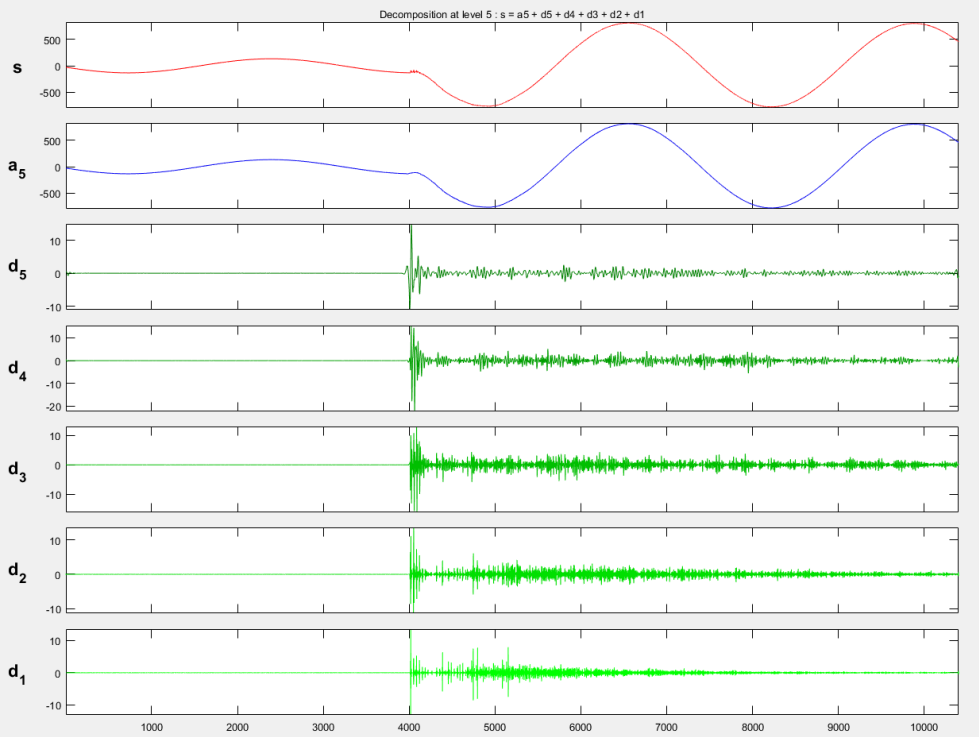

Figure 22. DWT for Phase A current for a 100-Ω fault

In summary, lightning strikes can be easily recognized using the magnitudes of the DWT coefficients as these attain extremely high values. Load switching can also be recognized using DWT coefficient magnitudes as these attain very low values. Line switching and faults cannot be easily differentiated from each other due to the overlap

that could occur between the magnitudes of the DWT coefficients for each of them. For this reason, suitable pattern recognition approaches will be evaluated to identify the best approach for classification.

2.6 Sensitivity analysis of disturbance events

In the next few sections, a study on how the high-frequency content changes with different loading conditions, contingency conditions and other parameters will be presented. This is important as we intend to design a pattern recognition approach. This study will help us design appropriate training, testing and validation scenarios.

2.6.1 Changes in features as the system load changes

One of the main issues that could be critical to the use of high-frequency components is the changes that could occur due to changing load throughout the day in the system. To investigate what could happen to the high frequency components due to changing load levels, the loads in the system shown in Figure 11 has been scaled to 50%, 90%, 110% and 120%. As can be seen in Figure 23 and Figure 24, the high-frequency oscillating components are more or less constant for load changes from 50% to 120% of the system load. The apparent deviations between fault current is because of changing load levels, but not due to changing high frequency components. Another example is given in Figure 25.

The results in this section should not come as a surprise as they are a direct consequence of the compensation theorem, which is another manifestation of the superposition principle [74]. The compensation theorem states that the response of the network to a disturbance is obtained by opening all current sources, shorting all voltage sources and representing the disturbance as a current source. This immediately shows

that the generation and load levels do not have a major effect on the high frequency oscillations as the variables that are left unchanged in the compensation theorem are the transmission line parameters while the load is electrically far away from the transmission system.

This is another strong point in using the high frequency components for classification. One can study the base case without worrying so much about changing load levels. This is to be contrasted with the process that the protection engineer must undergo to set up a distance relay where a power flow study must be done to set up load encroachment. In other words, the training, testing and validation scenarios need only to be designed under one load level and the same scenarios would be usable for other load levels, as long as the network does not affect the high frequency oscillations under various contingency conditions.

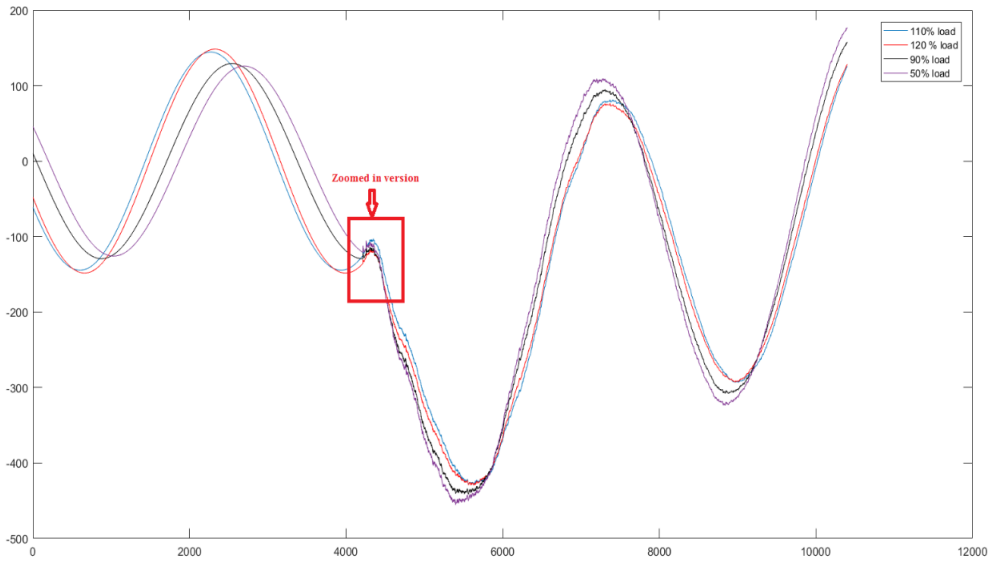

Figure 23. Pre-fault and post-fault phase A fault current on a certain line at various load levels

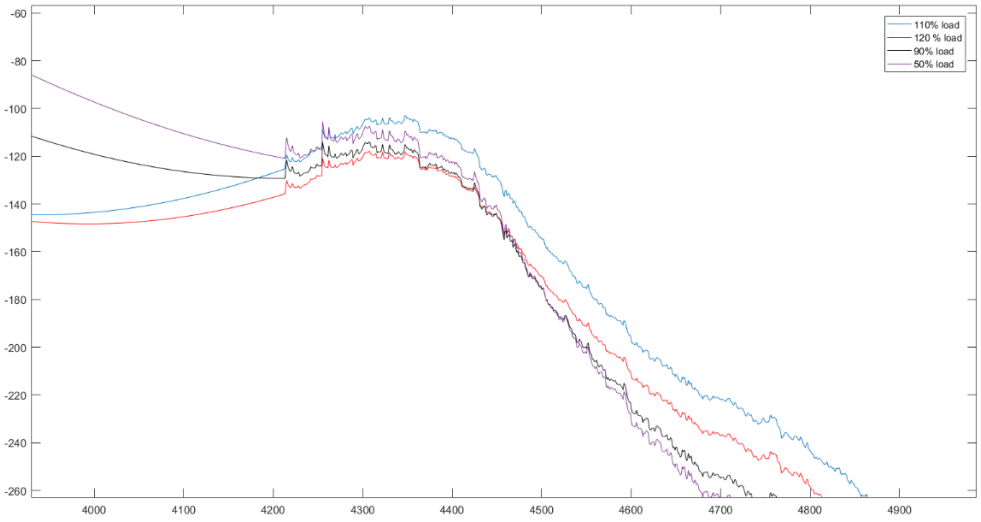

Figure 24. Zoomed in version of the current in Figure 23

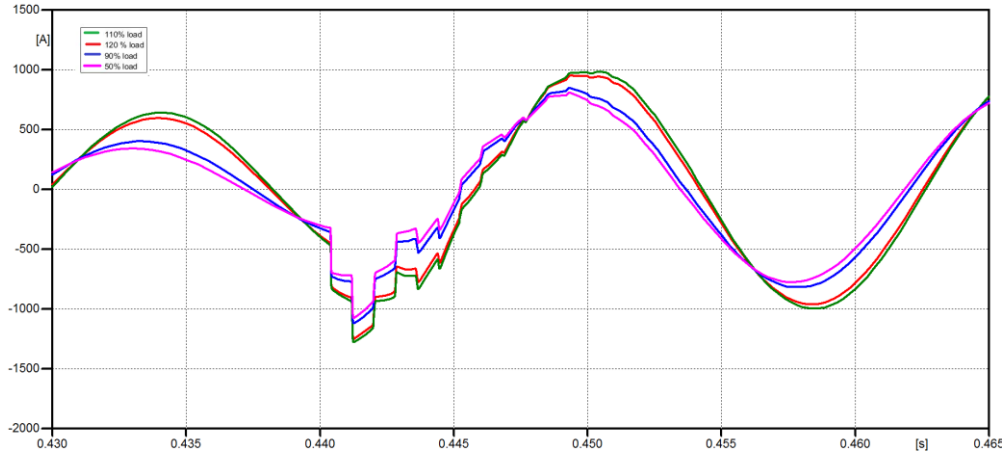

Figure 25. Pre-fault and post-fault phase A fault current on another line at various load levels

2.6.2 Changes in features as the system topology changes

Another issue that arises due to the use of high frequency components is whether the high frequency content of the disturbance data will change due to topology changes and system loading. The effects of system loading have been discussed in section 2.6.1.

To see what happens when the topology of the system changes, various fault cases have been created with N-1 and N-2 contingency conditions. Figure 26 shows phase A current of a three-phase to ground fault at mid-point of a certain line under different N-1 contingency conditions. As can be seen from the figure, contingency conditions have little or no effect on the features in the high-frequency oscillating components. Thus, by using those high frequency oscillating components, topology conditions can be ignored if the fault is internal. The same observation applies to other disturbance data as the high-frequency components have a strong dependence on the line being protected but not so much for N-1 contingency conditions.

However, the situation is a bit different under N-2 contingency conditions. Figure 28 and Figure 29 show phase A current of a three-phase fault on midpoint of another line under worst-case N-2 contingency conditions. Figure 28 shows that even though one can see that the mismatch is a bit worse than the case of N-1 contingency conditions, the mismatch can be accounted for from a practical point of view, if one allows for a frequency band with certain variations in its features. This is one of the main advantages of using high frequency components. Even though contingency conditions that are close to the relay causes the most severe topology changes for the line under study, they have little effect on the disturbance data to a great extent.

In other words, high frequency oscillations are a function of network topology in the large without much attention to N-1 and N-2 contingency conditions occurring around the relay. It is natural to ask whether the same observation applies to all transmission systems. The high frequency oscillations depend on the initial and

boundary conditions as explained before. The boundary conditions are expressed as the frequency response of the network at the line terminals [75]. If the frequency response does not change due to contingency conditions, then the high-frequency disturbance oscillations will not change due to those contingency conditions. Based on our experience with large networks, this is indeed the case. In fact, we have conducted a frequency scan of the ERCOT network contingency conditions up to N-10 in [76]. More than 320 scans of the ERCOT network contingency conditions up to N-10 have been performed, and they are attached in Figure 30. As can be seen from the figure, the frequency response of the ERCOT network is almost constant over a wide range of frequencies under highly improbable contingency conditions. This is also expected to be the case for large networks that are well connected.

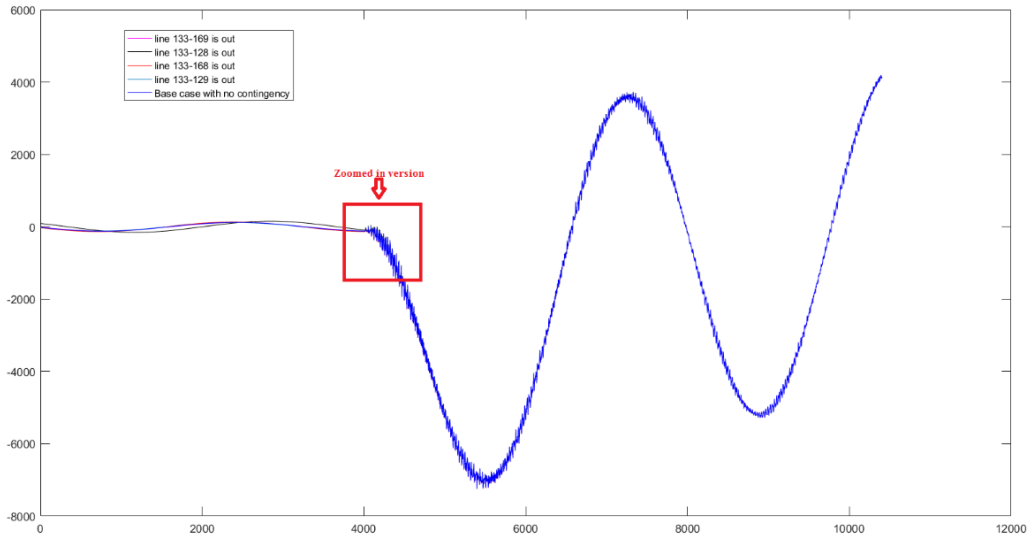

Figure 26. Phase A current at relay 137 of line 133-137 of IEEE 300 bus system for a line fault due to worst-case N-1 contingency conditions

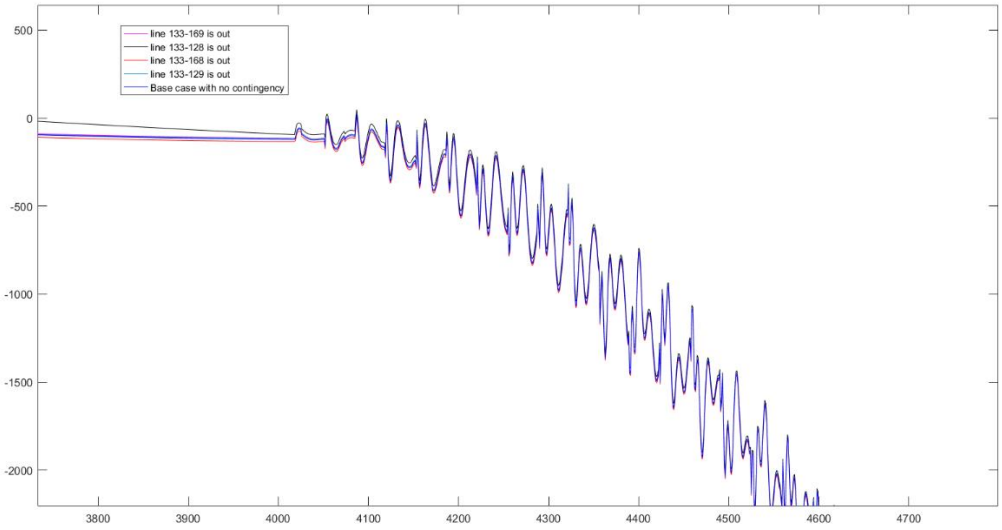

Figure 27. Zoomed in version of the current in Figure 26

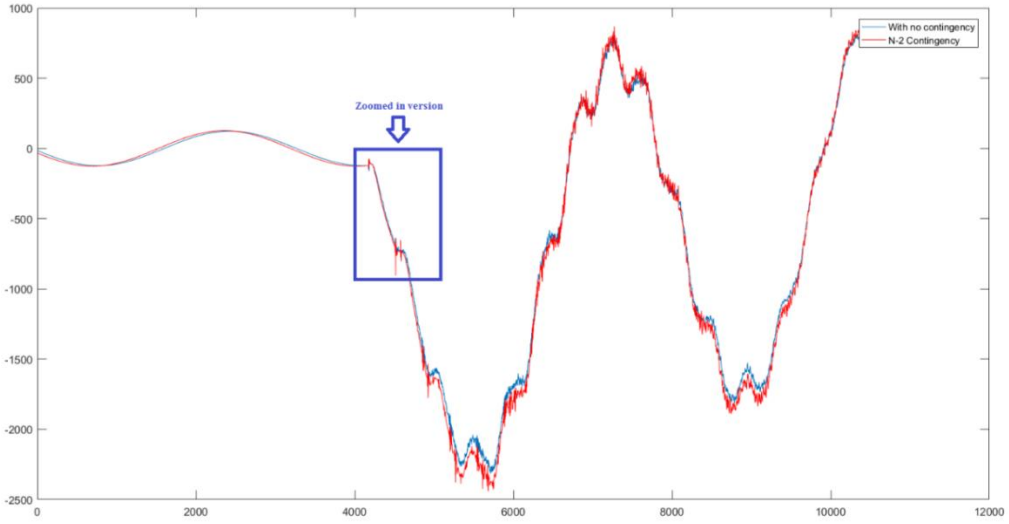

Figure 28. Phase A current of a fault case on line 133-137 of the IEEE 300 bus system with no contingency and N-2 contingency conditions

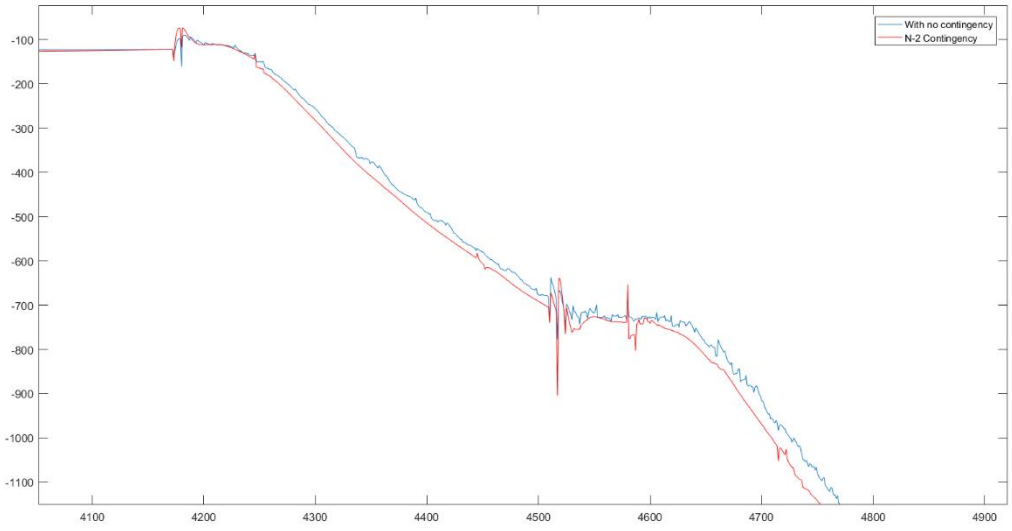

Figure 29. Zoomed in version of the current in Figure 28

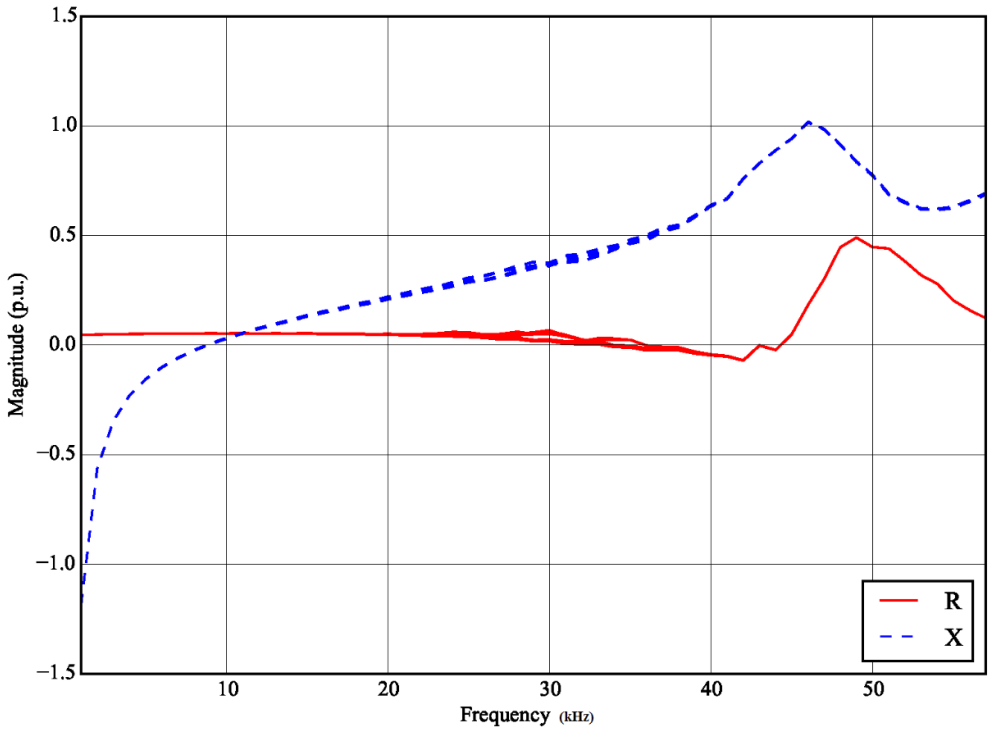

Figure 30. Frequency response of the ERCOT network

2.6.3 Changes of features as the tower configuration changes

Having shown that the high frequency oscillating components are more or less that same under different load conditions and topology changes, what remains is to study how these features change with regard to the tower configurations. For this purpose, one transmission line of a certain test case has been replaced by six tower configurations in Figure 31.

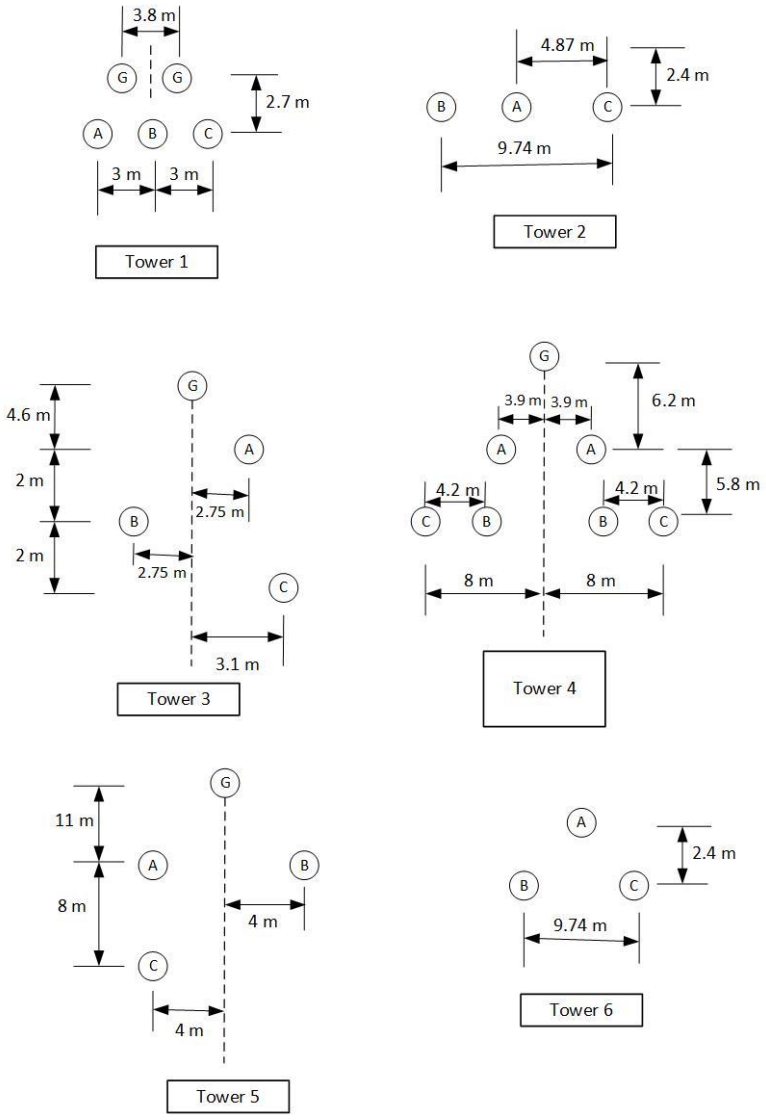

Figure 31. Tower Configurations

After the six tower configurations were created, three fault cases with different fault resistances were created: 0 Ohms, 20 Ohms and 100 Ohms. The results of these faults are shown in Figure 32, Figure 33, Figure 34, Figure 35, Figure 36, and Figure 37. As shown in these figures, the high frequency oscillating components are highly dependent on the tower configuration. In other words, for the same fault resistance given in Figure 32, the oscillatory components vary greatly according to the tower configuration.

The same observation applies to other disturbance events such as line switching and lighting strikes.

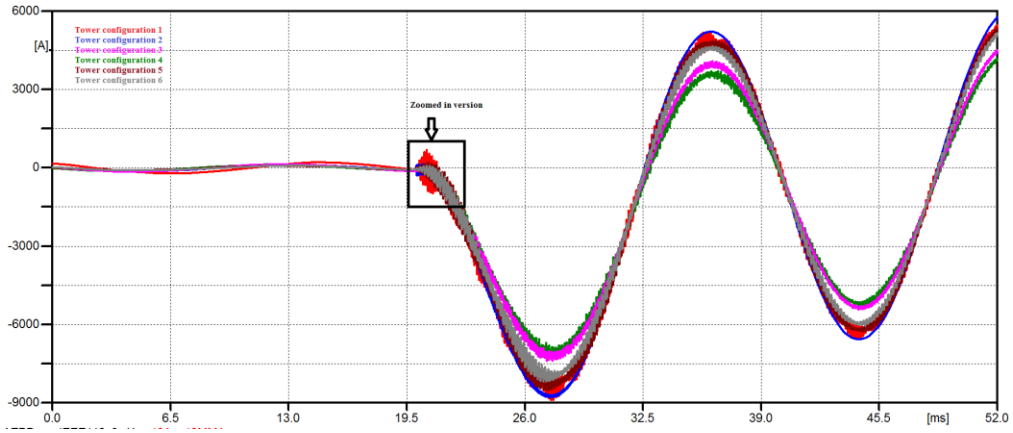

Figure 32. Zero fault resistance for different tower configurations

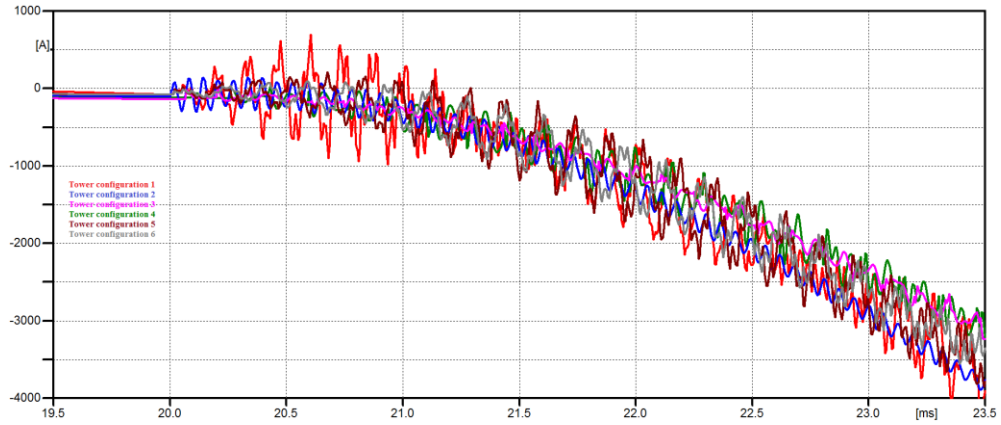

Figure 33. Zoomed in version of the currents in Figure 32

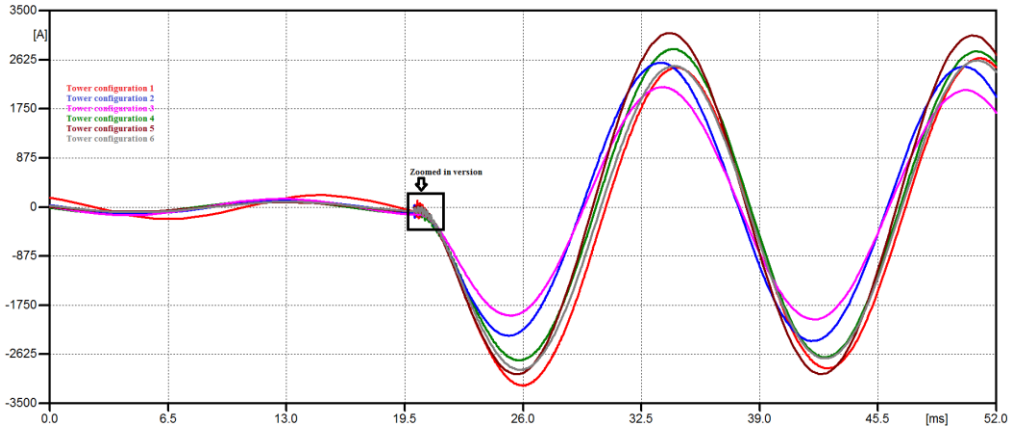

Figure 34. 20-Ohm fault resistance for different tower configurations

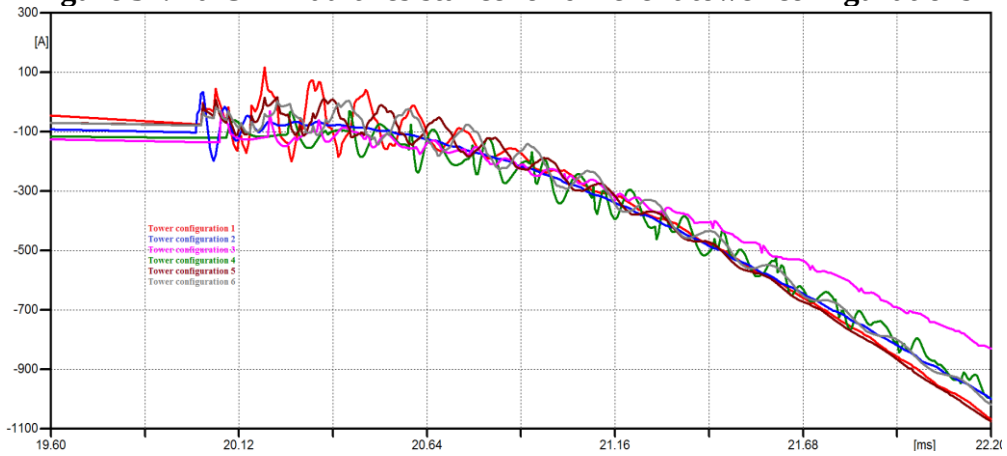

Figure 35. Zoomed in version of the currents in Figure 34

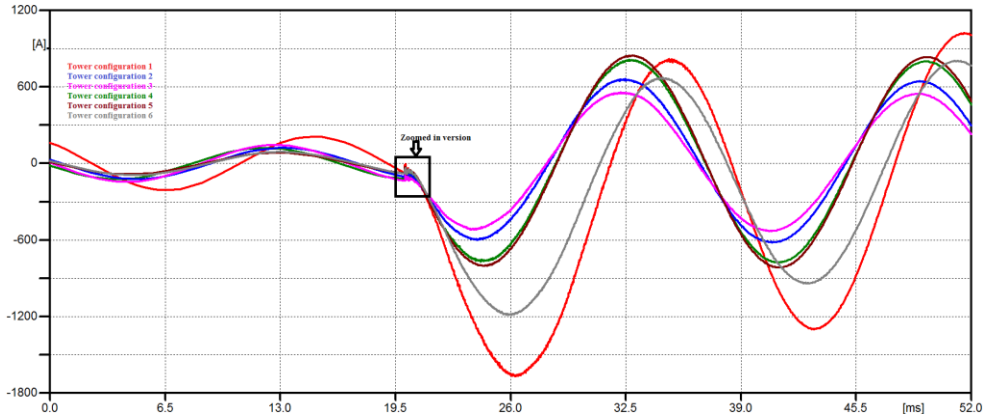

Figure 36. 100-Ohm fault resistance for different tower configurations

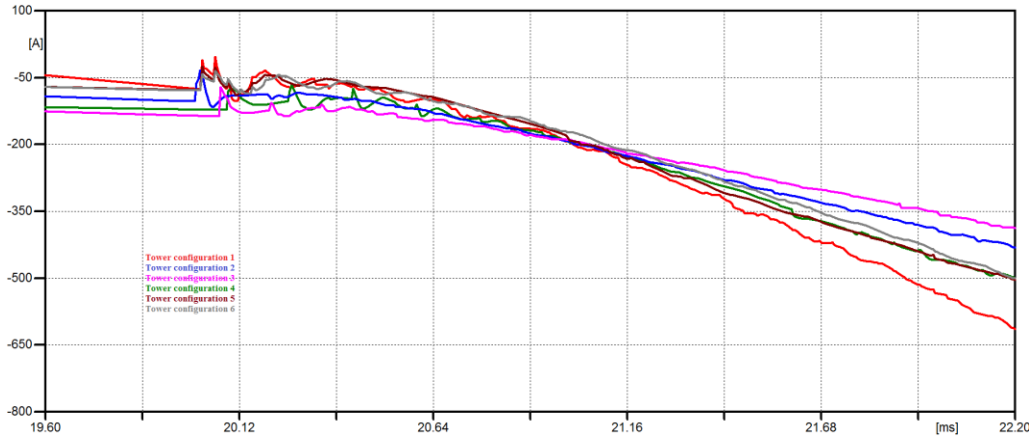

Figure 37. Zoomed in version of the currents in Figure 36

2.7 Considerations for acceptable solution methodology

In a typically cascading scenario that leads to distance relay misoperation, the currents seen at the local relay continuously increase as can be seen in Figure 38. A typical impedance locus during a wide-area cascading event is also shown in Figure 39. As can be seen from Figure 39, the impedance locus marches on steadily until it enters

zone 3. It should be noted that relay misoperation occurs because Point4 which corresponds to the final point of the impedance locus eventually settles in zone 3 and times out regardless of the locus that is outside zone 3. Based on the literature survey in chapter 1, it is impossible to use the steady state quantities observed locally by the relay to increase the security of the relay and prevent this type of misoperation.

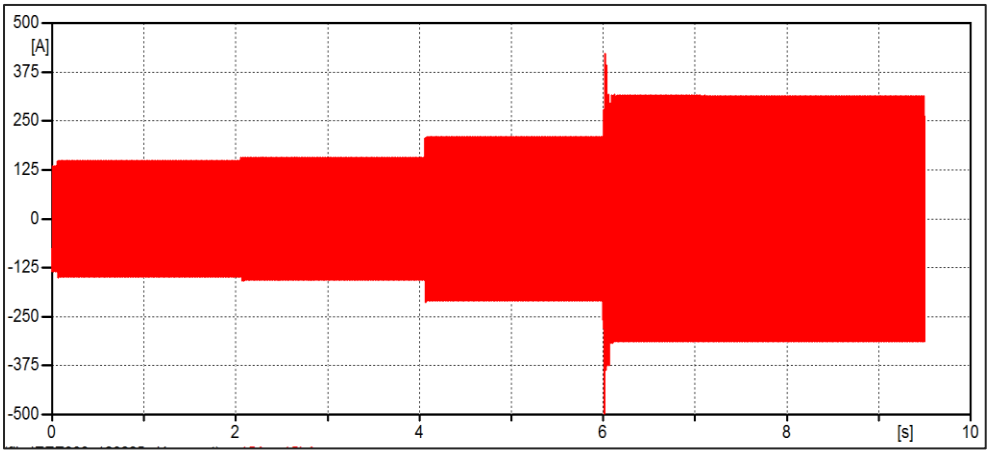

Figure 38. Typical current seen at a relay during a cascading event leading to relay misoperation.

It was determined, that the best solution approach to prevent misoperation is to use the high-frequency oscillatory components generated by disturbances to recognize zone 3 faults from line overloading, or any other event that could lead the impedance to enter the third zone when no fault exists on the system.

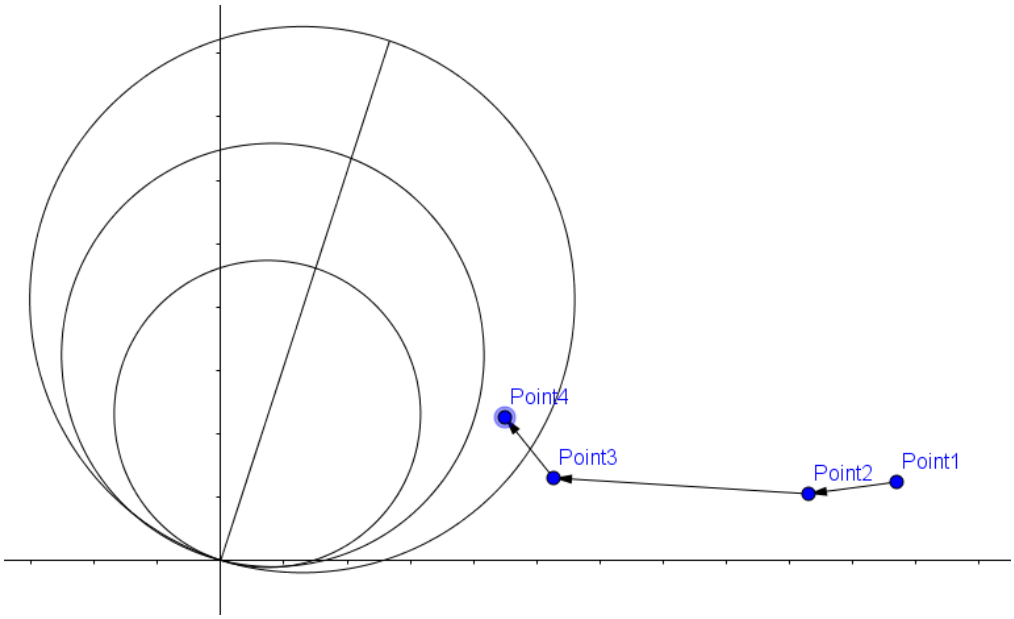

Figure 39. Distance locus during cascading event

The main argument is that since we are dealing exclusively with transmission systems, very few disturbance events cause high frequency oscillation components imposed on the fundamental current or voltage waveforms. This is to be contrasted against distribution systems where dozens of events occur daily and contaminate the fundamental waveform. In other words, transmission systems are operated in a more controllable manner and events in distribution systems that give rise to high frequencies are rarely, if ever, propagated to the transmission systems. The reason for this is that distribution systems are separated from bulk transmission systems by geographically distributed sub-transmission and sub-distribution networks which, due to their lengths, act as low-pass filters to the bulk transmission network. In any case, it will be shown in chapter 4 that a very accurate disturbance classifier can be developed. This classifier can

be used in conjunction with the classifiers given in chapter 3 to indicate that the disturbance events observed locally by the relay is outside its reach.

The problem can be solved easily if one assumes that impedance enters zone 3 either because of zone 3 faults or heavy loading resulting from wide-area cascading events. However, the problem is more complex than that. The complexity arises from the limited operational experience we have with respect to zone 3 misoperation. In other words, ISO operation engineers do not know for sure whether heavy loading or zone 3 faults alone cause zone 3 misoperation. It is known that power swing can also cause zone 3 misoperation, but it does not seem that these are the only three reasons for zone 3 misoperation. Consider the following situation: The network is under heavy loading and suddenly a transmission line is dropped due to circuit breaker failure. The dropping of this line yields the same effect as faulting the line then opening it. The opening of this line causes the power flow to be redistributed across the network which results in one of the lines carrying a heavy load. This heavy load causes the impedance to enter zone 3, thereby causing misoperation. Another example is that of lightning striking a line. This strike causes flashover, which prompts the associated relay to trip the line to clear the fault. Due to this, one of the lines in the system carries heavy load which causes the impedance to enter zone 3, which also causes the distance relay to misoperate. As a third example, consider a system that is undergoing a swing oscillation after tripping a line due to a fault. It is well documented in [77] that the impedance can enter zone 3 and cause misoperation.

The point in the above examples is that heavy loading and relay misoperation can occur due to many reasons even though they have not been observed in daily operations. In other words, one can design several practical system-wide scenarios such that the distance relay misoperates eventually even though those scenarios have not been observed in operation. If one plans on detecting every event and scenario that occurs and causes misoperation, an enormous amount of combinations need to be studied. Even when studying these combinations, a conclusive answer may not be reached because power systems are always evolving.

On the other hand, if one plans to use the high frequency components observed at the local relay to distinguish zone 3 faults from heavy loading conditions, then the disturbances that cause heavy loading must also studied. Heavy loading can occur due to:

1. Sudden load increase or ramping up a load,
2. lightning that knocks lines out of service that causes line loading to change,
3. line dropping that causes line loading to increase and enter zone 3, and
4. any other unknown reason

Even though points 2 and 3 of the above list results in the same outcome, the transient behavior of both cases are different. As shown before in section 2.5.1, a lightning strike causes the current to attain extreme values, which is not the case in line dropping.

As matter of fact, prevention of distance protection misoperation is a formidable task because of the reasons that can lead to this misoperation. For example, stable and

unstable power swings can cause the distance relay to see a fault when no fault exists in the system. Thus, the problem is totally unmanageable if the origin of heavy loading is investigated over a large network consisting of thousands of buses or even few hundred buses. However, if one realizes that the distance relay only needs to react to faults that are within the normal protection reach which is 220% of the line length, then the problem can be confined to a certain area. Distance relays provide primary protection for one transmission line and backup protection to circuit breakers down the line. This is shown in below in Figure 40.

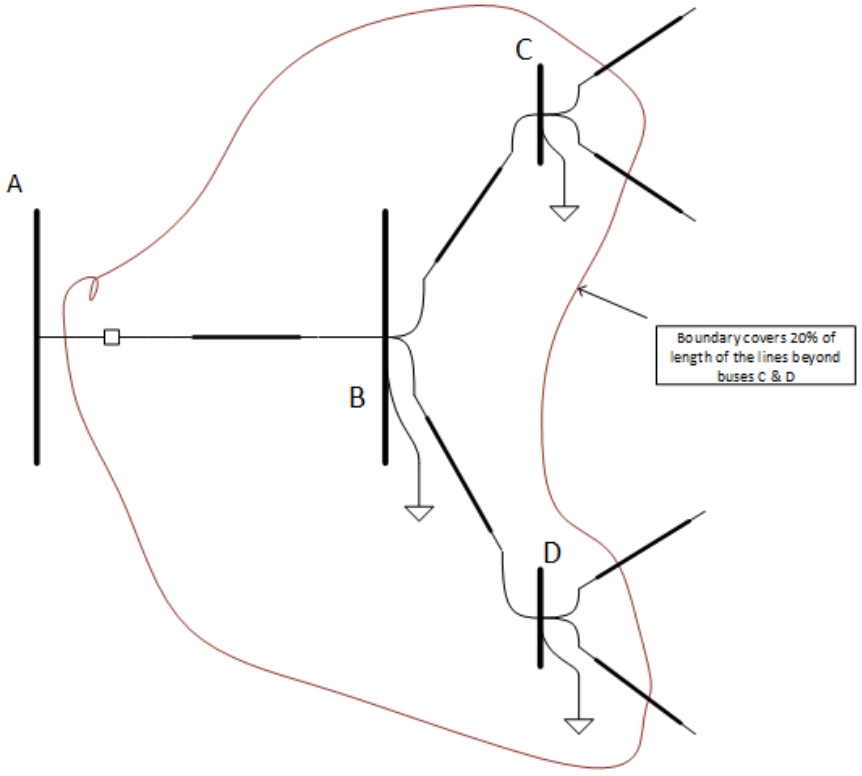

Figure 40. Distance protection reach of relay at Bus A

It should be noted that our field experience with distance protection misoperation is limited and our reasons for heavy loading are limited based on this lack of field experience. For these reasons, instead of trying to pinpoint the reasons for heavy loading, we focused on recognizing the faults that occur within zone 3 (or more generally within the reach of the relay) against all other events. In this manner, the solution will be general and does not depend on the reasons for heavy loading conditions that occur within or outside the relay reach. In this manner, a secure fault detection can be achieved without regard to non-fault conditions.

For this research, the solution is about asserting that a fault occurs within relay reach. Once the fault is asserted or unasserted, a logic will be invoked to trip or block the distance relay from operation. The use of high frequency components for asserting faults is thus advantageous because the high frequency components are very localized in nature; hence, events that are electrically far away from the relay will cause low-amplitude high-frequency transients [78] that are likely to be rejected by a denoising approach. Even if they pass through the denoising approach, they can still be identified as non-fault transients or faults that are outside the reach of the relay as will be explained in chapter 4.

The central point to remember is that the relay needs to respond to faults that are within its zone of protection, and it must be determined which faults are within the relay reach. The distance protection principle is not the only way to judge this because it may confuse heavy loading for faults.

Generally, faults anywhere in the network do not always cause high frequency transient oscillations imposed over the three-phase currents. In other words, non-zone 3 faults cannot always be detected locally using high-frequency current oscillations. However, a characteristic of relay misoperation due to heavy loading is the occurrence of a fault then clearing it which causes one transmission line to carry a substantially heavier load. Thus, programing logic to distinguish any heavy loading from any fault using local information available to the distance relay is an impossible task because:

1) The relatively high current level of heavy loading could correspond to any fault anywhere in the network, which means that we will not be able to use the steady state current to tell if this is a heavy loading condition or a fault in the network.

2) Faults anywhere in the network cannot always be detected by the local relays using the high frequency components because those components do not propagate very far away from the point of incipience.

It should also be kept in mind that the relay misoperates because it thinks that a fault is within its zone 3 when in fact it is a heavy load. Thus, by ensuring that all faults within the reach of the distance relays have been detected, we can rule out relay misoperation if we also make sure that those faults have been cleared. In other words, we do not care so much about the heavy loading being experienced by a transmission line as long as all faults that occurred within the reach of the relay have been cleared. However, if the line sags, the line must be tripped anyway. We are justified in doing this since the distance relay needs to react to faults within its zone of protection (zone 1, 2 and 3) only. If the impedance enters zone 3 yet no fault has been detected, then the relay should not

be operating at all. By detecting the fault as well as clearing the fault, we will be able to block the distance relay from operation. However, this should only be done for faults within the zone of protection of the distance relay.

Since we see heavy loading after clearing of the faults, as shown in Figure 38, it is mandatory to detect clearing of the fault locally to determine whether this heavy loading is due to a fault or a power flow shifting through the network. Clearly, this also makes the case for restricting the study area to the distance protection reach area only. By restricting the fault clearing detection area to the distance protection reach, the problem becomes more manageable. Thus, the elements of the solution methodology will be as follows:

1. A disturbance classification module that identifies all faults regardless of their location. We can also call this fault the detection module,
2. a classification module that determines whether the fault is within the relay protection reach, and
3. a fault-clearing detection module that is activated once faults are cleared within relay protection reach.

By detecting both the fault and its clearing, we can tell with confidence that a certain distance relay should not send a trip command even if the impedance falls into zone 3. The overall solution methodology is simplified in Figure 41.

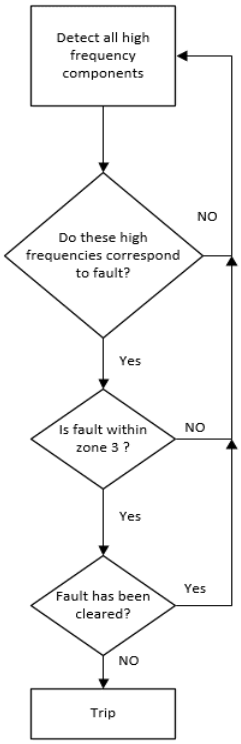

Figure 41. Simplifed solution methodology

2.8 Summary

As can be seen from the results in this chapter, the high frequency oscillations are highly dependent on the network configuration as a whole without much regard to the N-1 and N-2 contingency conditions occurring close to the line under study. As a matter of fact, as the network becomes larger, contingency conditions have a lesser effect on the high frequency oscillations observed by the relay as shown in Figure 30. Also, the high frequency oscillatory components are highly dependent on the tower configuration of the line under study. These two properties will enable us to design the algorithm without regard to the contingency conditions occurring throughout the network and without regard to the load level that changes over the day and over the year. Notably, we have already determined that the only way to distinguish zone 3 disturbance events versus non-zone zero disturbance events is shrinking zone 3 to a 200% reach. Thus, the solution methodology for fault detection must consist of two modules:

1. A module that determines whether the disturbance event is a fault
2. Based on the decision of the first module, another module will determine whether the fault is within or outside the modified relay reach.

It would not have been practically possible to develop both of these components if the features in the high frequency disturbance data changes considerably when the network topology or load level changes. Only if the high frequency components stay within a reasonable range, can these two components be created. Otherwise, the amount of data that is needed to train both pattern recognition modules would be massive and unpractical.

The fault detection module is presented section 3.1. Determining whether this fault is within relay reach is provided in section 3.2. In section 3.3, fault clearing detection is presented.

Since the purpose of this study is to increase relay security, it is important to apply the proposed method to the relays that misoperate and the ones that did not misoperate, which will be done in chapter 4. Since measurement error always exists in the field, a framework for error analysis will be provided in chapter 4.

3. THE PROPOSED METHOD*

The proposed solution method consists of three stages. Each of the stages is explained in this chapter.

3.1 Fault detection module

In this section, we explain all aspects of the fault detection module.

3.1.1 Pattern recognition approach for disturbance classification

The only disturbance which had features that were not obviously different from faults is line switching. For this purpose, several pattern recognition approaches were used to test the best approach for classification, not only between faults and line switching but also between all disturbance events. By including all disturbance events in the pattern classification approach, the classifier will be more general. As stated in chapter 2, the detail coefficients represent the high frequency content of the signal in a compressed form. By using various transformations, different versions of the detail coefficients can be defined. For example, one can apply the symmetrical components transform to the three-phase currents and then apply the DWT to those three-phase currents and then do a pattern recognition approach to see how it performs. The same can be done using Clarke components instead of the symmetrical components.

---

* Parts of this chapter were reprinted with permission from “A wavelet entropy approach for detecting lightning faults on transmission lines” by Ahmad Abdullah, 2016 IEEE/PES Transmission and Distribution Conference and Exposition (T&D), Pages 1–8, ©2016 IEEE, and from "Ultrafast Transmission Line Fault Detection Using a DWT-Based ANN" by Ahmad Abdullah, 2018. IEEE Transactions on Industry Applications, Volume 54, Pages 1182-1193, ©2018 IEEE

Even though load switching and lightning strikes have clear features to be recognized, it was determined that including these disturbance events in training the pattern recognition approach is more advantageous than handling them separately. The structure of the fault detection module is show in Figure 42. The next few sections provide an overview of the fault detection module. The fault detection module consists of two main stages: the first one is the disturbance classifier and the second one is the lighting fault detection module. We provide a detailed account about the pattern recognition approach that was found to produce the best classification accuracy in section 3.1.1, and then proceed to explain the lightning fault detection module in section 3.1.3.

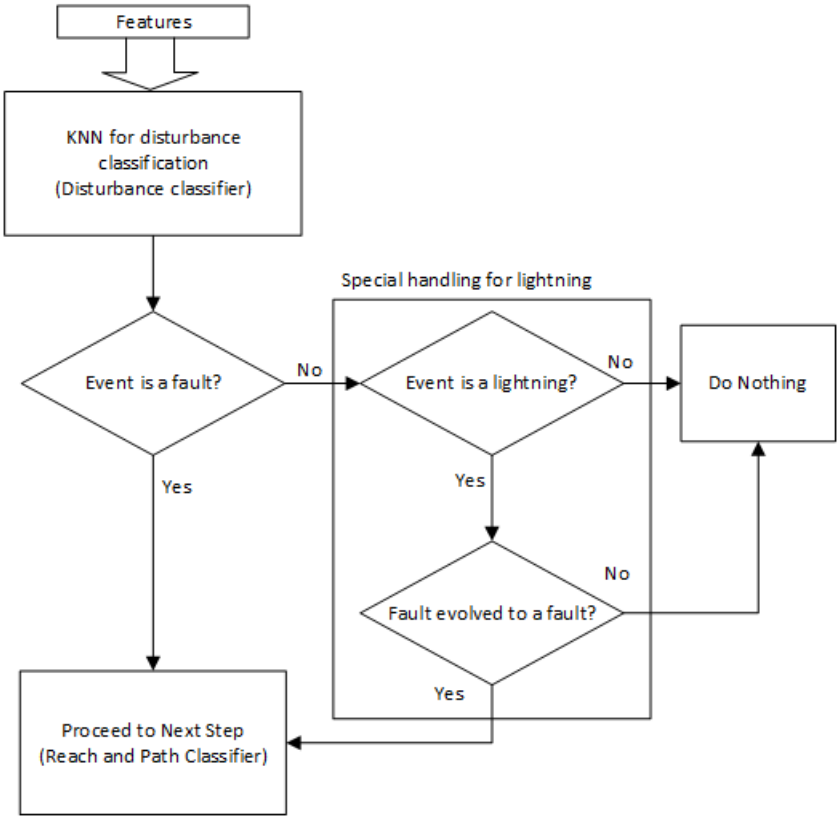

Figure 42. Stages of fault detection module

3.1.1.1 K-nearest neighborhood (KNN) classifiers

The output of the KNN [79] is a class membership. An object is assigned to a membership based on the number of neighbors it has. Thus in Figure 43, the red object is classifier as the purple triangle if one uses a KNN classifier with K=3. If one uses KNN with K=5, then the red object gets classified as a blue square.

For the following sections, the KNN is called a fine KNN if K=1, medium if K=10 and coarse if K=100. The main metric in KNN is the distance which is used to determine the proximity of the samples. Different ways exist to calculate the distance metric:

- Euclidian Distance = $\sqrt{\sum_{i=1}^{N} X_i^2}$, where $X_i = a_i - b_i$
- Minkowski Distance = $\sqrt[m]{\sum_{i=1}^{N} X_i^m}$, where m is the order of the metric which can be either quadratic, cubic …. etc.
- Cosine Distance = $1 - \frac{\sum_{i=1}^{N} a_i \times b_i}{\sqrt{\sum_{i=1}^{N} a_i^2} \times \sqrt{\sum_{i=1}^{N} b_i^2}}$
- Inverse Distance= $\frac{1}{\sqrt{\sum_{i=1}^{N} X_i^2}}$,

We found that the Euclidian metric as along with K=1 produces the best classification accuracy. The purpose of this classifier is to detect whether the disturbance is fault, lightning, line switching or any other event. We call this classifier the disturbance classifier.

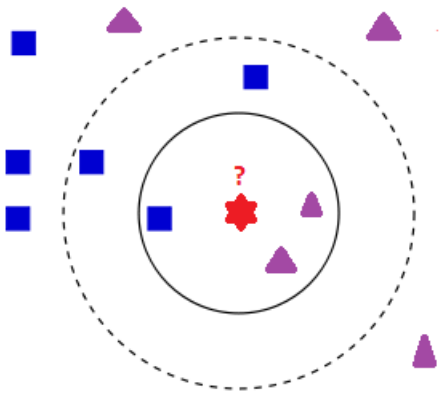

Figure 43. KNN classification

3.1.2 Features used for training and testing disturbance classifier

The features that were used to train and test the pattern classification approaches are presented in this section.

The feature vector can be built using any level of the DWT as shown in Figure 44. The feature vector will have this structure except for when the modal transformation

is applied, in which case, the feature vector will consist of the aerial modes only corresponding to half a cycle of post-event data.

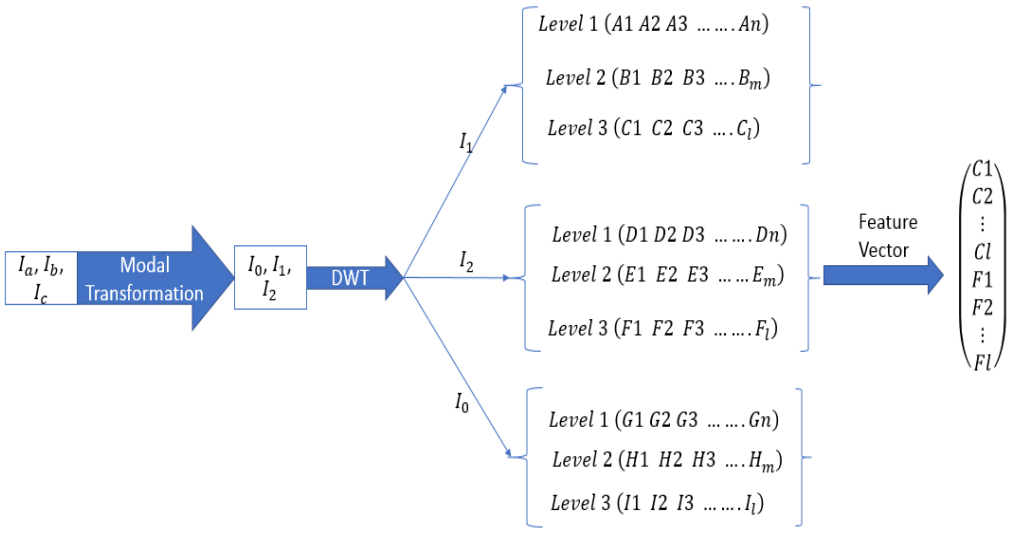

Figure 44. Structure of feature vector

A well-established procedure is given in [68] to extract optimal or near optimal features. We found that when using a sampling rate of 200 kHz, the optimality condition in [68] removes a considerable amount of detail coefficients from level 1 and level 2 decompositions but not from level 3 if certain conditions are met. The conditions are that we apply the modal transformation [44] to a half cycle of post disturbance data to remove the ground mode current and obtain the two aerial mode currents. After that, we apply the DWT to extract level 3 detail coefficients corresponding to half a cycle of post disturbance data of the two aerial mode currents. Thus, a design decision was made not to apply the optimality condition to trade complexity for simplicity and practicality. It should be noted that if the CT bandwidth is 10 kHz as is the case with some bushing

type CTs, then level 1, corresponding to a frequency band 10 kHz to 5 kHz will be used instead of level 3. In other words, we found that the detail coefficients have to correspond to frequencies of at least 5 kHz for accurate classification.

3.1.3 Detection of lightning faults

It not enough to detect lightning, since in many instances, lightning will evolve to fault [80]. In this section, we provide a way to detect lightning faults [81]. Many publications have dealt with the process of a lightning strike evolving to a fault [82], [83] (mainly as a flashover of insulators) or even a back flashover [84]. The process is summarized with simplifications as follows:

- A lightning strike either hits the phase or ground wire
- The voltage of the insulator rises rapidly with respect to ground due to that strike.
- A statistical time lag (in the range of microseconds) passes before the voltage peak of the insulator attains the high voltage peak of the strike. This basically means that the peak of the insulator voltage lags behind the peak of the lightning strike.
- In any case, this time lag is small and when the voltage reaches a certain value, a flashover occurs, which manifests itself as an arc from the insulator on the tower to ground or an arc between the phases.

It should be apparent from the evolution process of lightning faults described above that the fundamental frequency current increase in magnitude as the fault occurs. However, the magnitude of the fundamental frequency does not increase if the lightning strike does not evolve to a fault. It does not matter whether the arc is initiated from the

insulator to ground, conductor to ground or conductor to conductor. An arc will be initiated, and this causes the fundamental current to increase in magnitude. It should be clear as well that a fault following a lightning strike will occur within microseconds from the strike. This is because the statistical time lag and the traveling wave propagation time are very small.

So, if we take a window of one half of a cycle starting from the moment of the lightning strike, a fault should be seen within such a window.

The essence of the detection method is that when a lightning strike evolves to a fault, the 60 Hz current magnitude is increased, but when the strike does not evolve to a fault, the fundamental frequency does not change. Calculating the area of the squared value of a derived signal from the fundamental current and comparing it against a predetermined threshold should indicate whether a fault occurred or not.

A lighting strike could evolve to either an LG or LLG or a three-phase fault. In any case the need arises to determine which phase is faulted to apply our window to the phase faulted. Instead, we apply 0-α-β transformation [66] (Clarke transformation) to the three-phase currents and use the α-component (which is an aerial mode current) as the current that needs to be analyzed. This way, we need to analyze one current not three currents, which boosts relay speed if used in real time applications. We then apply a window of one half of a cycle to the α-component starting from the moment of the lightning strike. A detailed discussion on why the α-component is suitable for our analysis is given in [85]. The most important reason is that the α-component always has a higher amplitude than the phase current. Such a property makes the selection of the

threshold easier as it increases the area under study. We then normalize the α-component using the pre-lightning current fundamental peak value. Doing this, the pre-lightning peak current value will equal to unity.

DWT is then applied to the α-component to retrieve the approximation 5. This is done mainly to get rid of the noise imposed on the signal as much as possible. When a lightning strikes a line, oscillations will be imposed on the fundamental frequency. Applying DWT until we reach approximation 5 will eliminate this noise as shown in Figure 45.

Afterwards, we calculate the integral of the squared normalized α-component which corresponds to the energy by summing up the squared coefficients of the approximation 5. Since the current is assumed a sine wave, this integral should not increase beyond $\pi/2$ if there is no fault. If the strike evolves to a fault, then this integral will exceed $\pi/2$. The threshold should then be taken to equal $\pi/2$. In reality, the threshold will be slightly higher than this because approximation 5 will have more noise due to the lightning oscillations as shown in Figure 45.

It should be noted that the essential feature in the method above is that the once the lightning strike evolves to a fault, the fundamental current increases. If this condition does not occur, then the method fails, and it will be very difficult to detect that type of fault. It is worth mentioning that such a condition will not occur if the available short circuit MVA at the transmission line is low, which corresponds to a weak grid or when the lightning evolves to very high resistance fault. An example of a lightning strike that evolved to a fault in a weak grid system is shown in Figure 46. As can be seen from the

figure, the fundamental current does not increase in an appreciable manner making it difficult to judge whether the lighting actually evolved to a fault or not. These difficulties will not arise if we used double-ended methods.

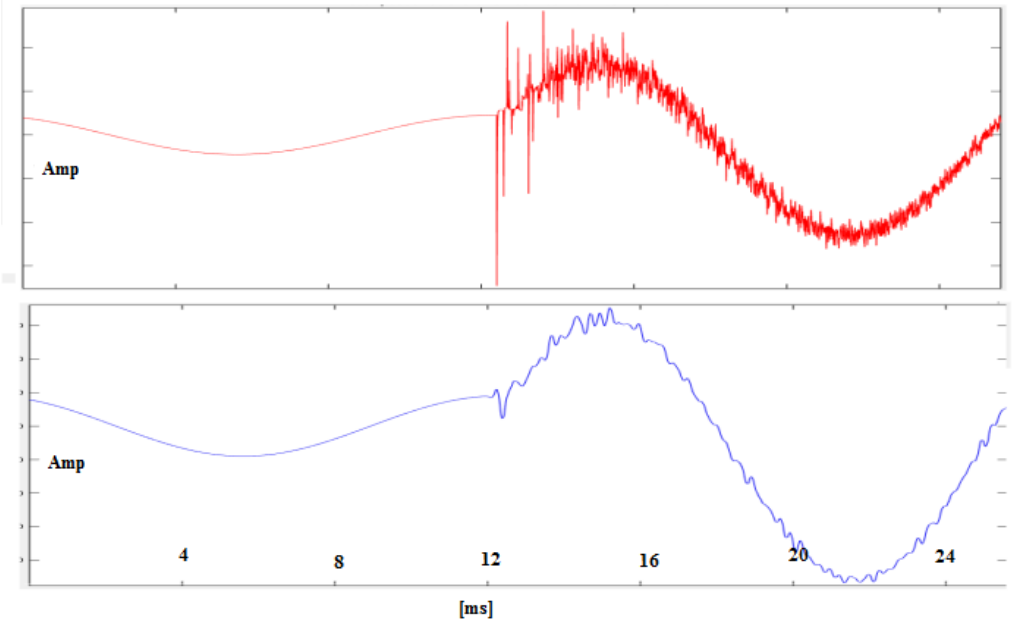

Figure 45. Phase current of a certain lighting fault (upper plot) and approximation 5 of the same current (lower plot)

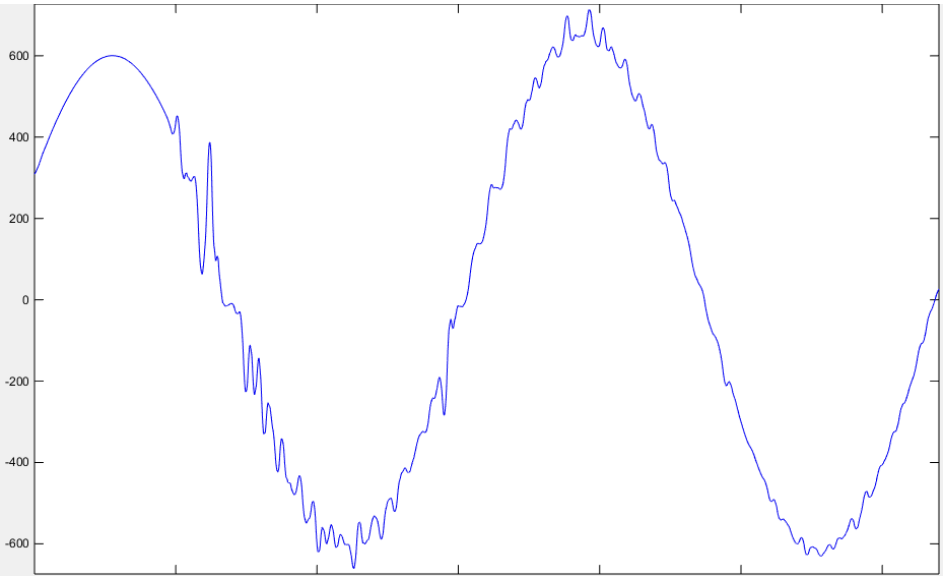

Figure 46. Lightning evolving fault when short circuit level is low

3.1.4 Training Scenarios

In this section, we describe the training scenarios that were used to train the classifiers.

3.1.4.1 Fault cases

Fault cases were created in batches, i.e., a batch for each line. Each batch has fault parameters, which are: incipient angle, fault resistance, fault location and fault type. All fault types have been created, i.e., AG, BG, CG, AB, BC, CA, ABG, CBG, ACG, ABC, ABCG. Incipient angles are from 0 to 350 degrees in 10-degree increments. Fault resistance assumes the values: 0, 100 Ω and 1000 Ω. The distance takes the following values: 5%, 15%, 35%, 50%, 65%, 80% and 95% which are all percentages of total line length. Based on the results that have been provided in [43], [86], not all cases have been used in training. Only the extreme cases corresponding to the highest and lowest DWT

coefficients have been used in training and validation of the pattern classification approaches.

3.1.4.2 Line Switching Cases

For line switching cases, a batch for each line was created. Each batch consists of smaller batches; each of the smaller batches corresponds to switching by one of the circuits breakers at each terminal. For example, a line connecting bus 37 and bus 58 would have a smaller batch for switching using the breaker installed on terminal 37 and another smaller batch for switching using the breaker on terminal 58. The variable in switching cases is the moment of switching. Switching times range from 0 to 360 degrees in 2-degree increments. This way 360 cases per batch were created. Again, only the cases corresponding to the extreme wavelet amplitudes were used in training and validation.

3.1.4.3 Lightning cases

For lightning strike cases, a batch of each line was again created. A Heidler type lightning source [69] with rising time equal to 4 μs and a τ equal to 10 μs has been used. The rising and tailing times were kept constant during simulations but amplitudes were varied, which were set to 5 kA, 10 kA, 15 kA, 20 kA and 30 kA. Striking distances were the same as the ones used for fault batches: 5%, 15%, 35%, 50%, 65%, 80% and 95%, which are all percentages of total line length. The incipient angle was 0, 90,180, 270 and 330 degrees. Again, only the cases corresponding to the extreme amplitudes were used in training and validation.

3.1.4.4 Load Switching cases

All loads in the area under study were switched ON or OFF at different incipient angles of 10, 90, 180, 270 and 330 degrees. Only the cases corresponding to the extreme cases were used in training and validation.

3.1.4.5 Bus fault cases

Bus faults were also created [87]. If a line connected buses 34 and 37, the faults that occurred at bus 34 and 37 were included in training in addition to the cases mentioned in sections 3.1.4.1, 3.1.4.2, 3.1.4.3, and 3.1.4.4.

All types of faults were created, i.e., AG, BG, CG, AB, BC, CA, ABG, CBG, ACG, ABC, ABCG. Incipient angles were from 0 to 350 degrees in 10-degree increments. Fault resistance assumed the values: 0, 50, 100 Ω and 1000 Ω.

In the following sections, we provide the classification results for both the disturbance classification module and the module for determining whether the fault is within or outside the reach of the distance relay.

3.1.5 Training the disturbance classifier

What remains to be discussed is whether we used all disturbance data from all over the network to train the pattern recognition approaches for each relay. For the disturbance classification module, certain criteria were used to select which disturbance events should be used to train the pattern recognition approach for each distance relay. The criterion was to select the disturbance events that belong to the lines within 300% of the line reach in the forward direction. This has been done to guard against false alarms. It was found that the disturbance events occurring in the network do not propagate

everywhere in the network unless they are electrically close enough to some distance relays. This will be explained in chapter 4. In that section, the faults that occur electrically far away from the distance relay did not cause any noticeable high frequency components. If we include those in training and label them as faults, when they have no high frequency components, we risk producing wrong classification results as the faults and non-fault disturbances will not be classified correctly. Using this simple trick, we can classify disturbance events that occur near the distance relay leaving the issue of determining whether the event is inside the protection reach or not to section 3.2. The validity of this procedure will be tested in chapter 4 where we applied the methodology at each single distance relay at the network during wide-area cascading events and detected what relays responded to the faults and whether each relay was supposed to respond to these faults or not.

3.2 Determining whether a fault is inside or outside relay reach

Once the event is determined to be a fault based on the results provided in chapter 3.1, the next step involves deciding whether the fault is inside or outside the modified reach of the distance relay. The modified reach is 200% as explained in section 2.4.

The success of the proposed method will depend on determining whether the fault is inside or outside the relay reach since detecting whether the disturbance was a fault is not sufficient to eliminate distance relay misoperation. It is this step of detecting whether the fault has occurred within zone 3 (the relay reach) and the clearing of the zone 3 fault that makes the proposed method viable. In this section, we will discuss how

to determine if the fault is within the relay reach or, in other words, whether the fault is a zone 3 fault.

3.2.1 Path and reach classifiers

It should be kept in mind that determining whether a fault is within the reach of relay or outside the reach of the relay is only activated after a fault has been detected. In other words, if a non-fault disturbance has been detected by the module given in Figure 42, no action will be taken.

Before stating how to determine that the fault is inside or outside the relay reach, a new term has to be introduced. This term is called a "current path." A current path is the path in the forward direction of a specific distance relay that allows the current to flow, leaving the line of that distance relay. This can be better visualized by referring to Figure 47. The current that is passing through line A-B, can take multiple paths once it arrives at bus B. Thus, three current paths exist in the figure: current path 1, current path 2 and current path 3. Current path 1 is line B-C and all lines connected to it beyond bus C, current path 2 is line B-E and all lines connected to it beyond bus E, and finally, current path 3 is line B-D and all lines connected to it beyond bus D.

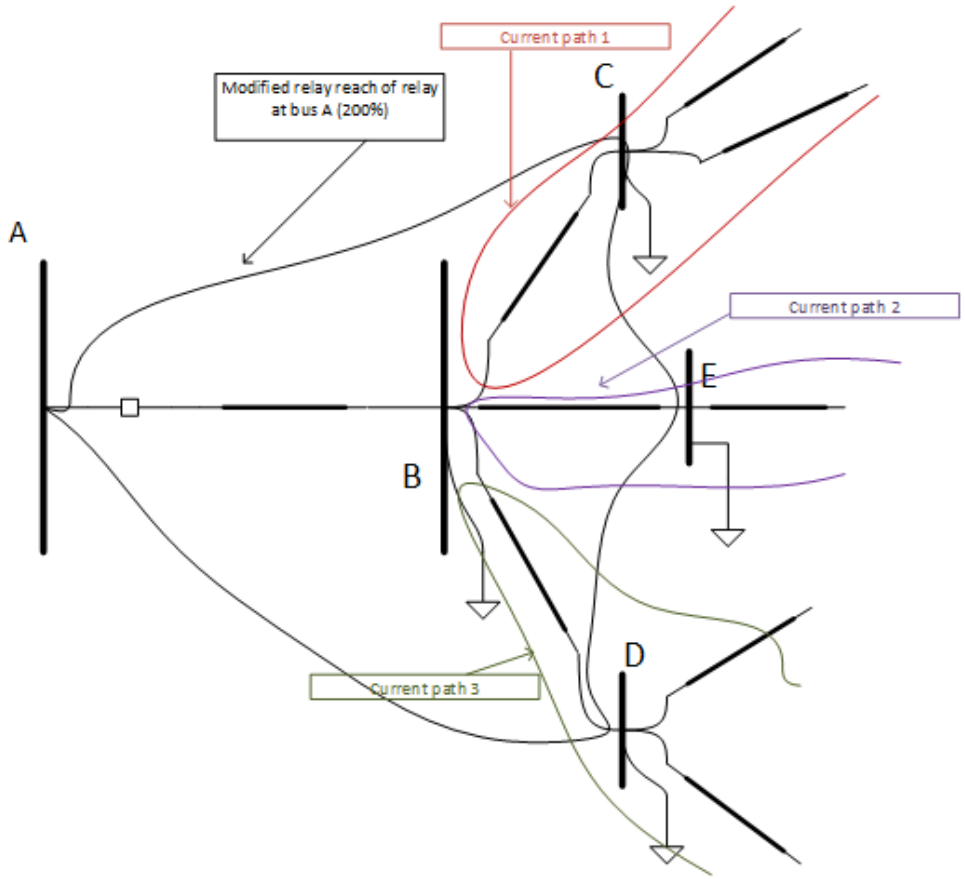

Figure 47. Current paths of relay at bus A of line A-B

For determining whether the fault is within the reach of the relay, there will be two pattern recognition approaches. The first one is called the path classifier which determines whether the fault is a zone 1 fault (belonging to line A-B in Figure 47), or which current path the fault belongs to. The second one is called the reach classifier and it will determine whether this fault belongs to the first line of the current path or not. There will be a reach classifier for each current path. For example, if the disturbance classifier detects a fault at relay A of line A-B of Figure 47, then the path classifier will determine which current path the fault corresponds to or even if the fault is on line A-B.

Let's say that the fault was on current path 1. Then the reach classifier of current path 1 will determine whether this fault belongs to line B-C or not. If it was found that the fault indeed is in line B-C, then this is a zone 3 fault, and we need to react only if the fault has not been cleared. This issue will be treated in section 3.3.

3.2.2 Feature vector and training scenarios

Now, we need to revisit what has been stated about the training scenarios in section 3.1.5. It was stated that the disturbances that are used to train the pattern recognition approach are created to be within 300% of the relay reach in the forward direction. This was done since the distance relay is only supposed to react to faults in the forward direction as faults in the reverse direction will not fall in the MHO characteristics and thus, no risk exists for misoperation. Additionally, using events that are within 300% of the relay reach guard against possible misclassification when the events do not cause strong enough high frequency oscillations to be seen by the relay or differentiated by the relay. In this section, we still use the faults that are created within 300% of the relay reach to train the path and reach classifiers. It could be asked how the pattern recognition approach will determine whether a fault occurred beyond the 300% reach. The answer is that we will, one more time, depend on the generalization capability of the pattern recognition approach to eliminate these faults that occurred beyond the 300% reach. For example, if a fault occurred at 425% of the relay reach, then first of all we are not sure that the disturbance classifier in section 3.1 will classify this as a fault since it is electrically far away from the relay, and it is highly likely that the event will be classified as non-fault because the DWT coefficients will be very small, which will

likely to cause the event to be mistaken as a non-fault disturbance. Even if the event is classified as a fault, the path classifier in this section may or may not be able to tell for sure which current path the fault belongs to. However, the reach classifier in this section should be able to tell whether it is within the 200% relay reach or not, i.e., we must depend on the generalization capability of the path and reach classifiers to eliminate faults that were not included in training of both classifiers. We can only make sure that this is feasible by examining the performance for the disturbance, path, and reach classifiers during wide-area cascading events which is explained in chapter 4.

It is clear from the description above that we have to select the features for training both classifiers in a manner that makes these two classifiers have the best generalization capability specifically for the faults that occur beyond 300% of the relay reach.

The features that were used to train and test the two classifiers in this section were designed in such a way that the classifiers have good generalization capabilities. The feature vector will be the same as the one given in section 3.1.2 which is a level 3 detail coefficient. The feature vector must have the frequency content of at least one half of a cycle of post-fault information. The feature vector is built using the two aerial modes.

3.3 Detection of fault clearing

The last component in this methodology is the detection of fault clearing. Numerous fault studies have been performed. The main characteristic of fault clearing is

the reduction of phase currents to values close to pre-fault values. This is shown in Figure 48.

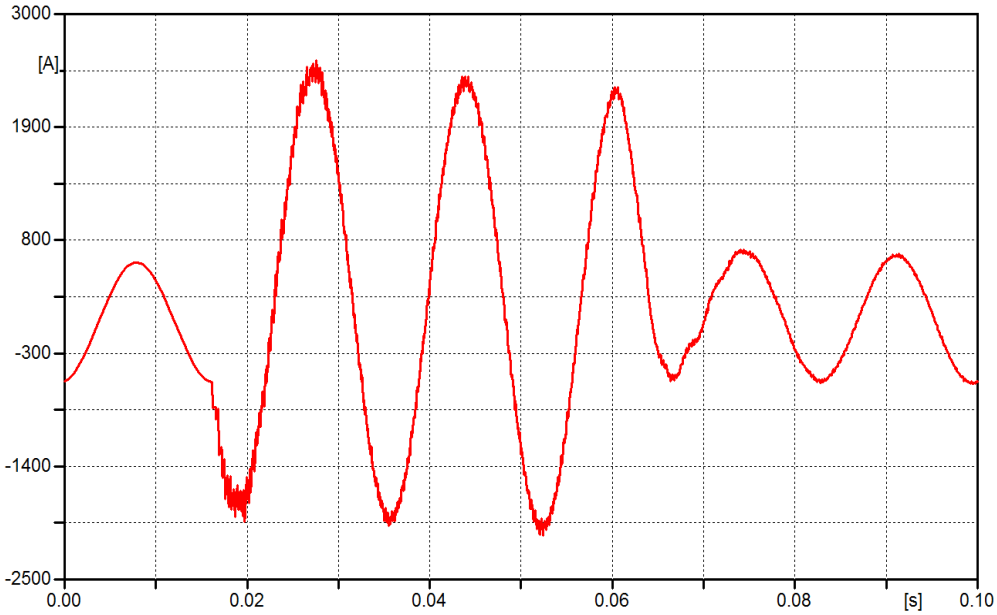

Figure 48. Pre-fault, fault and post-fault currents of a certain fault case

As can be seen from Figure 48, the main characteristic when it comes to fault clearing is that the phase current goes back to normal pre-fault levels. In this work, we determined that the fault has been cleared only if the fundamental current magnitude is reduced by more than 25% within 10 cycles after the reach classifier confirms that the fault is within zone 3. Most high voltage CBs clear the faults within six cycles, so a 10-cycle fault clearing time is a conservative measure to prevent confusing this reduction with fundamental current reduction due to system devices (regulators, exciters, tap changers, etc.). The only drawback in the way we detect remote circuit breaker operation is that it is not applicable to buses where the short circuit level is so low, the fault current will not increase dramatically.

3.4 Overall solution methodology

Any relay needs only to respond to faults that are within its protection reach. Thus, when all faults within the reach of the distance relays have been detected, we can rule out distance protection misoperation if we also make sure that those faults have been cleared. The use of high-frequency current oscillations (HFCOs) for asserting this condition is thus advantageous because the HFCOs are very localized in nature and events that are electrically far away from the relay will cause low-amplitude high-frequency transients that are likely to be classified as non-fault as will be shown in chapter 4.

The solution proposed in this dissertation has two main units: 1) the first unit, which detects all faults within the relay reach, and 2) the second unit, which detects fault clearing once the fault has been confirmed to be within the relay reach by the first unit.

In our investigations, we found that the first unit must have two modules: 1) a fault detection module that detects all disturbance-generated HFCOs and classifies them as fault or non-fault conditions, and 2) once the first module asserts that the disturbance is a fault, a second module will further take this fault and determine whether the fault is within the protection reach of the relay. Since we are using HFCOs to judge the occurrence of the fault in the network, we will have to study not only the fault HFCOs, but also HFCOs produced by all the other disturbance events. The first module was described as a disturbance classifier as explained in chapter 3.1. The second module will consist of two sub-modules as described in chapter 3.2.

One important aspect of the solution will be determining whether the fault is within the relay reach or outside that reach using the HFCOs. For this reason, the relay reach has to be changed such that a clear distinction can be made between the disturbances that are within the relay reach and the ones that are outside the relay reach. In this work, we propose that the zone 3 reach be reduced to 200% instead of 220%, i.e., we disabled remote backup protection provided by relay A of line A-B for the remote CBs of the lines emanating away from buses C, D and E as shown in cyan in Figure 47. Disabling this backup protection does not mean that those CBs are without backup as they are still backed up by the relays on the lines emanating away from bus B. We mentioned that this reduction should cause no problem unless, for example, the circuit breakers at bus A and B fail simultaneously, which is a rarity

Additionally, the proposed method in this work will never be put into operation unless the impedance enters one of the zones of distance protection to ensure maximum relay security. Lastly, based on the impedance jumps out of zone 3, the method will be deactivated immediately. The overall solution methodology is given in Figure 49.

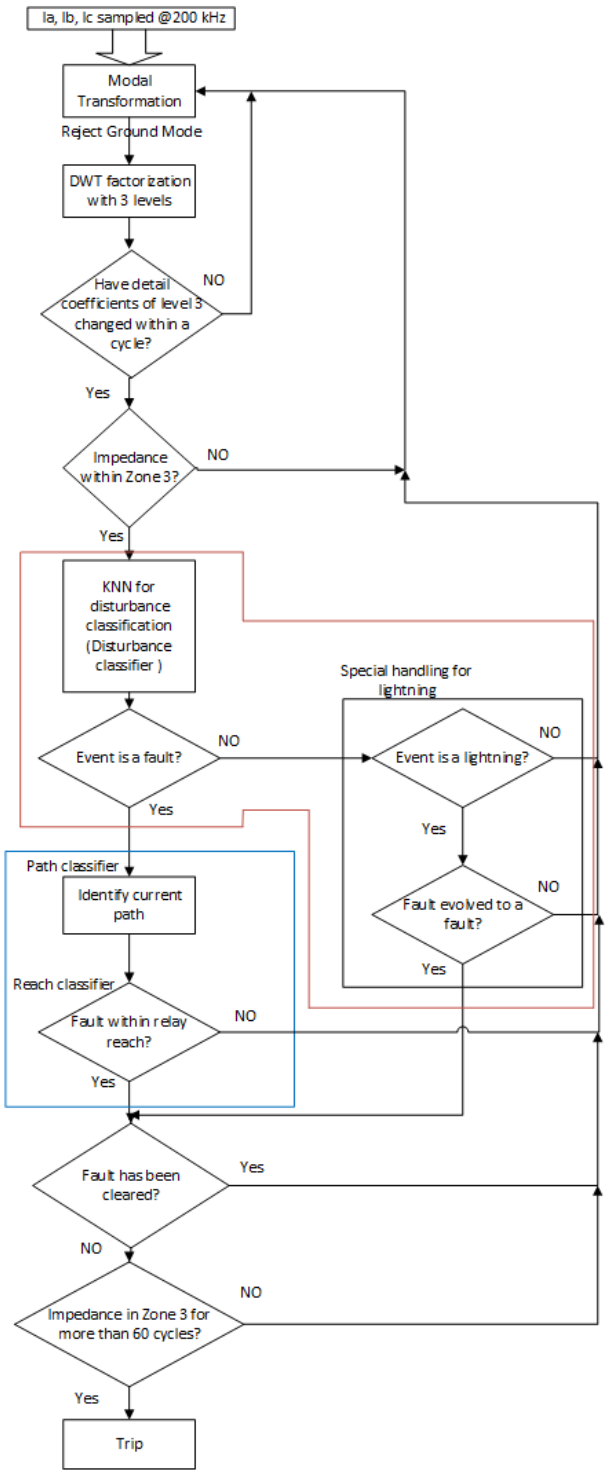

Figure 49. Overall solution methodology

3.5 Summary

In this chapter, we discussed the features used to train the disturbance, path and reach classifiers which constituted the first and second stages of the proposed methodology. We showed how the three classifiers work in harmony to determine that the fault is within the zone 3 reach of the relay. We overviewed the structure of the classifiers and their operation. We mentioned that lighting faults cause the disturbance classifier to fail, and we proposed a separate module that detects lightning faults. We presented the training scenarios used to train all classifiers.

Also, we presented the last stage on how to detect fault clearing and circuit breaker openings.

Finally, we showed how to piece together all three stages to construct the overall solution methodology.

4. CASE STUDIES AND PERFORMANCE ANALYSIS

In this chapter, we provide a couple of cascading scenarios that resulted in one distance relay misoperation as case studies. The proposed methodology was applied to each single distance relay in the simulated test systems, and it will be shown that the proposed method successfully blocks the affected relays from misoperation. We show the performance of certain relays under standard testing conditions. Lastly, we perform validation for the various classifiers proposed.

4.1 Creation of cascading scenarios and system model

In this chapter, two cascading scenarios are introduced. One cascading scenario is simulated in the IUTC 146 bus system [88], while the other one is simulated in the IEEE 300 bus system [89]. The cascading scenarios were created based on an automated program under certain load and generation conditions. First, the program would create all distance protection settings for all transmission lines in the network. Second, the program faults one transmission line and then takes it out of service by opening the two circuit breakers at each end. After clearing the fault, all distance relays in the network are checked to see if any of them misoperates. If no relay misoperates, the program continues by 1) adjusting the power flow in the network by redispatching the generation and letting system devices operate (regulators, tap changers, etc.) and 2) then by faulting another line and taking that line out of service and checking if any distance relay misoperates. This process continues till at least one zone 3 impedance element misoperates. The process is also restarted by starting from a different transmission line. By doing that, the program enumerates all possible combinations of successive faults

and successive transmission line outage operations that can lead to zone 3 distance protection misoperation. The sequence of faults and transmission line outage is called a cascading scenario. After that, the loads and generation levels are scaled by a certain percentage, the case is redispatched and the above process is restarted to create different cascading scenarios under new load and generation levels. This way, numerous cascading scenarios for each case and under different load and generation levels were created and studied. This process is summarized in Figure 50.

Before presenting the cascading scenarios, the measures that were taken to make the simulations realistic are:

1. Current transformer (CT) models [55] and capacitive transformer models (CVT) are included [90]
2. Tower configurations are taken into consideration. The tower configurations are taken from [91].
3. Power transformers are modeled according to [92]
4. Synchronous machines are modeled according to [93]
5. Standard Library PSCAD distance element was used. The proposed classifiers were modeled as well for each distance relay in the system.
6. Surge arresters were also modeled according to [94]

Hundreds of cascading scenarios were created in this way, but only two scenarios are presented in this chapter.

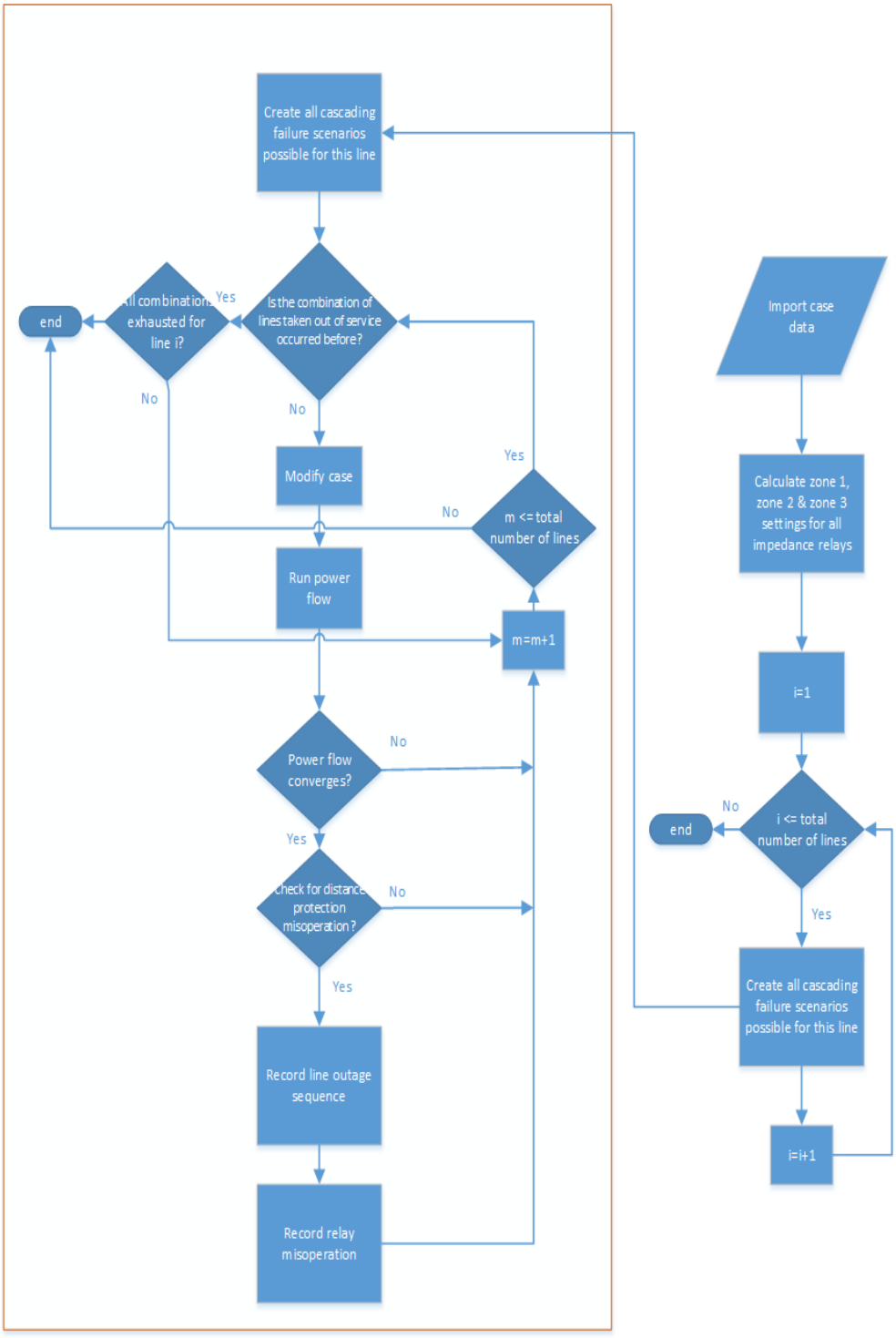

Figure 50. Algorithm for creating cascading scenarios

4.2 Cascading scenario in IEEE 300 bus system

The cascading scenario that has been created in the IEEE 300 bus system is shown in Figure 53. The cascading scenario proceeds as follows:

- A fault on line 7-131 is created and then cleared by opening the circuit breakers at both end within 5 cycles
- A fault on line 19-3 is created and then cleared by opening the circuit breakers at both ends within 5 cycles
- Another fault on line 176-173 is created and then cleared by opening the circuit breakers at both end within 5 cycles
- A fault on line 43-44 is created and then cleared by opening the circuit breakers at both end within 5 cycles

Due to the opening of these lines, the power flow is redistributed around the network and the line 52-55 is loaded at 123 % of its line rating. Due to that, the impedance seen by the relay at bus 52 enters zone 3 and the relay misoperates. The phase A current seen by the relay at bus 55 of line 52-55 is given in Figure 51. As can be seen from the Figure 51, the current seen by the relay continuously increases until misoperation occurs. The impedance seen by that relay is given in Figure 52. As can be seen from the Figure 52, the impedance trajectory marches until it enters zone 3 and settles there, causing the relay to misoperate.

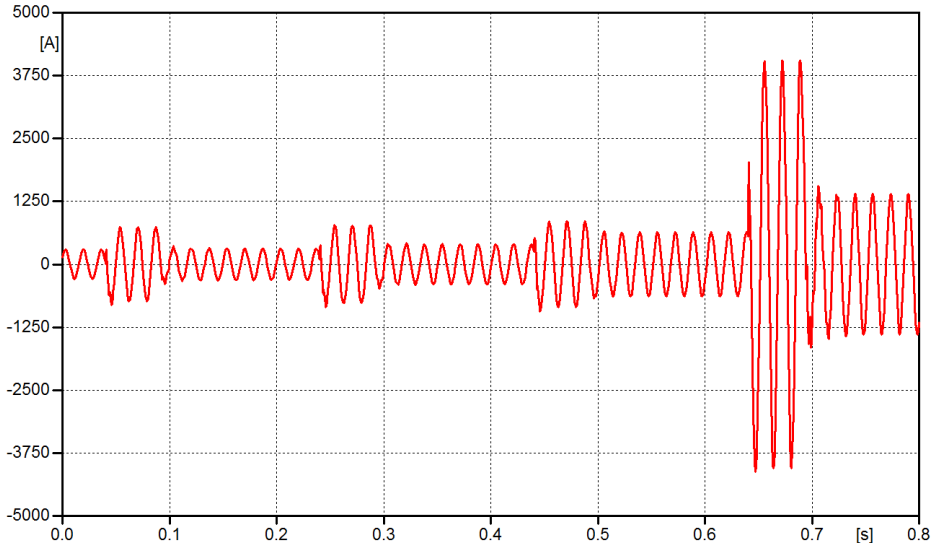

Figure 51. Current of Phase A seen by the relay at bus 52 of line 52-55 during the IEEE 300 cascading scenario under different power levels

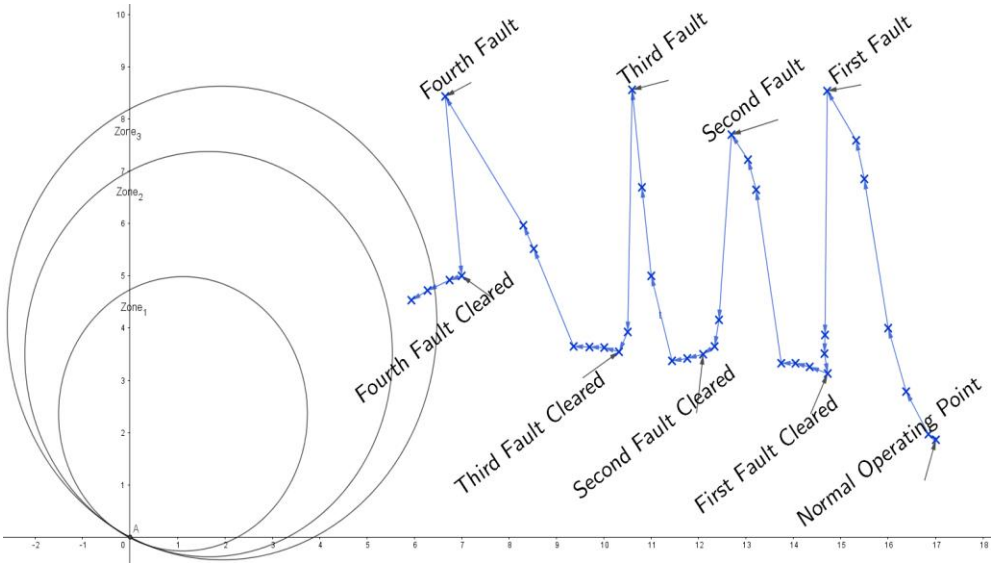

Figure 52. Positive sequence impedance seen by relay at bus 52 of line 52-55 during IEEE 300 cascading scenario

4.2.1 Response of the distance relays during cascading scenario

In this section, we show how all distance relays respond after modifying the distance protection functionality using our proposed methodology. Any relay that is not colored in the figures in this section means that it did not see a fault and did not operate. We relax the requirement of having the impedance falling within the zone 3 circle to activate the methodology. Instead, we activate the disturbance classifier once the fault is detected in the forward direction to test the effectiveness of the classifier throughout the network.

The first event of the scenario is the fault on line 7-131. The response of the solution methodology to the first event is shown Figure 54. As can be seen from the figure, the fault has been detected by all distance relays marked by the blue and green squares. The blue squares denote relays that recognized the fault, and these are the only relays that are supposed to respond to the fault. Green squares are the relays that saw the event and they are not supposed to respond to the fault because their impedance falls outside the zone 3 circle.

We continue the scenario and apply the path classifiers to all the marked relays. For all the relays marked in color (whether green or blue), the path classifiers successfully identify the current path. When it comes to the reach classifiers, the reach classifiers for the blue relays correctly identify the fault within zone 3 while the reach classifiers for the green relays correctly identify the fault outside zone 3. Once the fault has been cleared by the circuit breakers at the line terminals, all blue relays in the figure

identifies fault clearing because the fundamental current is highly reduced after fault clearing.

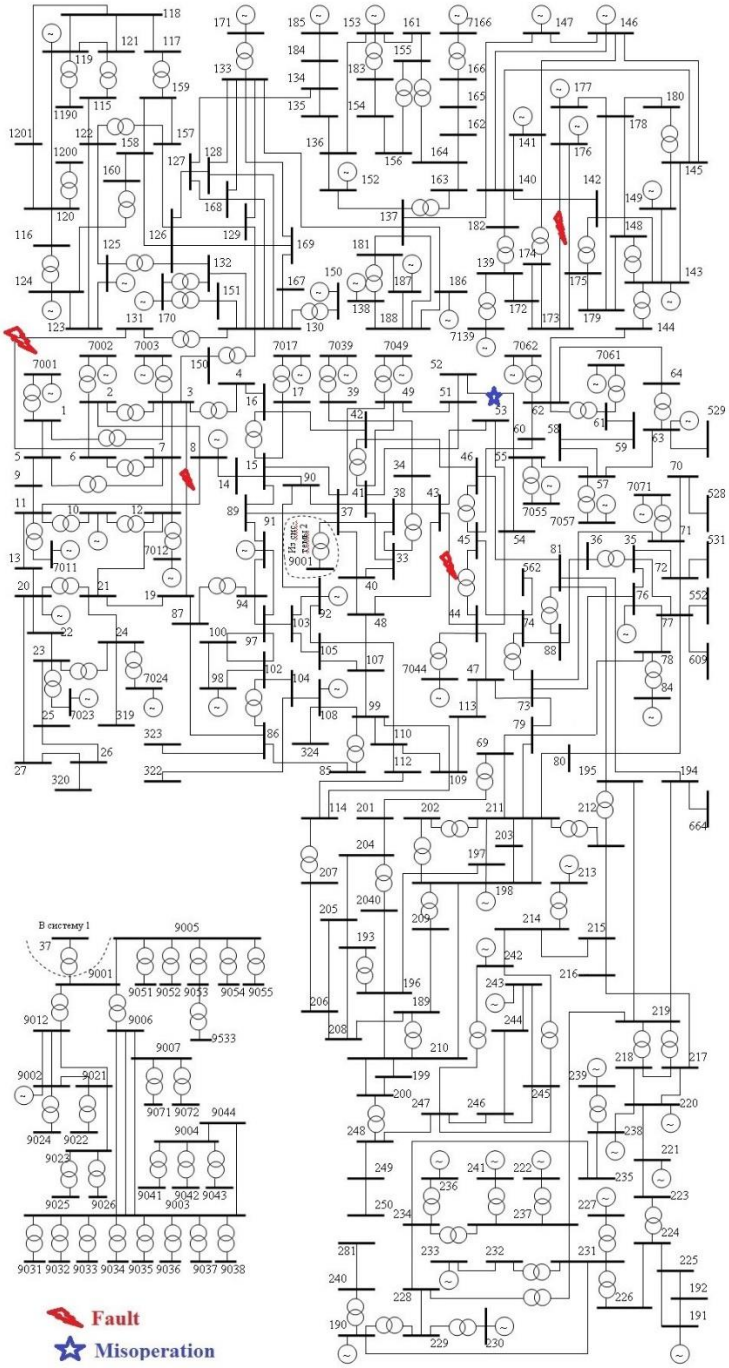

Figure 53. Cascading scenario in IEEE 300 bus system

The second event of the scenario is the fault on line 3-19. The response of the solution methodology to the first event is shown Figure 55, where the fault is detected by all distance relays that have line 3-19 in their zone 3 reach denoted by blue squares as well as some green relays that are electrically close to the fault but do not have that relay in their zone 3 reach. In other words, when the fault is in the forward direction the results of the disturbance classifier is given by the blue and green squares. The blue squares denote relays that recognized the fault, and these are the only relays that are supposed to respond to the fault. The green squares denote the relays that recognized the fault, but these are relays that are not supposed to respond to the fault since the fault is outside its protection zone. The recognition of the fault by the green relays should not come as a surprise since the disturbance classifier of those relays has been trained with faults that are within 300%**.**

At this step, it is worth mentioning that the green relay 85 of line 85-86 has seen the event as a fault even though the fault is beyond the 300% line reach. In other words, the disturbance classifier was able to generalize and see this event as a fault even though we have not trained that classifier with the faults on line 3-19. If we applied the methodology given in the section 3.4, then green squares would not exist since the fault impedance does not fall within their zone 3 (which reaches to 200%).

We continue the scenario and apply the path classifiers even for relay 85 of line 85-86 to all the blue and green relays. For all relays, the path classifiers successfully identify the current path. When it comes to the reach classifier, the reach classifiers of all green relays even for relay 85 of line 85-86 saw this fault as a fault outside the 200%

protection reach which means that they will not pick-up which is denoted by the orange circle in the figure. **Notably, the path classifier of relay 85 of line 85-86 was able to determine correctly the current path even though it had not been trained using any fault on line 3-19, which shows that the reach classifier generalization capability is doing what it is supposed to do**. **It is also noteworthy that the reach classifier of relay 85 of line 85-86 was able to determine that the fault is beyond its reach even though it was not trained using any fault on line 3-19, which shows that the reach classifier generalization capability is doing what it is supposed to do.**

On the other hand, the reach classifier for the blue relays correctly identifies the fault within zone 3. At this step, the green relays have stopped working and the blue relays are still trying to detect if the fault has been cleared. Finally, once the fault is cleared, all blue relays in the figure identify fault clearing because the fundamental current is highly reduced after fault clearing. The results of this step clearly show that limiting the training of the disturbance, path and reach classifiers to events within 300% of line length was advantageous in this situation as it limited the number of relays that saw the fault. **They also show that the disturbance, path, and reach classifiers were able to generalize to faults that were not included in the training.**

The third event of the scenario is the fault on line 176-173. The response of the solution methodology to the third event is shown Figure 56. As can be seen from the figure, the fault has been detected by all distance relays that have line 176-173 in their zone 3 reach denoted by blue squares as well as some green relays that are electrically close to the fault but do not have that relay in their zone 3 reach. In other words, when

the fault is in the forward direction, the results of the disturbance classifier are given by the blue and green squares. The blue squares denote relays that recognized the fault, and these are the only relays that are supposed to respond to the fault. The green squares denote the relays that recognized the fault, but these are relays that are not supposed to respond to the fault since the fault is outside its protection zone.

The recognition of the fault by the green relays should not come as a surprise since the disturbance classifier of those relays has been trained with faults that are within 300% of line length. If we applied the methodology given in section 3.4, then green squares would not exist since the fault impedance does not fall within their zone 3 (which reaches 200%). We continue the scenario and apply the path classifiers to all the blue and green relays. For all the relays, the path classifiers successfully identify the current path.

When it comes to the reach classifier, the reach classifiers of all green relays see this fault as a fault outside the 200% protection reach which means they will not pick-up, which is denoted by the orange circles in Figure 56. On the other hand, the reach classifier for the blue relays correctly identifies the fault within zone 3. At this step, the green relays have stopped working and the blue relays are still trying to detect whether the fault has been cleared. Finally, once the fault is cleared, all blue relays in the figure identify the fault clearing because the fundamental current is highly reduced after fault clearing.

The results of this step clearly show that limiting the training of the disturbance, path and reach classifiers to events within 300% of line length was advantageous in this situation as it limited the number of relays that saw the fault.

The fourth event of the scenario is the fault on line 43-44. The response of the solution methodology to the first event is shown in Figure 57. As can be seen from the figure, the fault has been detected by all distance relays that have line 43-44 in its zone 3 reach denoted by blue squares as well as some green relays that are electrically close to the fault but do not have that relay in its zone 3 reach. In other words, when the fault is in the forward direction, the results of the disturbance classifier is given by the blue and green squares. The blue squares denote relays that recognize the fault, and these are the only relays that are supposed to respond to the fault. The green squares denote the relays that recognized the fault, but these are relays that are not supposed to respond to the fault since the fault is outside its protection zone. The recognition of the fault by the green relays should not come as a surprise since the disturbance classifier of those relays has been trained with faults that are within 300% of the line length. **Notably, the fault has been recognized by relay 52 of line 52-55. It is also noted that that fault would be outside the zone 3 reach even if the zone 3 reach was maintained at 220% of the line length.** If we applied the methodology given in section 3.4, then green squares would not exist since the fault impedance does not fall within their zone 3 (which reaches 200%).

We continue the scenario and apply the path classifiers to all the blue and green relays. For all the relays, the path classifiers successfully identify the current path. When

it comes to the reach classifier, the reach classifiers of all green relays see this fault as a fault outside the 200% protection reach which means that they will not pick-up which is denoted by orange circle in the figure. On the other hand, the reach classifier for the blue relays correctly identify the fault within zone 3. At this step, the green relays have stopped working and the blue relays are still trying to detect whether the fault has been cleared. Once the fault has been cleared, all blue relays in the figure identify fault clearing because the fundamental current is highly reduced after fault clearing. **It should be emphasized that even though the disturbance classifier of relay 52 of line 52-55 did see the event as a fault, the reach classifier was successful in determining that the fault was outside zone 3 sending a blocking command to the relay, which signifies the success of the solution methodology to prevent the protection misoperation.**

After fault clearing, the impedance seen by relay 52/52-55 starts to enter zone 3 slowly due to power flow adjustments of the network. However, the disturbance classifier of 52/52-55 identified this disturbance as non-fault, as it was fault clearing, and the proposed method blocks relay operation. Thus, misoperation was avoided and system was saved from collapse.

The results of this scenario show that limiting the training of the disturbance, path and reach classifiers to events within 300% of line length was advantageous in this situation as it limited the number of relays that saw the fault. **Some relays outside the 300% training threshold (as mentioned in section 3.1.5) saw some faults but the**

path and reach classifiers were able to block those relays due to their generalization capability which shows that the security of the relays has been improved.

The overall results in this section confirms that the classifiers can indeed be trained using events occurring within 300%. Also, the features seen by the relay have a very strong correlation with the system topology as a whole without regard to the few contingencies that occurred in the network before the first misoperation occurred (the reader is reminded that classifier training was done under base case topology without regard to any contingency). These two observations make the proposed methodology attractive from a practical point of view.

4.3 Cascading scenario in the IUTC 146 bus system

The first cascading scenario that has been created in the IUTC 146 bus system [88] is shown in Figure 60. The cascading scenario proceeds as follows:

- A fault on line 39-49 is created and then cleared by opening the circuit breakers at both ends within five cycles
- Another fault on line 37-50 is created and then cleared by opening the circuit breakers at both end within five cycles
- Another fault on line 69-71 is created and then cleared by opening the circuit breakers at both end within five cycles

Due to the opening of these lines, the power flow is redistributed around the network and the line 30-33 was loaded at 115 % of its line rating. Due to that, the impedance seen by the relay at bus 30 entered zone 3 and the relay misoperated. Phase A current seen by the relay at bus 30 of line 30-33 is shown in Figure 58. The current is seen to increase until misoperation. The impedance seen by that relay is shown in Figure

59. The trend of the impedance trajectory is also seen to approach zone 3 until it settles indefinitely there causing misoperation.

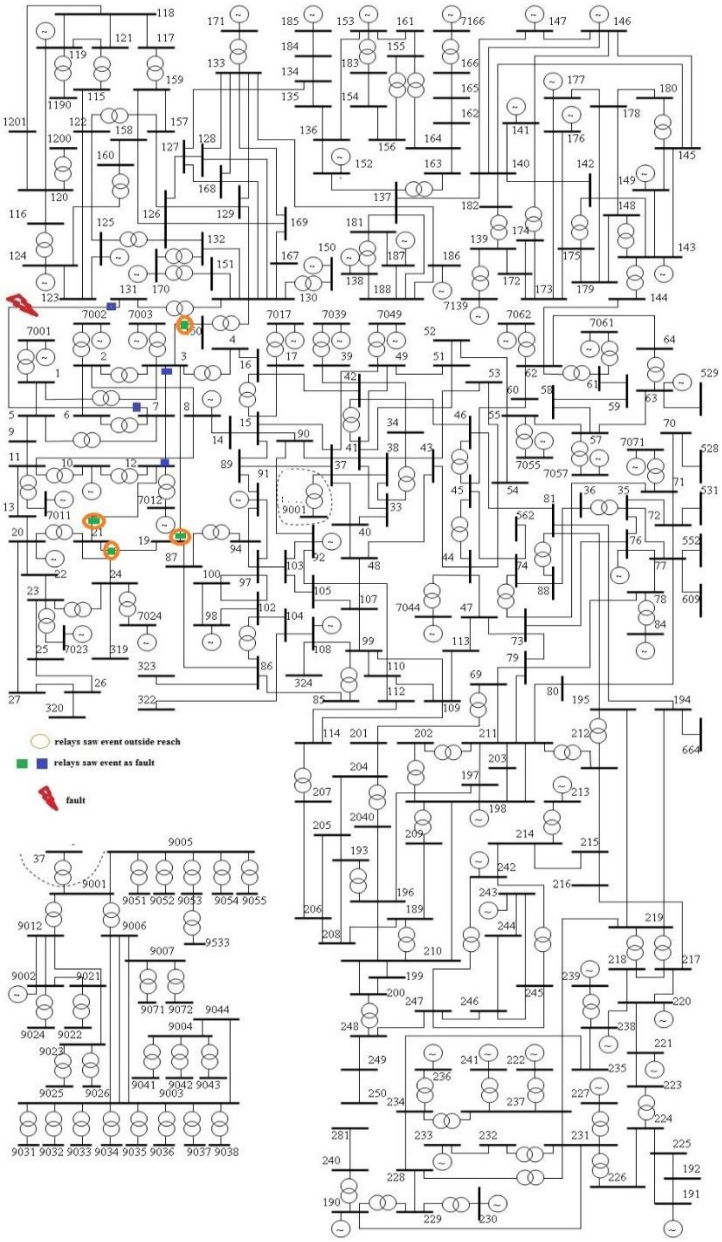

Figure 54. Application of solution methodology to first event of the IEEE 300 bus cascading scenario

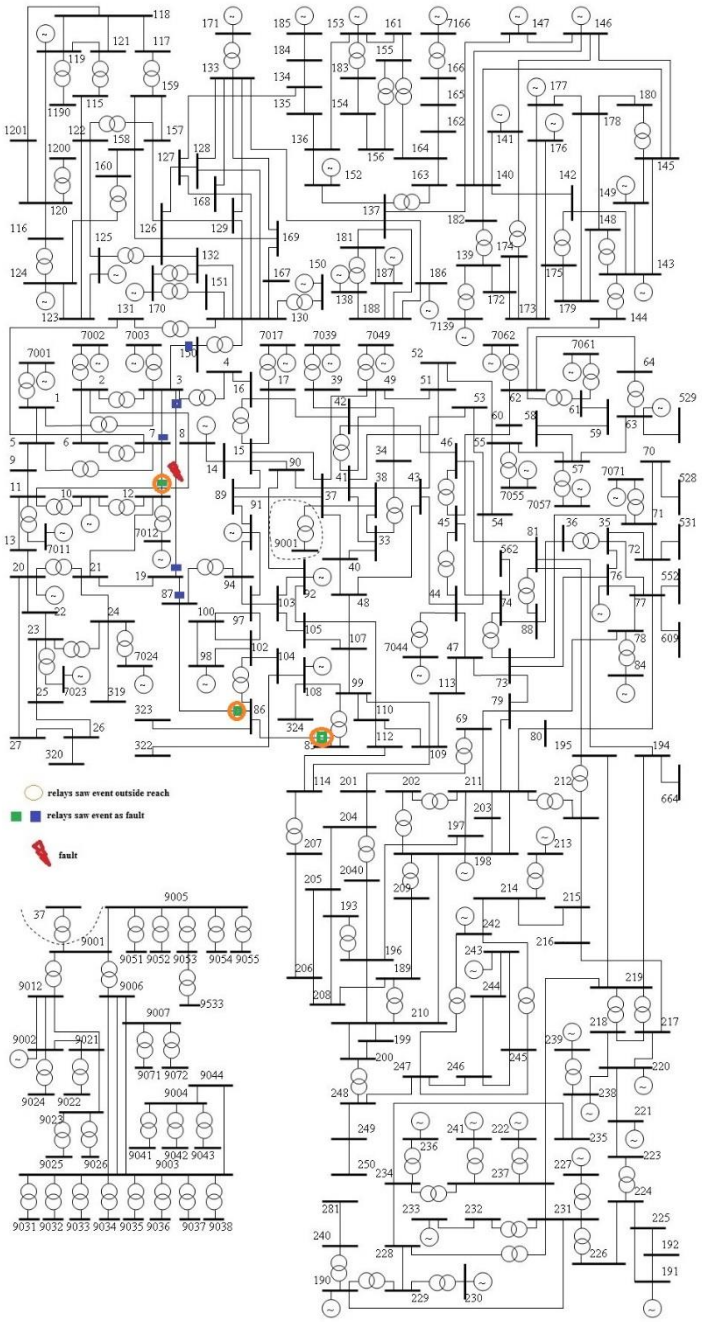

Figure 55. Application of the solution methodology to the second event of the IEEE 300 bus cascading scenario

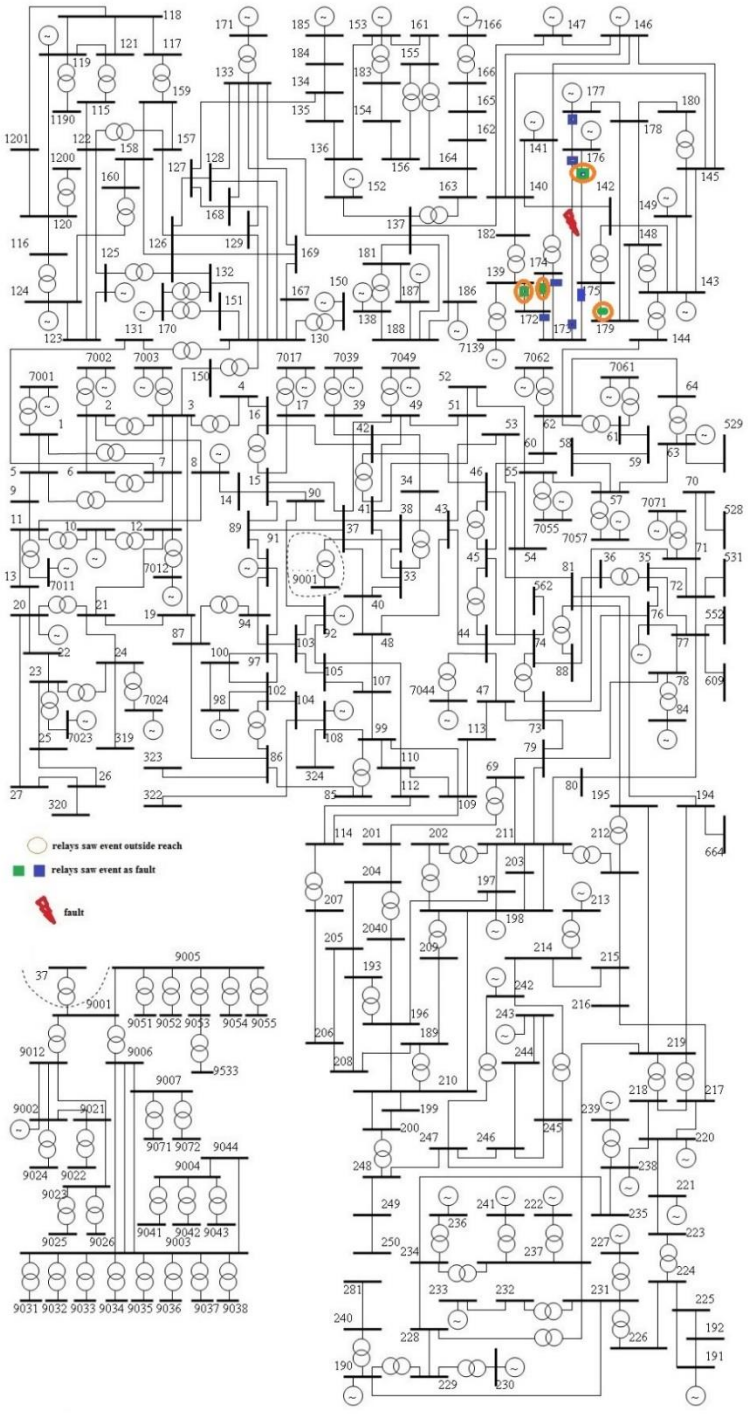

Figure 56. Application of the solution methodology to the third event of the IEEE 300 bus cascading scenario

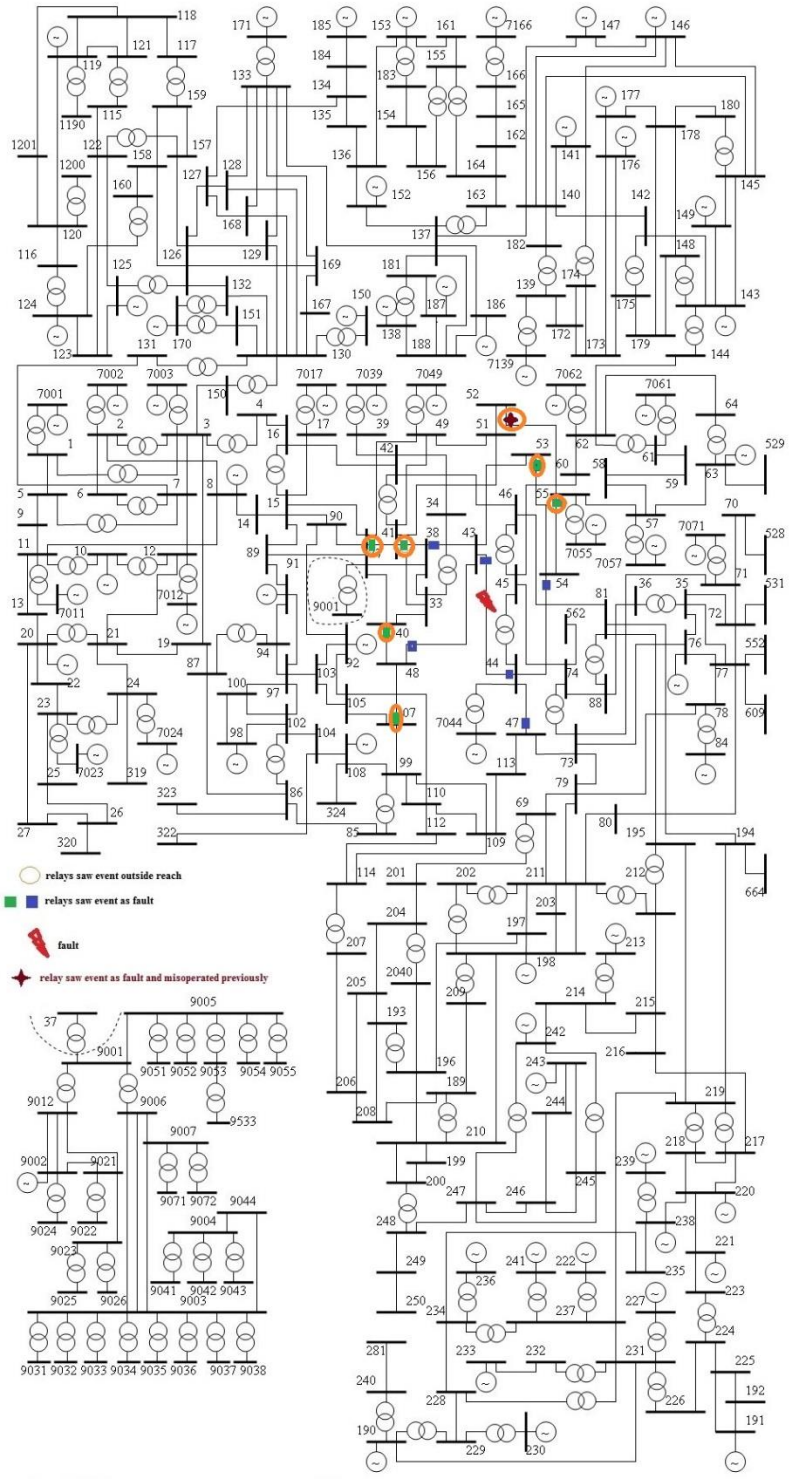

Figure 57. Application of solution methodology to fourth event of the IEEE 300 bus cascading scenario

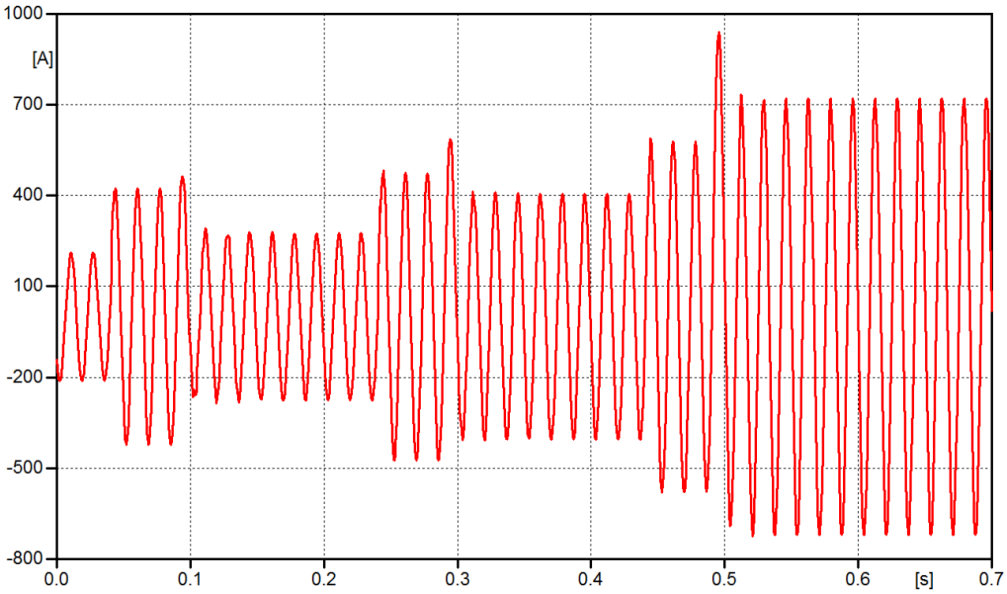

Figure 58. Current of Phase A seen by the relay at bus 30 of line 30-33 during the IUTC 146 cascading event

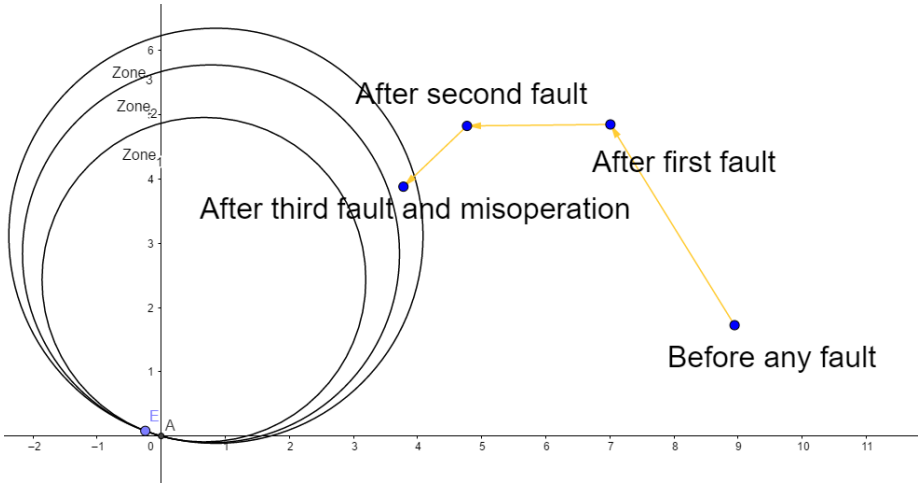

Figure 59. Positive sequence impedance seen by relay at bus 30 of line 30-33 during IUTC 146 cascading scenario under different power levels

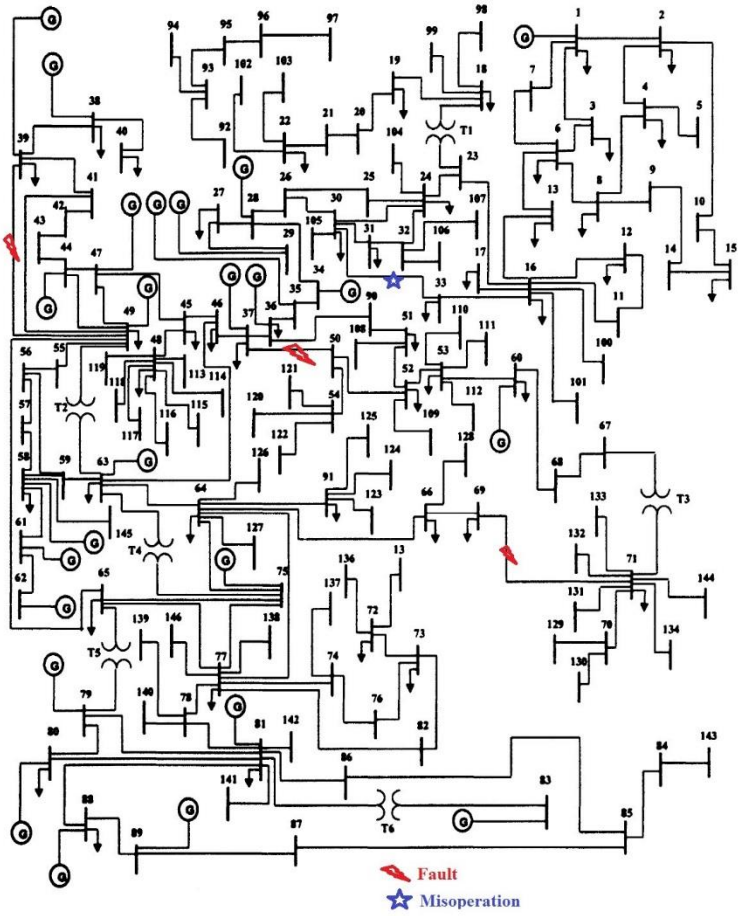

Figure 60. First cascading scenario at the IUTC 146 bus system

4.3.1 Response of the distance relays during cascading scenario

The first event of the scenario is the fault on line 39-49. The response of the distance protection functionality after the addition of the proposed methodology is shown Figure 61 for the first event. As can be seen from the figure, the fault is detected by all distance relays that have line 39-49 in its zone 3 reach denoted by blue squares as well as some green relays that are electrically close to the fault but do not have that relay

in its zone 3 reach. In other words, when the fault is in the forward direction, the results of the disturbance classifier is given by the blue and green squares. The blue squares denote relays that recognized the fault, and these are the only relays that are supposed to respond to the fault. The green squares denote the relays that recognized the fault, but these are relays that are not supposed to respond to the fault since the fault is outside its protection zone. The recognition of the fault by the green relays should not come as a surprise since the disturbance classifier of those relays has been trained with faults that are within 300% of the line length. If we applied the methodology given in section 3.4, then the green squares would not exist since the fault impedance does not fall within their zone 3 (which reaches to 200%). We continue the scenario and apply the path classifiers to all the blue and green relays. For all the relays, the path classifiers successfully identify the current path. When it comes to the reach classifier, the reach classifiers of all green relays see this fault as a fault outside the 200% protection reach, which means that they will not pick up which is denoted by the orange circle in Figure 56. On the other hand, the reach classifier for the blue relays correctly identify the fault within zone 3. At this step, the green relays have stopped working, and the blue relays are still trying to detect whether the fault has been cleared. Finally, once the fault is cleared, all the blue relays in the figure identify the fault clearing because the fundamental current is highly reduced after fault clearing. The results of this step clearly show that limiting the training of the disturbance, path, and reach classifiers to events within 300% of line length was advantageous in this situation as it limited the number of relays that saw the fault.

The second event of the scenario is the fault on line 37-50. The response of the solution methodology to the first event is shown Figure 62. As can be seen from the figure, the fault has been detected by all distance relays that have line 37-50 in its zone 3 reach denoted by blue squares as well as by some green relays that are electrically close to the fault but do not have that relay in its zone 3 reach. In other words, when the fault is in the forward direction, the results of the disturbance classifier are given by the blue and green squares. The blue squares denote relays that recognized the fault, and these are the only relays that are supposed to respond to the fault. The green squares also denote the relays that recognized the fault, but these are relays that are not supposed to respond to the fault since the fault is outside its protection zone. The recognition of the fault by the green relays should not come as a surprise since the disturbance classifier of those relays has been trained with faults that are within 300% of the line length. If we applied the methodology given in section 3.4, then the green squares would not exist since the fault impedance does not fall within their zone 3 (which reaches 200%).

We continue the scenario and apply the path classifiers to all the blue and green relays. For all the relays, the path classifiers successfully identify the current path. When it comes to the reach classifier, the reach classifiers of all green relays see this fault as a fault outside the 200% protection reach which means that they will not pick-up, which is denoted by the orange circles in Figure 56. On the other hand, the reach classifier for the blue relays correctly identifies the fault within zone 3. At this step, the green relays have stopped working and the blue relays are still trying to detect whether the fault has been cleared. Finally, once the fault is cleared, all blue relays in the figure identify fault

clearing because the fundamental current is highly reduced after fault clearing. Again, the results of this step clearly show that limiting the training of the disturbance, path, and reach classifiers to events within 300% of line length was advantageous in this situation as it limited the number of relays that saw the fault.

The third event of the scenario is the fault on line 69-71. The response of the solution methodology to the first event is shown in Figure 63. As can be seen from the figure, the fault has been detected by all distance relays that have line 69-71 in its zone 3 reach denoted by blue squares as well as some green relays that are electrically close to the fault but do not have that relay in its zone 3 reach—in other words—when the fault is in the forward direction, the results of the disturbance classifier is given by the blue and green squares. The blue squares denote relays that recognized the fault and these are the only relays that are supposed to respond to the fault. The green squares denote the relays that recognized the fault, but these are relays that are not supposed to respond to the fault since the fault is outside its protection zone. The recognition of the fault by the green relays should not come as a surprise since the disturbance classifier of those relays has been trained with faults that are within 300% of the line length. If we applied the methodology given in section 3.4, then green squares would not exist since the fault impedance does not fall within their zone 3 (which reaches 200%).

We continue the scenario and apply the path classifiers to all the blue and green relays. For all the relays, the path classifiers successfully identify the current path. When it comes to the reach classifier, the reach classifiers of all green relays see this fault as a fault outside the 200% protection reach, which means that they will not pick-up which is

denoted by the orange circles in the figure. On the other hand, the reach classifier for the blue relays correctly identifies the fault within zone 3. At this step, the green relays have stopped working, and the blue relays are still trying to detect whether the fault has been cleared. Once the fault has been cleared, all blue relays in the figure identify fault clearing because the fundamental current is highly reduced after fault clearing. **It should be emphasized that the disturbance classifier of relay 30 of line 30-33 did not see the event as a fault either in fault inception or clearing thus blocking relay operation even though the impedance falls in its zone 3 after fault clearing which signifies the success of the solution methodology to prevent the protection misoperation.**

The results of this scenario show that limiting the training of the disturbance, path and reach classifiers to events within 300% of the line length was advantageous in this situation as it limited the number of relays that saw the fault. No relay outside the 300% training threshold saw the event as a fault in all faults of the cascading scenario, which shows that security of the relays has been improved. Lastly, it should be emphasized that even though the scenario has been trained with the features at certain load levels, the same scenario has been repeated at different power levels, without retraining the classifiers, and all relays in the system had the same response. This is a direct consequence of the results provided in section 2.6.1.

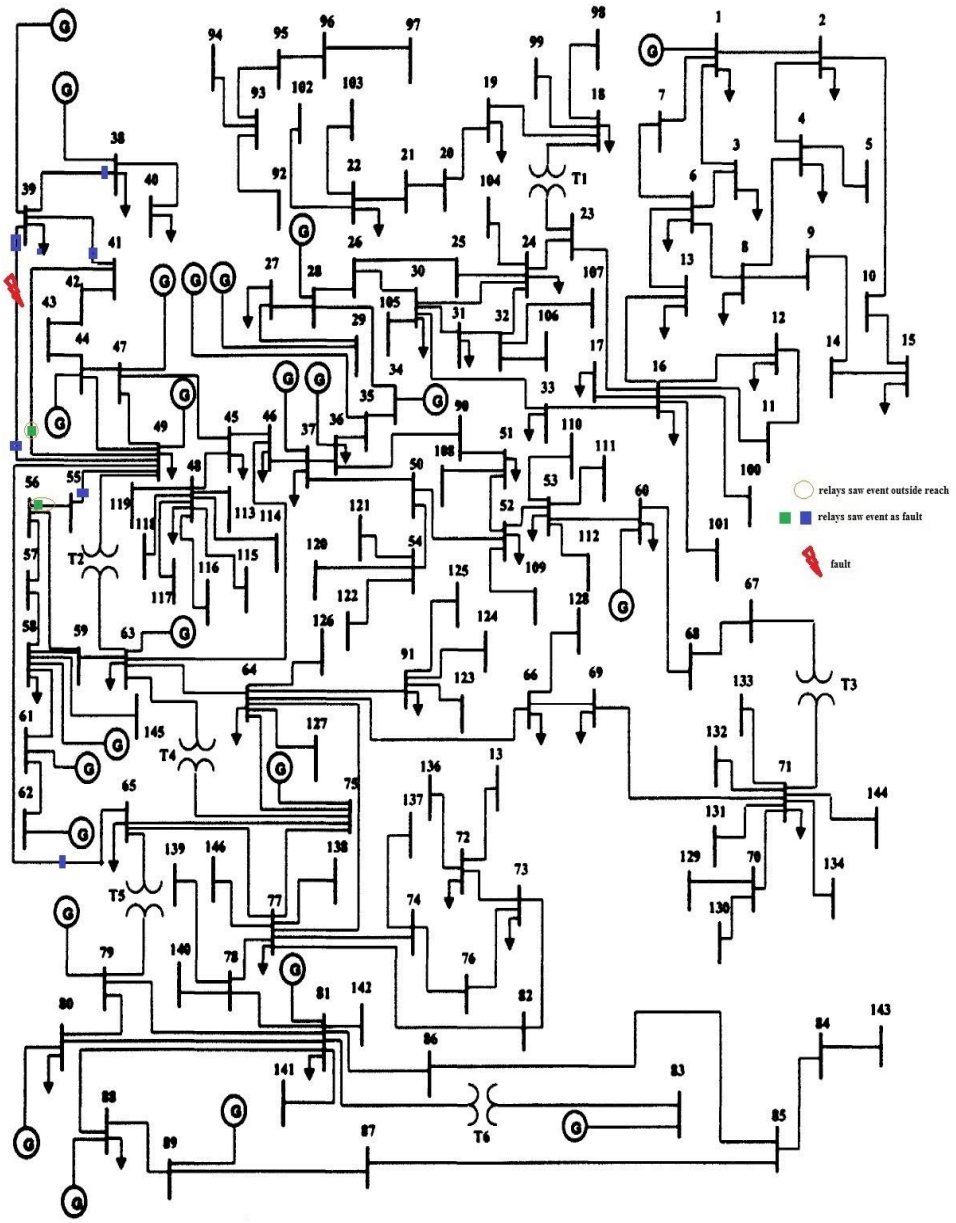

Figure 61. Application of solution methodology to first event of the IUTC 146 bus cascading scenario

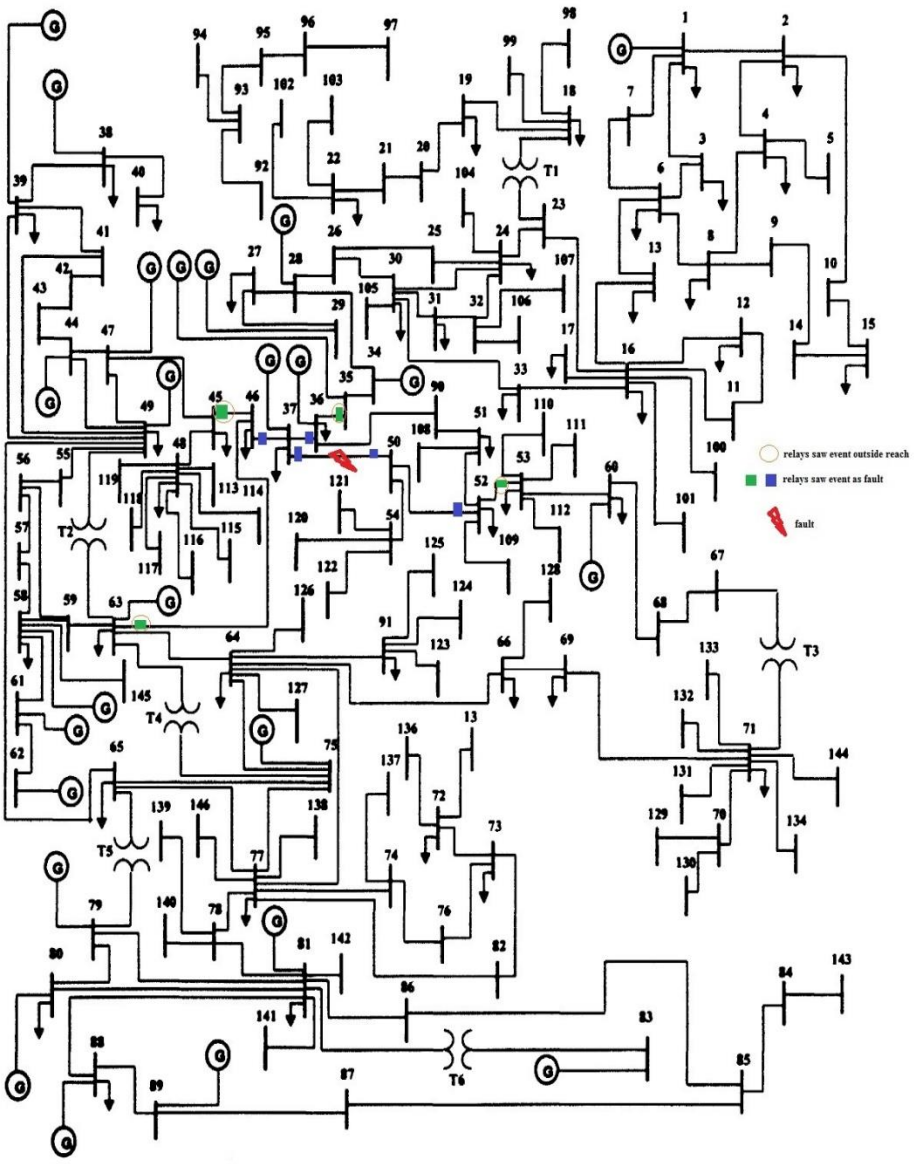

Figure 62. Application of solution methodology to the second event of the IUTC 146 bus cascading scenario

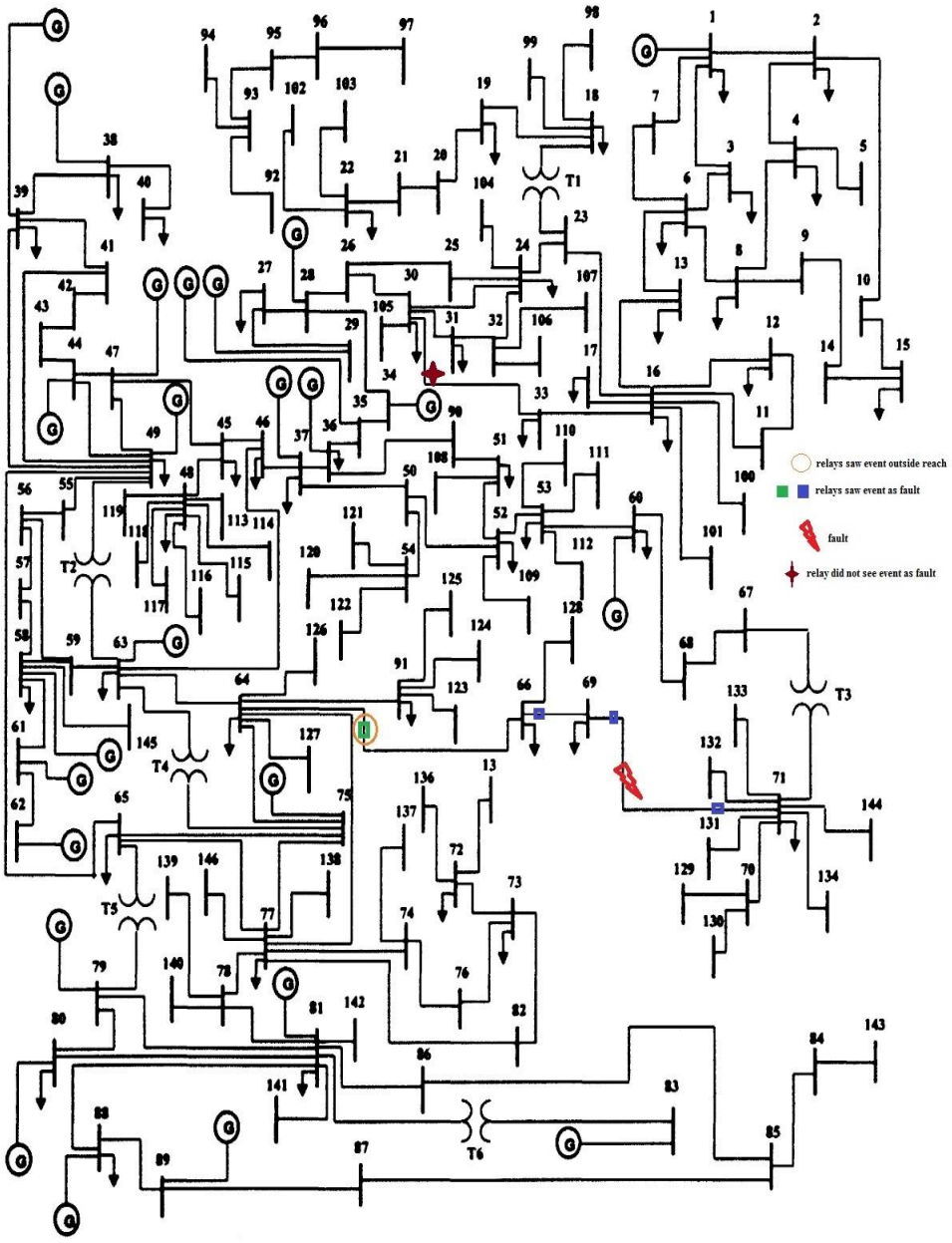

Figure 63. Application of solution methodology to third event of the IUTC 146 bus cascading scenario

4.4 Validation of the classifiers

A comprehensive error analysis is beyond the scope of this dissertation as field validation will need to be performed to understand the nature of the error. However, we provide a preliminary error analysis as a way to anticipate how the classifiers will perform when noise exists in the measurements.

All classifiers in this dissertation are KNN. As previously mentioned, let's assume that the training signal is given by a while the object to be classifier is b. Assuming that a is the closest neighbor to b, then the distance is given as $d = \sqrt{\sum_{i=1}^{n}(a_i - b_i)^2}$.

Now let's assume that the object b has an error of e such that $b' = b + e$. Then, the new distance between a and b' lies in between $|d| - |e|$ and $|d| + |e|$. This is illustrated in Figure 64.

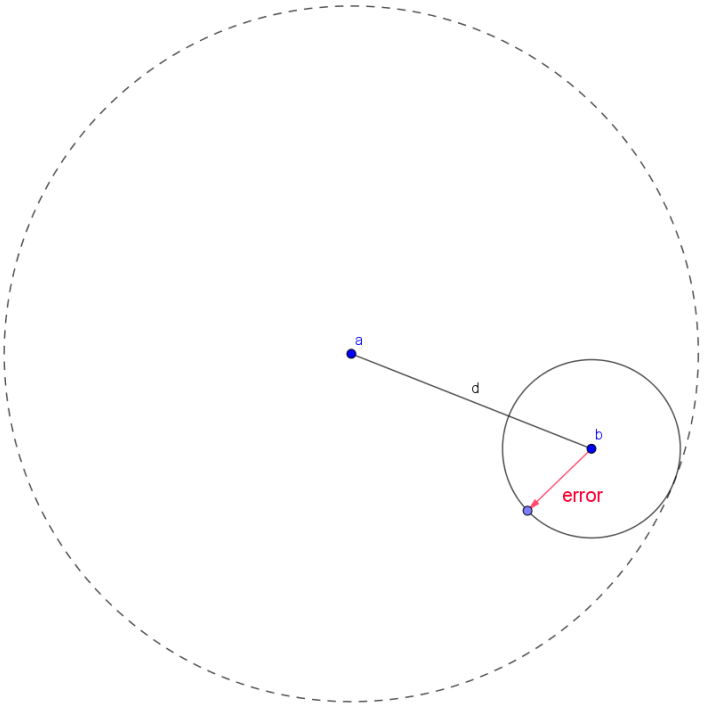

Figure 64. Error analysis

Clearly, object b will never be misclassified unless another object appears from a different class that is close to b than a. This can only happen if the error is large enough to cause the distance to change considerably. However, in our experience this situation is unlikely to occur unless for high resistance faults that can be confused for line switching operations. Simulations show the following:

1. Lightning strikes cause level 3 coefficients to attain extremely high values that are highly unlikely to be attained by any other disturbance event. This is shown in Figure 65.
2. Load switching, and ramping causes the detail coefficients to attain small amplitudes for a small period of time. This is shown in Figure 66.

3. Faults cause the detail coefficients to attain values that are less than lighting strikes but more than line switching and load switching. This is shown in Figure 67 and Figure 68.

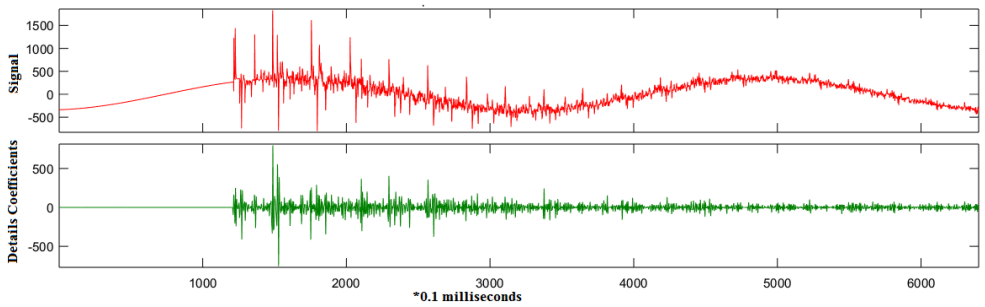

Figure 65. Mode 1 current and level 3 decomposition of a simulated lightning strike

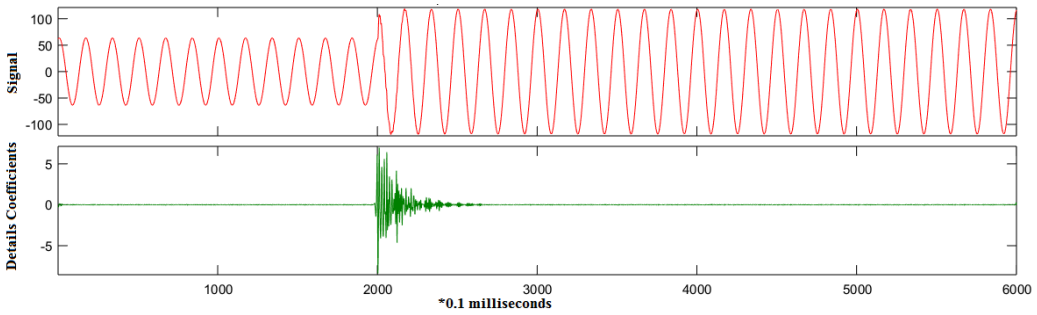

Figure 66. Mode 1 current and level 3 decomposition of a simulated load switching

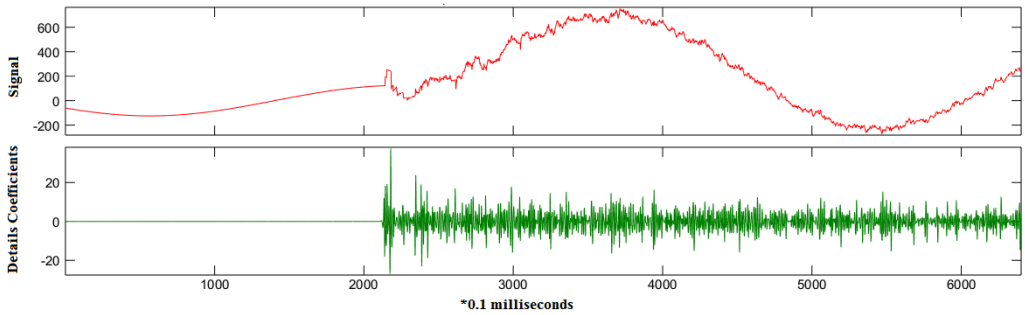

Figure 67. Mode 1 current and level 3 decomposition of a simulated fault

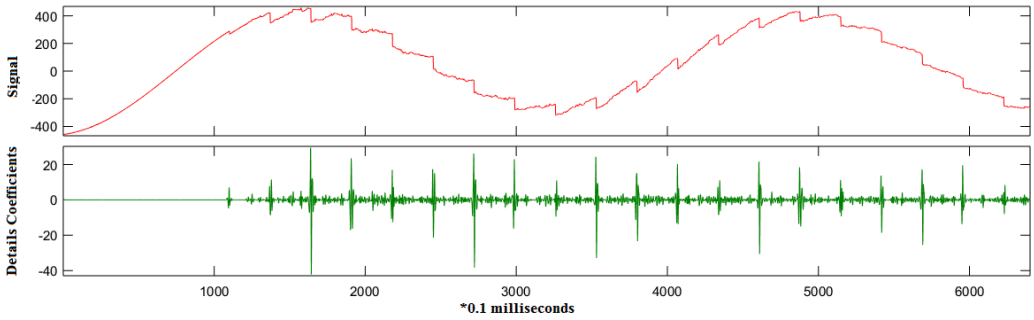

Figure 68. Mode 1 current and level 3 decomposition of a simulated line switching

All figures in this section are waveforms seen by 52/52-55 for comparison purposes. We have tested all classifiers for all distance relays in the system. The classification accuracy will depend on the tower configuration of the line that as shown in Figure 31. The cases that were used to test the classifiers were all within 600% and are described in section 3.1.4. The effectiveness of the disturbance classifier is given in Table 1 as several cases of SNR (signal to noise ratio). The effectiveness of the path classifier is given in Table 2. The effectiveness of the reach classifiers is given in Table 3. For the path classifier, path 1 is line 55-57 and the lines connected to it while path 2 is line 55-54 and all the lines connected to it. It should be noted that Table 1, 2 and 3 provide classification results for several cases of SNR (signal to noise ratio).

Table 1. Validation of the disturbance classifier

	Event type	Classification Accuracy (%)		
		SNR = 30	SNR = 15	SNR = 5
Tower Configuration 1	faults	100	99.21	97.99
	lightning	98.5	97.42	91.98
	non-fault	98	97.19	96.2
Tower Configuration 2	faults	100	99.92	93.59
	lightning	99.2	98.26	97.2
	non-fault	96	95.13	91.13
Tower Configuration 3	faults	100	99.17	94.78
	lightning	99.5	98.97	98.67
	Non-fault	98.32	97.01	92.69
Tower Configuration 4	faults	100	99.12	95.41
	lightning	99	97.83	95.1
	non-fault	99.6	98.77	90.24
Tower Configuration 5	faults	100	99.04	96.9
	lightning	99.5	99.14	98.3
	non-fault	98.52	96.16	95.72
Tower Configuration 6	faults	100	99.45	90.33
	lightning	98.8	96.84	94.3
	non-fault	98.52	97.89	96

Table 2. Validation of path classifier

	Which path?	Classification Accuracy (%)		
		SNR = 30	SNR = 15	SNR = 5
Tower Configuration 1	Line 52-55	99.03	98.8	97.2
	path 1	94.2	93.4	91.6
	path 2	97.84	97.1	90.5
Tower Configuration 2	Line 52-55	98.94	98	94.9
	path 1	95.06	94.1	92.7
	path 2	98.3	98.1	93.6
Tower Configuration 3	Line 52-55	98.21	97.4	94.4
	path 1	96.45	95.5	88.3
	path 2	98.81	97.9	89.1
Tower Configuration 4	Line 52-55	99.04	98.7	91.7
	path 1	98.56	97.7	89.5
	path 2	98.93	97.9	93.6
Tower Configuration 5	Line 52-55	99.47	98.6	92.4
	path 1	99.11	99	92.5
	path 2	98.91	98.5	92

Table 3. Validation of reach classifier

	Event type	Classification Accuracy (%)		
		SNR = 30	SNR = 15	SNR = 5
Tower Configuration 1	path 1	100	99.41	93
	path 2	99.5	99.1	92.3
Tower Configuration 2	path 1	95.06	95	93.24
	path 2	99.7	98.3	89.32
Tower Configuration 3	path 1	99.8	99.2	93.34
	path 2	100	99.66	91.83
Tower Configuration 4	path 1	100	99.16	90.23
	path 2	99.5	99.1	93.5
Tower Configuration 5	path 1	100	99.5	92.84
	path 2	99.3	98.5	94.05

4.5 Operation under power swing conditions

One of the main issues that need to be addressed by the proposed method is correct operation during power swing conditions because swing scenarios were not included in the training of any of the classifiers. A power swing scenario has been created in the IEEE 300 bus system. A bolted three-phase fault was created at mid-point of line 105-110 of Figure 53. The fault was created at 0.2 s and cleared at 0.5 s. This intentional delay in clearing the fault caused a power swing. Consequently, the impedance seen by relay 8 of line 8-14 entered zone 3 as shown in Figure 69. In Figure 70, the level 3 decomposition of the mode 1 current of the three-phase currents of line 8-14 is zero at all times except for small edges corresponding to the instants when the fault

is created and cleared. The disturbance classifier of relay 8 of line 8-14 sees these two edges as non-fault because the DWT coefficients are so small in comparison to the fault level 3 detail coefficients. The relay is thus blocked and misoperation is avoided.

Another concern is when a zone 3 fault occurs during a power swing. To simulate this scenario, a single-phase fault with a 20-Ω resistance was created on line 15-90 after the zone 3 fault was cleared during the power swing condition. Figure 71 shows the DWT coefficients of the zone 3 fault are much larger than the small edges of Figure 70, and the proposed method applied at relay 8 of line 8-14 correctly sees this disturbance as a fault. It is clear from these two scenarios that low frequency oscillations such as power swing or inter-area oscillations do not affect the operation of the proposed method because these low frequency disturbances will not appear in a level 3 decomposition.

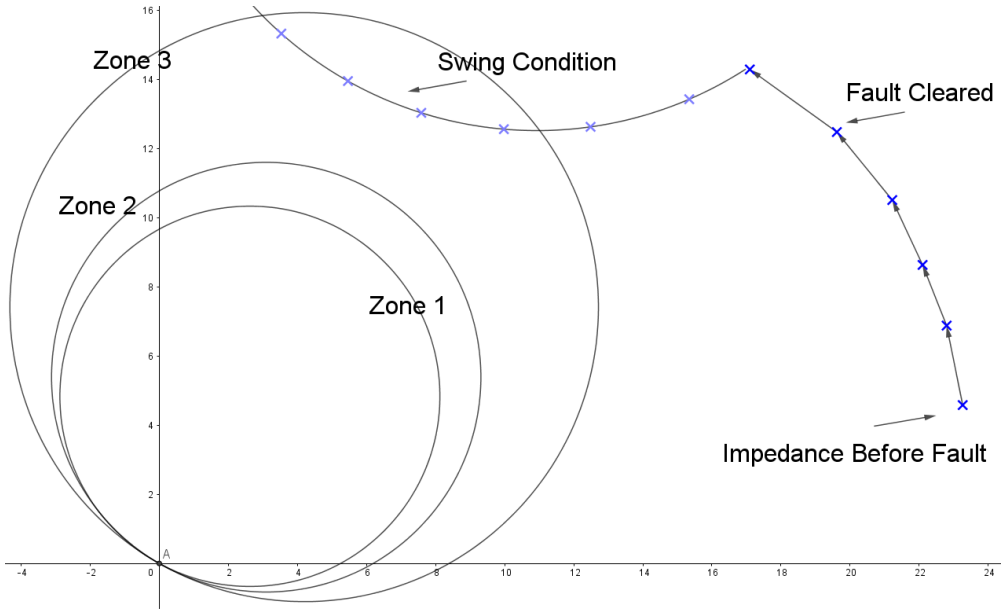

Figure 69. Positive sequence impedance trajectory of relay 8 of line 8-14

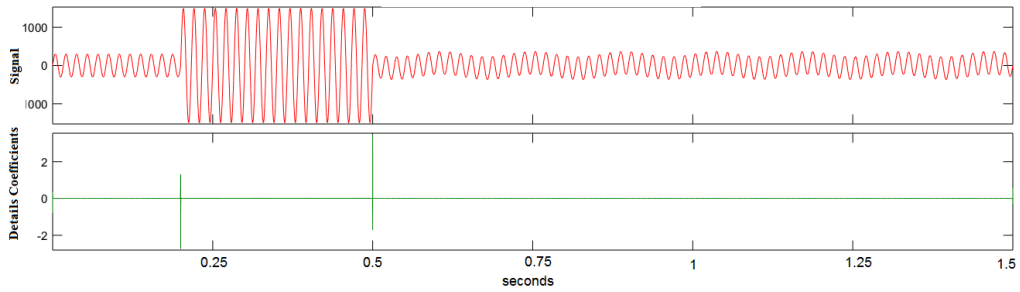

Figure 70. Mode 1 current and Level 3 decomposition of relay 8 of line 8-14 during power swing

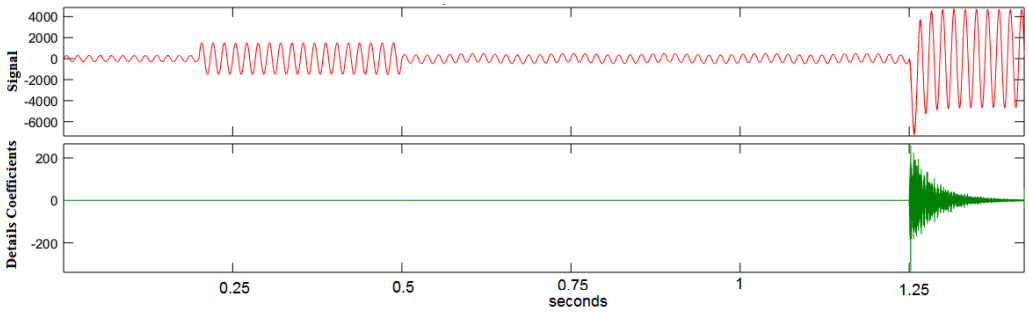

Figure 71. Mode 1 current and level 3 decomposition of relay 8 of line 8-14 during power swing

4.6 Effect of reducing zone 3 reach

One of the cornerstones of the proposed methodology is the reduction in the zone 3 reach from 220% to 200%. To see how this reduction affects the operation of zone 2 and zone 3 distance elements, several faults were created, and the operation of zone 3 relays was compared. The results are given in Table 4 and Table 5 for the IEEE 300 bus system and the IUTC 146 bus system, respectively. For example, refer to relay 7/7-12 in the IEEE 300 bus system. A fault was simulated just front of relay 7/7-12. As can be seen from the Table 4, relay 150/3-150 used to detect this fault in the forward direction

with the original distance relaying functionality. However, with the modification of distance relay functionality, the relay 150/3-150 does not detect this fault anymore.

As can be seen from the tables, the effect of the proposed method is to completely eliminate the operation of the second layer of the backup relays.

Table 4. Effect of Zone 3 reach reduction in the IEEE 300 bus system

		Conventional Operation		Proposed Method
Line	**Fault Location**	**Zone 2**	**Zone 3**	**Relays Identified Event on Adjacent Line**
7-12	5%	3/3-7,131/7-131	3/3-19,150/3-150,21/12-21	3/3-7,131/7-131,21/12-21
181-187	50%	None	137/137-181,138/181-138,188/187-188	Same as Zone 3
19-21	95%	24/21-24,12/12-21	3/3-19,87/19-87,7/7-12,319/24-319	3/3-19,87/19-87,24/21-24,12/12-21

Table 5. Effect of Zone 3 reach reduction in the IUTC 146 bus system

		Conventional Operation		Proposed Method
Line	**Fault Location**	**Zone 2**	**Zone 3**	**Relay identified event on adjacent line**
2-14	50	None	21/2-21,11/11-14,6/6-14	21/2-21,11/11-14,6/6-14
14 1-17	95 %	10/10-141,15/141-15,3/141-3,141/141-3,19/19-3	23/19-23,4/4-19	10/10-141,15/141-15,3/141-3,141/141-3,19/19-3
31-38	5%	37/37-38,7/7-38	41/31-41,40/31-40,8/7-8,33/33-37,35/35-37	41/31-41,40/31-40,37/37-38,7/7-38

4.7 Performance studies of the proposed method

In this section, we show the performance of a few relays under standard testing conditions. We select as examples a few relays from the IEEE 300 bus system [89] given in Figure 53. For this type of analysis, we use the usual procedure of testing distance relays given in [14] and [15], namely creating disturbances inside and outside the reach of the relay to gauge relay performance metrics. The setup used for testing the performance of the relay was previously described in section 4.1. We provide a theoretical discussion on the various metrics used to evaluate the performance of the relay. The cases used to test relay performance are presented in section 3.1.4. Lastly, we provide results of performance analysis in tabular format.

4.7.1 Performance metrics

In this section, we show the performance of a few relays under standard testing conditions. We select the IEEE 300 bus system as a benchmark system. For this type of analysis, we use the usual procedure of testing distance relays given in [95], [96], namely creating disturbances inside and outside the zones of the relays to gauge relay performance metrics. We describe the setup used for testing the performance of the relays in the benchmark system. We provide a theoretical discussion on the various metrics used to evaluate the performance of the relays. The cases used to test relay performance are presented. Lastly, we discuss the results of performance analysis.

4.7.2 Setup of the IEEE 300

The test system that was used is the IEEE 300 bus system [89] given in Figure 53.

The test system was built in PSCAD. The following were made to make the computer models realistic:

1. Current transformer (CT) models [55] and capacitive transformer models (CVT) are included [90]
2. Tower configurations are taken into consideration. The tower configurations are taken from [91] and are given in Figure 31. All lines in the system are modeled in phase domain.
3. Power transformers are modeled according to [92]
4. Synchronous machines are modeled according to [93]
5. Standard Library PSCAD distance element was used. The proposed classifiers were modeled as well for each distance relay in the system.
6. Surge Arresters were also modeled according to [94]
7. Distance relays are built with half-cycle Fourier filters for all zones.

4.7.3 Various metrics

In this section, we discuss the various performance metrics used to evaluate the operation of the overall distance protection functionality. This refers to the combined performance of the proposed method and the distance elements. The power system community uses four main metrics to assess the performance of any relay: speed, dependability, security, and sensitivity. All are delineated in the following sections.

4.7.3.1 Dependability

Dependability can be defined as the ability of the relay to trip line faults under assumed operating and faulty conditions with the required speed and sensitivity correctly [95]. Mathematically speaking, dependability in percentage is

$$\frac{in-zone\ faults\ detected\ Successfully}{Total\ number\ of\ in-zone\ faults} \times 100.$$

It should be noted that dependability is a holistic measure for all faults that occur within each of the zones of the relay. A fault case is ruled detected if the relay can detect that case in the allotted protection time. If the relay detects the fault case in a time that is more than the trip time allotted, the case will be counted as not detected and counted against the relay performance. To gain a detailed look into the operation of the relay, a sensitivity study needs to be performed. Sensitivity will be dealt with in section 4.7.3.3.

4.7.3.1.1 Description of the parameters of the study

Since the IEEE 300 bus system has more than 600 distance relays, we picked a few relays that are representative of the response of all relays in the system. Here, relay 52/52-55 in the IEEE 300 bus system is shown as an example of coverage for the surrounding region; which is shown in Figure 72. The region shown in Figure 72 represents all three zones of the distance relays.

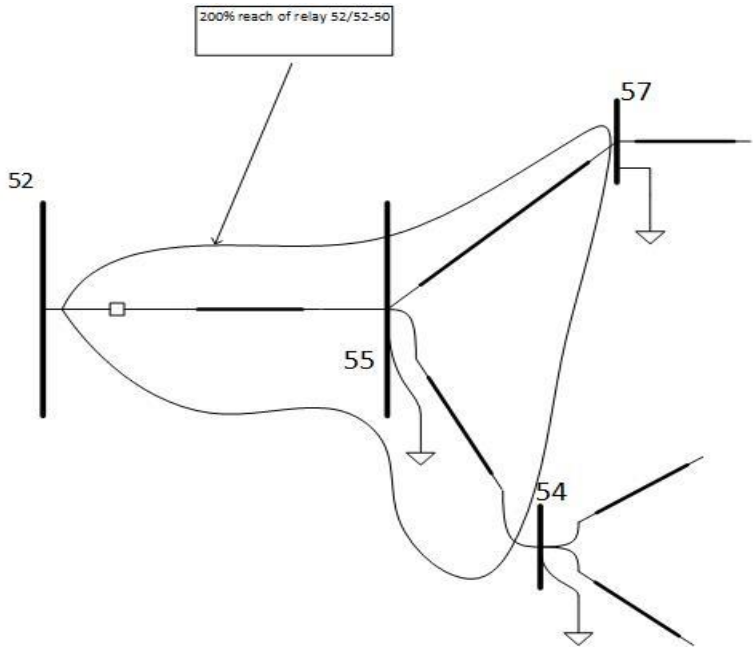

Figure 72. Testing dependability of relay 52/52-55

4.7.3.1.2 Fault cases

All disturbance cases were created with the tool released in [97]. Fault cases were created in batches; i.e., a batch for each line. Each batch has fault parameters, these parameters are the following: incipient angle, fault resistance, fault location and fault type. All types of faults have been created, i.e., AG, BG, CG, AB, BC, CA, ABG, CBG, ACG, ABC, ABCG. Incipient angles are from 0 to 350 degrees in 2-degree increments. Fault resistance assumes the values: 0, 5, 50, 100 Ω, 200 Ω and 1000 Ω. The distance takes the following values: 5%, 15%, 35%, 50%, 65%, 80% and 95% which are all percentages of the total line length. Faults used in this type of analysis are assumed permanent and never cleared.

4.7.3.1.3 Findings and discussions

In traditional distance relaying, the relay is judged based on whether it successfully detected the fault. We continue this tradition and study the performance of the overall distance protection functionality in each of its zones.

Since we use high-frequency current oscillations (HFCO) to enhance the distance protection functionality, the tower configuration affects performance. However, we averaged the performance for all tower configurations based on selections that together can represent all. Thus, Table 6 summarizes the dependability of a few relays in the IEEE 300 bus system in various areas.

We elect to explain the cases that were wrongly classified as faults as well as cases that were not detected as faults even though they were later found to be such. First and foremost, the horizontal tower configuration poses great challenges for model analysis as explained in [98]. Due to the phase arrangement of the horizontal tower configurations (Tower 2 in Figure 31), one of the aerial modes gets totally removed due to the structure of the modal matrix, which greatly affects the feature vector. This issue becomes more pronounced when two adjacent towers have horizontal tower configurations as is the case with relays that have a dependability of less than 96% in Table 6 regardless of the area. It should be noted that a 50 Ω fault is a high resistance fault on the 66-kV level but is not considered as such on the 345 kV level. This is the main reason for the discrepancy in dependability between the relays. Second, some faults were not detected and were thus classified as non-fault cases. This was apparent for cases of high-resistance faults that cause very low amplitude HFCO and a very low

short circuit current for the relays that have a dependability of less than 96% as shown in Table 6 regardless of the area. Third, single line to ground faults that occur around the current zero crossing were not detected because no HFCO are present when the disturbance occurs at a current zero crossing; this was equally correct for all relays in all areas and all zones. Clearly, Table 6 shows that the performance of the relays can be comparable to each other even when they are for different transmission lines at different voltage levels at different areas in the network. Lastly, a handful of cases were not detected correctly as zone 1 faults, and the majority of misclassifications occur beyond the 100% relay reach. The same observations apply to Zone 2 and Zone 3 as shown in

Table 7 and Table 8. The tables in this section indicate the absence of a high correlation between the dependability of the relay and the area it covers. Even when the available short circuit is relatively low, the dependability in Zone 2 or Zone 3 could be higher than that in Zone 1. This will be a subject for further research.

Finally, we provide few graphs that summarize the performance of relay 52/52-55 with respect to fault location, fault resistance and fault type in Figure 73, Figure 74, and Figure 75, respectively.

Table 6. Zone 1 dependability of select relays in IEEE 300 bus system

Relay	Area	Event type	Percentage Successful Detection
52/52-55	1	faults	98.13
3/3-19	1	faults	96.7
123/123-124	2	faults	96.9
115/115-122	2	faults	95.3
194/194-219	3	faults	99.6
203/203-198	3	faults	98.4

Table 7. Zone 2 dependability of few relays in IEEE 300 bus system

Relay	Area	Event type	Percentage Successful Detection
52/52-55	1	faults	97.4
3/3-19	1	faults	96.4
123/123-124	2	faults	97.2
115/115-122	2	faults	98.4
194/194-219	3	faults	97.3
203/203-198	3	faults	97.8

Table 8. Zone 3 dependability of few relays in IEEE 300 bus system

Relay	Area	Event type	Percentage Successful Detection
52/52-55	1	faults	96
3/3-19	1	faults	95.5
123/123-124	2	faults	95.6
115/115-122	2	faults	95.9
194/194-219	3	faults	98.2
203/203-198	3	faults	98

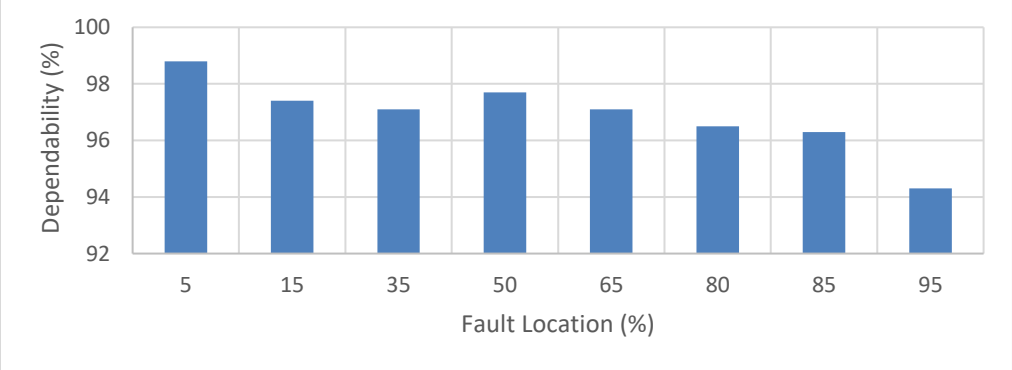

Figure 73. Dependability of relay 52/52-55 versus fault locations

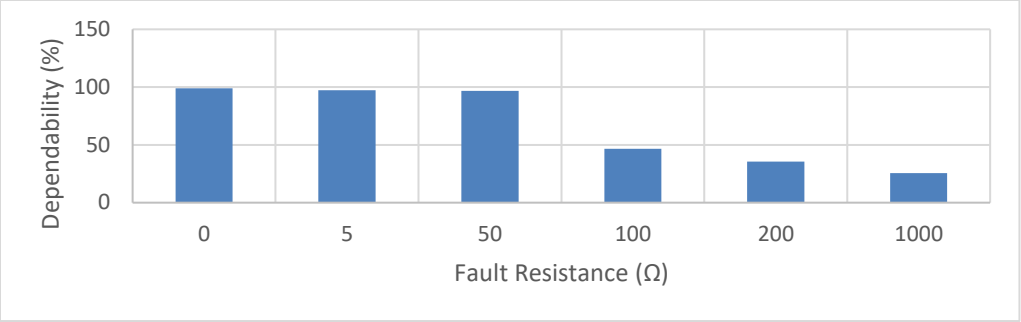

Figure 74. Dependability of relay 52/52-55 versus fault resistance

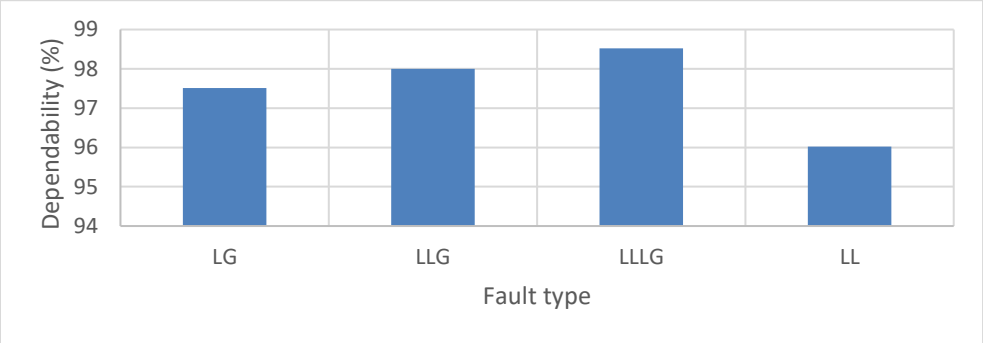

Figure 75. Dependability of relay 52/52-55 versus fault types

4.7.3.2 Security

The second metric used to quantify relay operation is security. Security can be defined as the ability to restrain for all conditions other than line faults, especially out of zone faults [99]. Thus, security is defined as $(1 - \frac{disturbances\ detected\ as\ internal\ faults}{total\ number\ of\ \ disturbances}) \times 100$.

As clear from the definition, several non-fault disturbances need to be created inside and outside of the relay reach to assess relay security. Also, several out-of-zone fault cases need to be created to test the security of the distance relay. All cases will be explained in the following sections.

4.7.3.2.1 Description of the parameters of the study

Unlike relay dependability, which is not affected by non-fault disturbances, relay security is affected by both out-of-zone faults and non-fault disturbances [100]. The relay could confuse some out-of-zone faults as internal faults which could affect its security. As mentioned in [95], non-fault disturbances such as switching could mislead distance relaying. For this reason, we include line switching cases to test relay performance.

For non-fault disturbances and out-of-zone faults, we focus on the same relays presented in the preceding section as they are representative of all relays in the system.

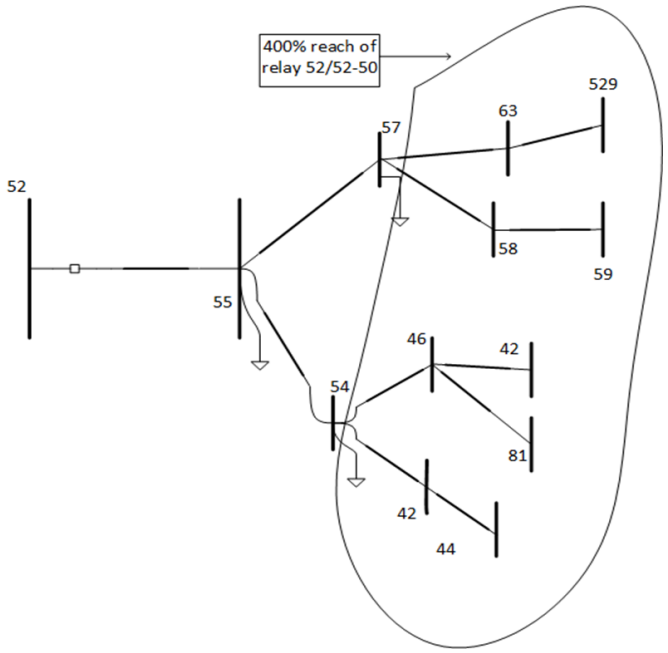

Figure 76. 400% reach of relay 52/52-55

4.7.3.2.2 Security of majority of the relays in IEEE 300 bus system

The out-of-zone fault disturbance cases were created for locations beyond the 200% relay reach but less than 400% of the relay reach as given in Figure 76 using ATPMAT [97] and are similar to the ones given in section 3.1.4.1.

Switching operations were created within 400% of relay reach (including 200% of the relay reach). Switching was done for each line, reactor and capacitor bank in the system. For line switching cases, a batch for each line was created. Each batch consists of smaller batches, and each of the smaller batches has their switching controlled by one of the circuit breakers at each terminal. For example, a line connecting bus 37 and bus 58 would have a smaller batch for switching using the breaker installed on terminal 37, and another smaller batch for switching would use the breaker on terminal 58. The variable in these switching cases is the moment of switching. Switching angles range from 0 to 360 degrees in 2-degree increments. In this way, 360 cases per batch were created. The same process holds true for reactor and capacitor bank switching. Each bank in the system was switched. The switching variable was the timing of the switch. Switching angles are much like line switching.

4.7.3.2.3 Findings and discussion

Table 9 summarizes the security of the select relays for non-fault disturbances and out-of-zone faults. We count a case as a failure if any of the distance protection elements fail to detect it correctly.

Table 9. Security of few relays in IEEE 300 bus system

	Area	Event type	Successful Detection (%)
52/52-55	1	faults	99
		line switching	99
3/3-19	1	faults	97
		line switching	98.2
123/123-124	2	faults	98.5
		line switching	98.6
115/115-122	2	faults	97.9
		line switching	97.5
194/194-219	3	faults	97.2
		line switching	98
203/203-198	3	faults	97
		line switching	98.2

As can be seen from the table, the security of the relays is very high. In most cases, we can reject non-fault disturbance more than 96% of the time irrespective of the area. The out-of-zone faults are detected correctly 97% of the time. This shows how the method enhances the security of relays. The fault cases that were not classified correctly as out-of-zone faults were very close to the 200% relay reach and were detected as in-zone faults. Some line switching operations, which occur around current zero crossing, were detected as high-resistance three-phase faults. Also, some non-fault conditions were incorrectly identified as high-resistance faults. Obviously, as noted in this account of our research results, high-resistance faults pose great challenges to the proposed method. Further research is needed to see if a statistical correlation exists between relay performance and the area; however, our results so far do not show that such a relationship exists.

4.7.3.3 Sensitivity

Sensitivity studies focus on the variations in relay operation, looking for various changes in fault conditions. Historically, sensitivity is defined as the ability to respond to low current line faults as per the assumed fault resistance and system short circuit level [99]. With this definition in mind, sensitivity is a qualitative study of relay dependability in a more granular manner with respect to fault resistance, fault location, and operating time.

The parameters of the study are the same as the ones given in section 4.7.3.1.1.

4.7.3.3.1 Findings and discussion

To gain a more detailed or granular view into the operation of the relays, their sensitivity with respect to the fault parameters were studied. Figure 77 provides an overview of the sensitivity of relay 52/52-55 under various values of fault resistance for different fault locations. As can be seen from the figures, the method takes much longer to respond to high resistance faults. It should also be noted that the figure shows the high-resistance faults that were detected, which were a minority. Also, as the fault moves to the end of the line, it takes the relay more time to detect it.

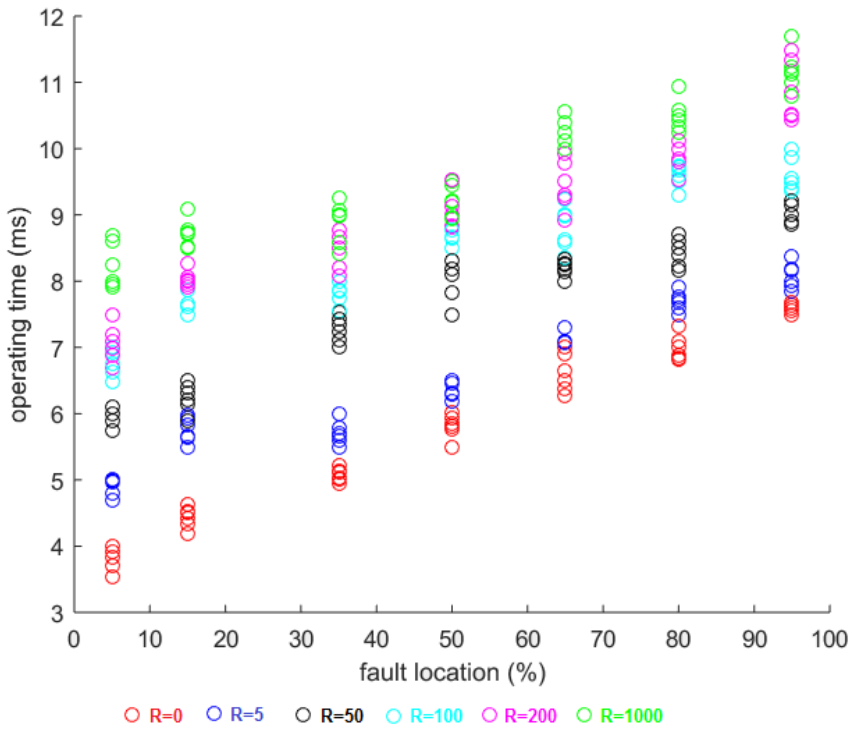

Figure 77. Sensitivity of relay 52/52-55 to fault conditions

4.7.3.4 Conclusions

Various relay performance metrics were evaluated. Dependability of the relay is highly reliant on the fault resistance in this study. The proposed method is not suitable for detection of high resistance faults. Even though the proposed method enhances relay security, it cannot enhance relay security in all imaginable situations. This is especially true when the available short circuit MVA at the relay location is small compared to the line rating. This situation arises in remote power systems; thus, more research and solutions need to be found for this problem.

4.8 Summary

Various case and performance studies were presented. The case studies consisted of simulated cascading scenarios in two test systems as well as power swing cases. The distance protection functionally for distance relays in the test systems were all modified per the solution methodology. It was found that the security of the distance relays was improved and misoperation was avoided.

The performance studies were created to verify that the proposed methodology does not affect the traditional operation of zone 1, zone 2, and zone 3 relays. Based on the results of the performance studies, it was found that the usual operation of distance protection is not affected by the proposed methodology except for a slight reduction in zone 3 reach.

5. CONCLUSIONS AND FUTURE WORK

5.1 Conclusions

Wide-area cascading scenarios can have major social impacts. A large portion of these cascading scenarios is due to distance protection misoperation. In this dissertation, a method was proposed to increase the security of distance protection. The backbone of the method is asserting that the impedance that falls in the operating characteristics of the relay is due to a fault within the relay reach. Once this is asserted, another module detects whether the fault is cleared, and the trip decision is made.

Through advanced signal processing techniques and artificial intelligence, several classifiers were designed. Those classifiers work in harmony with each other to prevent distance protection misoperation.

One classifier asserts that a fault occurred in the transmission network. Once this is done, other classifiers process the fault data to determine whether the fault is within the relay reach. If so, another stage detects whether the fault is cleared. If the fault is cleared, a blocking command will be sent to the relay to prevent misoperation. Since not all faults are initialized via broken conductors, a separate module was created to detect lightning faults as they are responsible for the majority of transmission line faults. For the proposed method to work well, a slight reduction in zone 3 reach had to be made. This reduction only disables the second layer of back-up protection for any circuit breaker and should not be of a great practical concern.

Several cases and performance metrics were used to study and evaluate the proposed method. The case studies included dozens of wide-area cascading scenarios.

The proposed method was tested for each relay in those case studies and for each event in the cascading scenarios. The performance metrics evaluated the proposed method under standard testing conditions. We found that the proposed method does not affect the traditional zone 1, zone 2, and zone 3 operation except for a slight reduction on zone 3 reach. We also found that the proposed method does not perform very well when a fault occurs close to zero incipient angle. Lastly, we found that the proposed method does not perform very well in systems with low short circuit MVA.

5.2 Comments and recommendations

The addition of the proposed method was shown to make the distance relay achieve high operation security. However, it was found that the proposed method is not adequate for detecting high-resistance faults. The proposed method was also found to be inapplicable to low short circuit levels in the transmission network.

5.3 Future work

Even though a preliminary error analysis was done in this dissertation, an extensive error analysis is still needed to quantify the nature of errors in high frequency oscillations. This is needed to guard against any possible nuisance tripping. The purpose of this error analysis is to ensure maximum security when using field measurements, and inevitably, to prevent errors due to harsh power system conditions.

Additionally, field validation needs to be undertaken. This is needed as it is not possible to model every aspect of the power system. For example, insulation failure following a lightning strike occurs very often. However, this phenomenon cannot be

modeled in the detailed modeling of EMTP. Transmission line conductance and Corona losses were ignored as well.

Moreover, the classifiers in this dissertation are staged one after the other. Recent research in pattern recognition indicates that the case at hand can be a candidate for a deep neural network. Whether this is correct is an open question.

Another improvement is the way the classifiers were designed. Half a cycle of post-disturbance data was used to train the classifiers. This fixed window approach raised the need to handle lightning faults differently as it is not possible to distinguish fault transients occurring milliseconds after lightning strikes. Whether we can use a recurrent pattern recognition approach to eliminate the need to handle this phenomenon in an exceptional manner is left for future research.

For the two simulated test systems, there were a limited number of cascading failures which led to zone 3 misoperation. Therefore, zone 3 misoperation should be studied in additional simulated test systems to determine how the characteristics of the new method needs to be enhanced to be more generalizable

Lastly, a good method for detecting high-resistance faults needs to be incorporated in the overall methodology.

REFERENCES

[1] P. Hines, J. Apt, and S. Talukdar, "Large blackouts in North America: Historical trends and policy implications," *Energy Policy*, vol. 37, no. 12, pp. 5249–5259, 2009.

[2] K. Yamashita, J. Li, P. Zhang, and C.-C. Liu, "Analysis and control of major blackout events," in *Power Systems Conference and Exposition, 2009. PSCE'09. IEEE/PES*, 2009, pp. 1–4.

[3] J. Chen, J. S. Thorp, and I. Dobson, "Cascading dynamics and mitigation assessment in power system disturbances via a hidden failure model," *Int. J. Electr. Power Energy Syst.*, vol. 27, no. 4, pp. 318–326, 2005.

[4] R. Baldick *et al.*, "Initial review of methods for cascading failure analysis in electric power transmission systems, IEEE PES CAMS task force on understanding, prediction, mitigation and restoration of cascading failures," in *Power and Energy Society General Meeting-Conversion and Delivery of Electrical Energy in the 21st Century, 2008 IEEE*, 2008, pp. 1–8.

[5] B. Liscouski and W. Elliot, "Final report on the august 14, 2003 blackout in the united states and canada: Causes and recommendations," *A Rep. to US Dep. Energy*, vol. 40, no. 4, 2004.

[6] NERC, "Standard PRC-004-3 - Protection System Misoperation Identification and Correction (PRC-004-3)." Feb-2014.

[7] D. Novosel, M. M. Begovic, and V. Madani, "Shedding light on blackouts,"

Power Energy Mag. IEEE, vol. 2, no. 1, pp. 32–43, 2004.

[8] D. N. Kosterev, C. W. Taylor, and W. A. Mittelstadt, "Model validation for the August 10, 1996 WSCC system outage," *Power Syst. IEEE Trans.*, vol. 14, no. 3, pp. 967–979, 1999.

[9] Entoso-E, "Final Report on Blackout in Turkey on 31st March 2015," 2015.

[10] A. Abdullah, A. Esmaeilian, G. Gurrala, P. Dutta, T. Popovic, and M. Kezunovic, "Test Bed for Cascading Failure Scenarios Evaluation," in *International Conference on Power Systems Transients (IPST) 2013*, 2012, pp. 18–20.

[11] A. M. Abdullah and K. Butler-Purry, "Distance protection zone 3 misoperation during system wide cascading events: The problem and a survey of solutions," *Electr. Power Syst. Res.*, vol. 154, 2018.

[12] M. J. Thompson and D. L. Heidfeld, "Transmission line setting calculations-beyond the cookbook," in *Protective Relay Engineers, 2015 68th Annual Conference for*, 2015, pp. 850–865.

[13] S. Protection and C. T. F. of the NERC Planning Committee, "Increase Line Loadability by Enabling Load Encroachment Functions of Digital Relays." Dec-2005.

[14] S. Protection and C. T. F. of the NERC Planning Committee, "NERC Standard PRC-023-2." Dec-2005.

[15] S. H. Horowitz and A. G. Phadke, "Third zone revisited," *Power Deliv. IEEE Trans.*, vol. 21, no. 1, pp. 23–29, 2006.

[16] ERCOT, "ERCOT Nodal Protocols-Section 5: Transmission Security Analysis

and Reliability Unit Commitment." 2017.

[17] CAISO, "California ISO Planning Standards." 2015.

[18] S. H. Li, N. Yorino, and Y. Zoka, "Operation margin analysis of zone 3 impedance relay based on sensitivities to power injection," *IET Gener. Transm. Distrib.*, vol. 1, no. 2, pp. 312–317, 2007.

[19] S. Li, N. Yorino, M. Ding, and Y. Zoka, "Sensitivity analysis to operation margin of zone 3 impedance relays with bus power and shunt susceptance," *IEEE Trans. Power Deliv.*, vol. 23, no. 1, pp. 102–108, 2008.

[20] M. R. Aghamohammadi, S. Hashemi, and A. Hasanzadeh, "A new approach for mitigating blackout risk by blocking minimum critical distance relays," *Int. J. Electr. Power Energy Syst.*, vol. 75, pp. 162–172, 2016.

[21] H. Song and M. Kezunovic, "A new analysis method for early detection and prevention of cascading events," *Electr. Power Syst. Res.*, vol. 77, no. 8, pp. 1132–1142, 2007.

[22] B. Ravikumar, D. Thukaram, and H. P. Khincha, "An approach using support vector machines for distance relay coordination in transmission system," *IEEE Trans. Power Deliv.*, vol. 24, no. 1, pp. 79–88, 2009.

[23] B. Ravikumar, D. Thukaram, and H. P. Khincha, "An approach for distance relay co-ordination using support vector machines," in *TENCON 2008-2008 IEEE Region 10 Conference*, 2008, pp. 1–6.

[24] M. Tasdighi and M. Kezunovic, "Automated review of distance relay settings adequacy after the network topology changes," *IEEE Trans. Power Deliv.*, vol.

31, no. 4, pp. 1873–1881, 2016.

[25] J. Joe-Air, Y. Jun-Zhe, L. Ying-Hong, L. Chih-Wen, and M. Jih-Chen, “An adaptive PMU based fault detection/location technique for transmission lines. I. Theory and algorithms,” *IEEE Trans. Power Deliv.*, vol. 15, no. 2, pp. 486–493, 2000.

[26] S.-I. Lim, C.-C. Liu, S.-J. Lee, M.-S. Choi, and S.-J. Rim, “Blocking of zone 3 relays to prevent cascaded events,” *Power Syst. IEEE Trans.*, vol. 23, no. 2, pp. 747–754, 2008.

[27] P. Dutta, A. Esmaeilian, and M. Kezunovic, “Transmission-line fault analysis using synchronized sampling,” *IEEE Trans. Power Deliv.*, vol. 29, no. 2, pp. 942–950, 2014.

[28] A. Esmaeilian, T. Popovic, and M. Kezunovic, “Transmission line relay mis-operation detection based on time-synchronized field data,” *Electr. Power Syst. Res.*, vol. 125, pp. 174–183, 2015.

[29] P. V Navalkar and S. A. Soman, “Secure remote backup protection of transmission lines using synchrophasors,” *IEEE Trans. Power Deliv.*, vol. 26, no. 1, pp. 87–96, 2011.

[30] P. Kundu and A. K. Pradhan, “Synchrophasor-assisted zone 3 operation,” *Power Deliv. IEEE Trans.*, vol. 29, no. 2, pp. 660–667, 2014.

[31] S. Garlapati, H. Lin, A. Heier, S. K. Shukla, and J. Thorp, “A hierarchically distributed non-intrusive agent aided distance relaying protection scheme to supervise Zone 3,” *Int. J. Electr. Power Energy Syst.*, vol. 50, pp. 42–49, 2013.

[32] M. A. Haj-ahmed and M. S. Illindala, “Intelligent coordinated adaptive distance relaying,” *Electr. Power Syst. Res.*, vol. 110, pp. 163–171, 2014.

[33] M. K. Neyestanaki and A. M. Ranjbar, “An Adaptive PMU-Based Wide Area Backup Protection Scheme for Power Transmission Lines,” *IEEE Trans. Smart Grid*, vol. 6, no. 3, pp. 1550–1559, 2015.

[34] M. M. Eissa, M. E. Masoud, and M. Elanwar, “A novel back up wide area protection technique for power transmission grids using phasor measurement unit,” *Power Deliv. IEEE Trans.*, vol. 25, no. 1, pp. 270–278, 2010.

[35] Z. He, Z. Zhang, W. Chen, O. P. Malik, and X. Yin, “Wide-Area Backup Protection Algorithm Based on Fault Component Voltage Distribution,” *IEEE Trans. Power Deliv.*, vol. 26, no. 4, pp. 2752–2760, 2011.

[36] X. Lin *et al.*, “Countermeasures on preventing backup protection mal-operation during load flow transferring,” *Int. J. Electr. Power Energy Syst.*, vol. 79, pp. 27–33, 2016.

[37] P. K. Nayak, A. K. Pradhan, and P. Bajpai, “Secured zone 3 protection during stressed condition,” *Power Deliv. IEEE Trans.*, vol. 30, no. 1, pp. 89–96, 2015.

[38] M. Jonsson and J. E. Daalder, “An adaptive scheme to prevent undesirable distance protection operation during voltage instability,” *Power Deliv. IEEE Trans.*, vol. 18, no. 4, pp. 1174–1180, 2003.

[39] K. Vu, M. M. Begovic, D. Novosel, and M. M. Saha, “Use of local measurements to estimate voltage-stability margin,” *IEEE Trans. Power Syst.*, vol. 14, no. 3, pp. 1029–1035, 1999.

[40] M. Sharifzadeh, H. Lesani, and M. Sanaye-Pasand, “A new algorithm to stabilize distance relay operation during voltage-degraded conditions,” *Power Deliv. IEEE Trans.*, vol. 29, no. 4, pp. 1639–1647, 2014.

[41] S. A. Probert and Y. H. Song, “Detection and classification of high frequency transients using wavelet analysis,” in *Power Engineering Society Summer Meeting, 2002 IEEE*, 2002, vol. 2, pp. 801–806 vol.2.

[42] N. Perera and A. Rajapakse, “Recognition of Fault Transients Using a Probabilistic Neural-Network Classifier,” *2011 Ieee Power Energy Soc. Gen. Meet.*, 2011.

[43] A. Abdullah, “Towards a new paradigm for ultrafast transmission line relaying,” in *2016 IEEE Power and Energy Conference at Illinois (PECI)*, 2016, pp. 1–8.

[44] D. E. Hedman, “Propagation on overhead transmission lines I-theory of modal analysis,” *IEEE Trans. Power Appar. Syst.*, vol. 84, no. 3, pp. 200–205, 1965.

[45] H. K. Zadeh and Z. Li, “Adaptive load blinder for distance protection,” *Int. J. Electr. Power Energy Syst.*, vol. 33, no. 4, pp. 861–867, 2011.

[46] H. K. Zadeh and Z. Li, “Artificial neural network based load blinder for distance protection,” in *Power and Energy Society General Meeting-Conversion and Delivery of Electrical Energy in the 21st Century, 2008 IEEE*, 2008, pp. 1–6.

[47] J. M. Zurada, *Introduction to artificial neural systems*, vol. 8. West St. Paul, 1992.

[48] V. C. Nikolaidis, N. Savvopoulos, A. S. Safigianni, and C. D. Vournas, “Adjusting third zone distance protection to avoid voltage collapse,” in *Power Systems Computation Conference (PSCC), 2014*, 2014, pp. 1–7.

[49] V. Nikolaidis, “Emergency Zone 3 Modification as a Local Response-Driven Protection Measure against System Collapse,” *IEEE Trans. Power Deliv.*, vol. PP, no. 99, p. 1, 2016.

[50] J. Ma, C. Liu, Y. Zhao, S. Kang, and J. S. Thorp, “An Adaptive Overload Identification Method Based on Complex Phasor Plane,” *IEEE Trans. Power Deliv.*, vol. 31, no. 5, pp. 2250–2259, 2016.

[51] A. Boggess and F. J. Narcowich, *A first course in wavelets with Fourier analysis*. John Wiley & Sons, 2015.

[52] Z. O. Bo, K. Aggarwal, A. T. Johns, B. H. Zhang, and Z. Y. Ge, “New concept in transmission line reclosure using high-frequency fault transients,” *IEE proceedings-generation, Transm. Distrib.*, vol. 144, no. 4, pp. 351–356, 1997.

[53] J. J. Grainger and W. D. Stevenson, *Power system analysis*. McGraw-Hill, 1994.

[54] S. Mallat, *A wavelet tour of signal processing*. Academic press, 1999.

[55] J. R. Lucas, P. G. McLaren, W. W. L. Keerthipala, and R. P. Jayasinghe, “Improved simulation models for current and voltage transformers in relay studies,” *IEEE Trans. Power Deliv.*, vol. 7, no. 1, pp. 152–159, 1992.

[56] S. Sefidpour, J. Wang, and K. Srivastava, “Factors affecting traveling wave protection,” in *Advanced Power System Automation and Protection (APAP), 2011 International Conference on*, 2011, vol. 2, pp. 1359–1365.

[57] E. H. Shehab-Eldin and P. G. McLaren, “Travelling wave distance protection-problem areas and solutions,” *IEEE Trans. Power Deliv.*, vol. 3, no. 3, pp. 894–902, 1988.

[58] M. Kezunovic and I. Rikalo, “Detect and classify faults using neural nets,” *IEEE Comput. Appl. Power*, vol. 9, no. 4, pp. 42–47, 1996.

[59] T. Dalstein and B. Kulicke, “Neural-Network Approach to Fault Classification for High-Speed Protective Relaying,” *IEEE Trans. Power Deliv.*, vol. 10, no. 2, pp. 1002–1011, 1995.

[60] M. Oleskovicz, D. V Coury, and R. K. Aggarwal, “A complete scheme for fault detection, classification and location in transmission lines using neural networks,” *Seventh Int. Conf. Dev. Power Syst. Prot.*, no. 479, pp. 335–338, 2001.

[61] K. M. Silva, B. A. Souza, and N. S. D. Brito, “Fault detection and classification in transmission lines based on wavelet transform and ANN,” *Power Deliv. IEEE Trans.*, vol. 21, no. 4, pp. 2058–2063, 2006.

[62] P. L. L. Mao and R. K. Aggarwal, “A novel approach to the classification of the transient phenomena in power transformers using combined wavelet transform and neural network,” *Ieee Trans. Power Deliv.*, vol. 16, no. 4, pp. 654–660, 2001.

[63] F. Martin and J. A. Aguado, “Wavelet-based ANN approach for transmission line protection,” *IEEE Trans. Power Deliv.*, vol. 18, no. 4, pp. 1572–1574, 2003.

[64] G. Zwe-Lee, “Wavelet-based neural network for power disturbance recognition and classification,” *Power Deliv. IEEE Trans.*, vol. 19, no. 4, pp. 1560–1568, 2004.

[65] J. L. Blackburn, *Symmetrical components for power systems engineering*. CRC Press, 1993.

[66] E. Clarke, *Circuit analysis of AC power systems*, vol. 1. Wiley, 1943.

[67] J. A. B. Faria and J. H. Briceno, “On the modal analysis of asymmetrical three-phase transmission lines using standard transformation matrices,” *IEEE Trans. Power Deliv.*, vol. 12, no. 4, pp. 1760–1765, 1997.

[68] S. Pittner and S. V. Kamarthi, “Feature extraction from wavelet coefficients for pattern recognition tasks,” *IEEE Trans. Pattern Anal. Mach. Intell.*, vol. 21, no. 1, pp. 83–88, 1999.

[69] W. Scott-Meyer, “EMTP Rule Book,” *BPA*, 1982.

[70] H. W. Dommel and W. S. Meyer, “Computation of electromagnetic transients,” *Proc. IEEE*, vol. 62, no. 7, pp. 983–993, 1974.

[71] D. E. Hedman, “Propagation on Overhead Transmission Lines II-Earth-Conduction Effects and Practical Results,” *IEEE Trans. Power Appar. Syst.*, vol. 84, no. 3, pp. 205–211, 1965.

[72] P. M. Anderson, *Power system protection*. Wiley, 1998.

[73] A. J. Eriksson, “The incidence of lightning strikes to power lines,” *IEEE Trans. Power Deliv.*, vol. 2, no. 3, pp. 859–870, 1987.

[74] A. J. Pointon and others, *AC and DC network theory*. Springer Science & Business Media, 2012.

[75] A. S. Morched, J. H. Ottevangers, and L. Marti, “Multi-port frequency dependent network equivalents for the EMTP,” *IEEE Trans. Power Deliv.*, vol. 8, no. 3, pp. 1402–1412, 1993.

[76] A. Abdullah and B. Yancey, “SSO study of a wind farm in ERCOT,” in *IEEE IAS Annual meeting 2017*, 2017, pp. 287–295.

[77] E. W. Kimbark, *Power system stability*, vol. 1. John Wiley & Sons, 1995.

[78] D. C. Robertson, O. I. Camps, J. S. Mayer, and W. B. Gish, "Wavelets and electromagnetic power system transients," *Power Deliv. IEEE Trans.*, vol. 11, no. 2, pp. 1050–1058, 1996.

[79] T. Cover and P. Hart, "Nearest neighbor pattern classification," *IEEE Trans. Inf. theory*, vol. 13, no. 1, pp. 21–27, 1967.

[80] M. Saito, M. Ishii, F. Fujii, M. Matsui, H. Kawamura, and N. Itamoto, "Evaluation of lightning fault rate of transmission line on the coastal area of the Sea of Japan in winter," *IEEJ Trans. Power Energy*, vol. 129, pp. 157–163, 2009.

[81] A. Abdullah, "A wavelet entropy approach for detecting lightning faults on transmission lines," in *Transmission and Distribution Conference and Exposition (T&D), 2016 IEEE/PES*, 2016, pp. 1–5.

[82] S. Okabe, T. Tsuboi, and J. Takami, "Analysis of aspects of lightning strokes to large-sized transmission lines," *IEEE Trans. Dielectr. Electr. Insul.*, vol. 18, no. 1, 2011.

[83] H. Motoyama, "Experimental study and analysis of breakdown characteristics of long air gaps with short tail lightning impulse," *IEEE Trans. power Deliv.*, vol. 11, no. 2, pp. 972–979, 1996.

[84] A. Inoue and S.-I. Kanao, "Observation and analysis of multiple-phase grounding faults caused by lightning," *IEEE Trans. power Deliv.*, vol. 11, no. 1, pp. 353–360, 1996.

[85] E. O. Schweitzer, A. Guzmán, M. V Mynam, V. Skendzic, B. Kasztenny, and S.

Marx, “Locating faults by the traveling waves they launch,” in *Protective Relay Engineers, 2014 67th Annual Conference for*, 2014, pp. 95–110.

[86] A. Abdullah, “Ultrafast Transmission Line Fault Detection Using a DWT Based ANN,” *IEEE Trans. Ind. Appl.*, pp. 1–1, 2017.

[87] A. Abdullah, “Busbar protection using a wavelet based ANN,” in *Power and Energy Conference (TPEC), IEEE Texas*, 2017, pp. 1–5.

[88] R. Gnanadass, “IUTC 146-Bus System,” Pondicherry University, 2005.

[89] I. C. for a Smarter Electric Grid (ICSEG), “IEEE 300-Bus System.” .

[90] M. Kezunovic, L. Kojovic, V. Skendzic, C. W. Fromen, D. R. Sevcik, and S. L. Nilsson, “Digital models of coupling capacitor voltage transformers for protective relay transient studies,” *IEEE Trans. Power Deliv.*, vol. 7, no. 4, pp. 1927–1935, 1992.

[91] ALSTOM and A. (Firm), *Network Protection & Automation Guide*. ALSTOM, 2002.

[92] S. D. Cho, “Parameter estimation for transformer modeling,” Michigan Technological University, 2002.

[93] H. K. Lauw and W. S. Meyer, “Universal machine modeling for the representation of rotating electric machinery in an electromagnetic transients program,” *IEEE Trans. Power Appar. Syst.*, no. 6, pp. 1342–1351, 1982.

[94] J. Woodworth, “Arrester Selection Guide.” 2011.

[95] B. K. M. V. M. A. G. N. F. E. O. Schweitzer III and V. Skendzic, “Defining and Measuring the Performance of Line Protective Relays,” in *2016 70th Annual*

Georgia Tech Protective Relaying Conference, 2016, pp. 1–19.

[96] M. Kezunovic, Y. Q. Xia, Y. Guo, C. W. Fromen, and D. R. Sevcik, "Distance relay application testing using a digital simulator," *IEEE Trans. Power Deliv.*, vol. 12, no. 1, pp. 72–82, 1997.

[97] A. Abdullah, "ATPMAT: An open source toolbox for systematic creation of EMTP cases in ATP using Matlab," in *2015 North American Power Symposium, NAPS 2015*, 2015.

[98] A. Ametani, N. Nagaoka, Y. Baba, and T. Ohno, *Power system transients: Theory and Applications*. CRC Press, 2013.

[99] E. O. Schweitzer, B. Kasztenny, and M. V Mynam, "Performance of Time-Domain Line Protection Elements on Real-World Faults," in *42nd Annual Western Protective Relay Conference, Spokane, Washington USA*, 2015.

[100] S. M. Brahma, "Distance relay with out-of-step blocking function using wavelet transform," *IEEE Trans. Power Deliv.*, vol. 22, no. 3, pp. 1360–1366, 2007.